

Spring 1-1-2011

# Excipient Effects on Humanized Monoclonal Antibody Interactions with Silicone Oil Emulsion

Keith A. Britt

University of Colorado at Boulder, keith.britt09@gmail.com

Follow this and additional works at: [http://scholar.colorado.edu/chbe\\_gradetds](http://scholar.colorado.edu/chbe_gradetds)

 Part of the [Biological and Chemical Physics Commons](#), [Chemical Engineering Commons](#), and the [Pharmacy and Pharmaceutical Sciences Commons](#)

---

## Recommended Citation

Britt, Keith A., "Excipient Effects on Humanized Monoclonal Antibody Interactions with Silicone Oil Emulsion" (2011). *Chemical & Biological Engineering Graduate Theses & Dissertations*. Paper 3.

This Thesis is brought to you for free and open access by Chemical & Biological Engineering at CU Scholar. It has been accepted for inclusion in Chemical & Biological Engineering Graduate Theses & Dissertations by an authorized administrator of CU Scholar. For more information, please contact [cuscholaradmin@colorado.edu](mailto:cuscholaradmin@colorado.edu).

# EXCIPIENT EFFECTS ON HUMANIZED MONOCLONAL ANTIBODY INTERACTIONS WITH SILICONE OIL EMULSION

by

Keith A. Britt

B.S., University of California, Irvine, 2009

A dissertation submitted to the  
faculty of the Graduate School of the  
University of Colorado in partial fulfillment  
of the requirement for the degree of  
Master of Science

Department of Chemical and Biological Engineering

2011



This thesis for the degree of Master of Science entitled:  
“Excipient Effects on Humanized Monoclonal Antibody Interactions with Silicone  
Oil Emulsion”

by Keith A. Britt

has been approved for the Department of Chemical and Biological Engineering

by

---

Professor Theodore W. Randolph

---

Professor Daniel K. Schwartz

Date: \_\_\_\_\_

The final copy of this thesis has been examined by the signatories, and we  
find that both the content and the form meet acceptable presentation standards  
of scholarly work in the above mentioned discipline

## ABSTRACT

Britt, Keith A. (M.S., Chemical and Biological Engineering)

Excipient Effects on Humanized Monoclonal Antibody Interactions with Silicone Oil Emulsion

Thesis directed by Professor Theodore W. Randolph and Professor Daniel K. Schwartz

Silicone oil is a lubricant used for plunger depression in prefilled glass syringes. Many therapeutic protein products are stored in prefilled syringes and may be exposed to the silicone oil-water interface for up to 18-24 months. At the present, our understanding of how proteins interact with this interface remains poorly understood. In this work, the interaction of three humanized monoclonal antibodies (humAbs) with silicone oil emulsion was assessed in presence of sodium chloride, sucrose, Tween® 20, Tween® 80, and poloxamer 188. It was found that the amount of humAb adsorbed was antibody- and excipient-dependent. Once adsorbed, the tryptophan exposure to solvent resembled that of unfolded protein and was independent of the identity of different excipients present in the formulation buffer. Protein aggregation was not detected in solution. But, colloidal destabilization of silicone oil emulsion resulting from protein adsorption lowered the activation energy barrier to flocculation thereby enabling heterogeneous aggregates comprised of protein-coated silicone oil microdroplets to form. The size of these flocs was dependent on the solution ionic strength. Flocculation occurred in the presence of all excipients examined except in the presence of surfactant. In formulations

containing surfactant, there was competition between humAb and surfactant molecules for adsorption sites at the silicone oil-water interface. The results suggest that the kinetics of humAb displacement from the silicone oil interface was surfactant-dependent. Whether the mechanism of this replacement involved the formation of protein-surfactant complex remains uncertain.

## ACKNOWLEDGEMENTS

I want to thank my advisors Theodore W. Randolph and Daniel K. Schwartz for their insightful guidance for the duration of this project. Their vision and mentoring made this research possible. I want to also thank the other thesis committee members Joel Kaar and Stephanie Bryant, Randolph and Schwartz group members for their day-to-day assistance, John Carpenter and his lab members for letting me use their facilities, Kristi Anseth and her lab members for letting me use their light microscope, and Brent Palmer and Michelle De Souza for helping me use their flow cytometer. Lastly, I want to thank my family and friends, for without your presence in my life, I would be lost.

I want to acknowledge our collaborators at F. Hoffmann-La Roche in Basel, Switzerland for funding this project and providing the protein used in experiments. In particular, I want to thank Christine Wurth for her input during teleconferences.

# TABLE OF CONTENTS

Abstract.....	iii
Acknowledgements.....	v
List of Tables.....	x
List of Figures.....	xi
Chapter 1: Motivation and Background Literature.....	1
1.1 Introduction.....	1
1.2 Antibody Structure, Function, Instability, and Therapeutic Potential.....	1
1.2.1 Structure.....	1
1.2.2 Function.....	3
1.2.3 Instability.....	5
1.2.4 Therapeutic Potential.....	6
1.3 Pharmaceutical Excipients.....	7
1.3.1 Definition of ‘Excipient’.....	7
1.3.2 Excipient Selection and Formulation Design.....	7
1.3.3 Excipient-Excipient and Drug-Excipient Interactions.....	8
1.3.4 Classes of Excipients used in Pharmaceutical Formulations.....	9
1.4 Protein Adsorption to Interfaces.....	10
1.5 Protein Aggregation Pathways.....	12
1.6 Conformational Stability of Therapeutic Proteins Exposed to Interfaces.....	14
1.7 Problems Associated with Perturbed Protein Conformation and Aggregates.....	16
1.8 Thesis Objectives.....	18
1.9 References.....	19
Chapter 2: Excipient Effects on Humanized Monoclonal Antibody Interactions with Silicone Oil Emulsion.....	24
2.1 Introduction.....	24
2.2 Materials and Methods.....	26

2.2.1	Proteins.....	26
2.2.2	Buffer Conditions.....	26
2.2.3	Preparation of Silicone Oil Emulsion.....	27 iii
2.2.4	Concentration of Silicone Oil Emulsion.....	28 v
2.2.5	Particle Size Distribution of Silicone Oil Emulsion.....	29
2.2.6	Silicone Oil-Induced humAb Loss from Solution.....	30
2.2.7	humAb Conformation at the Silicone Oil- Water Interface.....	32
2.2.8	Colloidal Stability.....	33
2.2.9	Fluorescence-Activated Particle Analysis.....	35
2.2.10	Light Microscopy.....	37
2.2.11	Statistical Analysis.....	38
2.3	Results.....	38
2.3.1	Characterization of Stock Silicone Oil Emulsion.....	38
2.3.2	Silicone Oil-Induced humAb Loss from Solution.....	39
2.3.3	humAb Conformation at the Silicone Oil- Water Interface.....	41
2.3.4	Colloidal Stability of humAbs.....	44
2.3.5	Colloidal Stability of Silicone Oil Emulsion.....	45
2.3.6	Fluorescence-Activated Particle Analysis.....	47
2.3.7	Light Microscopy to Inspect Silicone Oil Droplet Flocculation.....	52
2.4	Discussion.....	52
2.4.1	Characterization of Stock Silicone Oil Emulsion.....	52
2.4.2	Silicone Oil-Induced humAb Loss from Solution.....	53
2.4.3	humAb Conformation at the Silicone Oil- Water Interface.....	55
2.4.4	Colloidal Stability of humAbs.....	56
2.4.5	Colloidal Stability of Silicone Oil Emulsion.....	57

2.4.6	Fluorescence-Activated Particle Analysis.....	59
2.4.7	Light Microscopy to Inspect Silicone Oil Droplet Flocculation.....	61
2.5	Conclusions.....	62
2.6	References.....	63
Chapter 3:	Light Scattering Analysis of Humanized Monoclonal Antibody Interactions with Silicone Oil Emulsion.....	69
3.1	Introduction.....	69
3.2	Materials and Methods.....	71
3.2.1	Materials.....	71
3.2.2	Light Scattering Analysis.....	71
3.3	Results.....	72
3.3.1	humAb Adsorption to the Silicone Oil- Water Interface.....	72
3.3.2	Bridging Flocculation of Silicone Oil Emulsion.....	73
3.4	Discussion.....	73
3.4.1	humAb Adsorption to the Silicone Oil- Water Interface.....	73
3.4.2	Bridging Flocculation of Silicone Oil Emulsion.....	76
3.5	Conclusions.....	77
3.6	References.....	77
Chapter 4:	Competitive Adsorption of Humanized Monoclonal Antibody and Surfactants at the Silicone Oil-Water Interface.....	78
4.1	Introduction.....	78
4.2	Materials and Methods.....	80
4.2.1	Materials.....	80
4.2.2	Zeta Potential Analysis.....	80
4.2.3	Statistical Analysis.....	81
4.3	Results.....	81
4.3.1	Zeta Potential of humAb-surfactant Solution.....	81
4.3.2	Competitive Adsorption of humAbs	

and Surfactants to the Silicone Oil- Water Interface.....	82
4.4 Discussion.....	86
4.4.1 Zeta Potential of humAb-surfactant Solution.....	86
4.4.2 Competitive Adsorption of humAbs and Surfactants to the Silicone Oil- Water Interface.....	88
4.5 Conclusions.....	90
4.6 References.....	90
Chapter 5: Conclusions and Future Recommendations.....	93
5.1 Final Conclusions.....	93
5.2 Future Recommendations.....	94
5.3 References.....	97
Bibliography.....	98



## LIST OF TABLES

### CHAPTER 1

TABLE 1.1. Class and purpose of common pharmaceutical excipients. Sources: 1.10, 1.28.

TABLE 1.2. Factors enhancing protein aggregation. Source: 1.39.

### CHAPTER 2

TABLE 2.1. Summary of some physical properties of each humAb

### CHAPTER 3

none

### CHAPTER 4

none

### CHAPTER 5

none

## LIST OF FIGURES

### CHAPTER 1

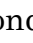
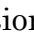
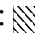
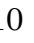
FIGURE 1.1. Representative images of an IgG. (A) Ribbon Model. Light chains are green and dark blue, heavy chains are light blue and orange, disulfide bonds are yellow, and oligosaccharide is red. (B) Y-shape Model. Different regions are labeled. Sources: 1.41, 1.42.

### CHAPTER 2

FIGURE 2.1. Standard curve showing the area of the peak at  $1260\text{ cm}^{-1}$  as a function of mass concentration of silicone oil in n-hexane. The area of the peak at  $1260\text{ cm}^{-1}$  was determined from  $1245\text{ cm}^{-1}$  to  $1275\text{ cm}^{-1}$ . This area was determined for silicone oil concentrations of 12.5, 6.25, 3.13, 1.56, 0.781, 0.391, 0.195, 0.0977 mg/mL in n-hexane. The dotted line is a linear fit of the data. The equation of this line is  $y = 0.036x$  with an  $R^2$  value of 0.99. Data represents the arithmetic mean of three replicate samples. Error bars represent the standard error of the mean.

FIGURE 2.2. Representative particle size distributions of silicone oil emulsion prepared in water. Droplet diameters are grouped into bins and represented as a percent of the total number of droplets analyzed. (A) Percent number particle size distribution. (B) Percent surface area particle size distribution.

FIGURE 2.3. Representative chromatograms from SE-HPLC. A control that was not incubated with silicone oil emulsion is represented by the solid line. A sample that was incubated with silicone oil emulsion is represented by the dashed line. There is a peak at roughly 17 minutes that corresponds to native humAb monomers. The formation of small homogeneous protein aggregates would appear at times before the monomer peak.

FIGURE 2.4. Loss of protein from solution after incubation of humAbs with silicone oil emulsion for 72 hours. Data for humAb 1, humAb 2, and humAb 3 are labeled accordingly. For each protein, there are four bars representing different excipient conditions:  10 mM L-histidine at pH 6.0 containing 0.01% (w/v) sodium azide,  10 mM L-histidine at pH 6.0 containing 0.01% (w/v) sodium azide and 140 mM sodium chloride,  10 mM L-histidine at pH 6.0 containing 0.01% (w/v) sodium azide and 240 mM sucrose,  10 mM

L-histidine at pH 6.0 containing 0.01% (w/v) sodium azide and 0.03% (w/v) Tween® 20. Data represents the arithmetic mean of three replicate samples. Error bars represent the standard error of the mean.

FIGURE 2.5. Representative Stern-Volmer plot obtained from front-face fluorescence quenching. These plots were linear with an  $R^2$  of ca. 0.99. Data represents the arithmetic mean of three replicate samples. Error bars represent the standard error of the mean.


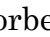
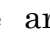
FIGURE 2.6. Measured Stern-Volmer constants after incubation of humAbs with silicone oil emulsion for at least 2 hours. (A) humAb 1. (B) humAb 2. (C) humAb 3. Data for each protein in 10 mM L-histidine at pH 6.0 containing 0.01% (w/v) sodium azide in the presence of no excipients, 140 mM sodium chloride, or 240 mM sucrose are labeled accordingly. For each protein, there are three bars representing different states of the protein:  native protein,  protein adsorbed to silicone oil,  unfolded protein in 9.5 M urea. Data represents the arithmetic mean of three replicate samples. Error bars represent the standard error of the mean.


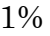
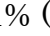

FIGURE 2.7. Zeta potential of native humAbs. Data for humAb 1, humAb 2, and humAb 3 are labeled accordingly. For each protein, there are four bars representing different excipient conditions:  10 mM L-histidine at pH 6.0, containing 0.01% (w/v) sodium azide,  10 mM L-histidine at pH 6.0 containing 0.01% (w/v) sodium azide and 140 mM sodium chloride,  10 mM L-histidine at pH 6.0 containing 0.01% (w/v) sodium azide and 240 mM sucrose,  10 mM L-histidine at pH 6.0 containing 0.01% (w/v) sodium azide and 0.03% (w/v) Tween® 20. Data represents the arithmetic mean of three replicate samples. Error bars represent the standard error of the mean.

FIGURE 2.8. Zeta potential of silicone oil in emulsion in water plotted versus incubation time. Data represents the arithmetic mean of three replicate samples. Error bars represent the standard error of the mean.


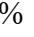


FIGURE 2.9. Zeta potential of humAb-coated silicone oil droplets plotted versus incubation time. (A) No protein. (B) humAb 1. (C) humAb 2. (D) humAb 3. For each case, there are four data sets representing different excipient conditions in 10 mM L-histidine at pH 6.0 containing 0.01% (w/v) sodium azide:  No excipients,  140 mM sodium chloride,  240 mM sucrose,  0.03% (w/v) Tween® 20. Symbols represent the arithmetic mean of three replicate samples. Error bars represent the standard error of the mean.

FIGURE 2.10. Representative plot of the fluorescence intensity of humAb labeled with Alexa Fluor® 647 versus the fluorescence intensity of silicone oil emulsion labeled with BODIPY® 493/503. Each of the 30,000 dots on the plot represents one silicone oil droplet with adsorbed humAb. The vertical axis reflects fluorescence due to Alexa Fluor® 647; the horizontal axis corresponds to fluorescence from silicone oil stained with BODIPY® 493/503.

FIGURE 2.11. Scaling exponents determined from fluorescence-activated particle analysis plotted versus incubation time. (A) humAb 1. (B) humAb 2. (C) humAb 3. For each protein, there are three data sets representing different excipient conditions in 10 mM L-histidine at pH 6.0 containing 0.01% (w/v) sodium azide: □ No excipients, ○ 140 mM sodium chloride, △ 240 mM sucrose. Symbols represent the arithmetic mean of three replicate samples. Error bars represent the standard error of the mean.

FIGURE 2.12. Representative plot of the fluorescence intensity of humAb labeled with Alexa Fluor® 647 versus the fluorescence intensity of silicone oil emulsion labeled with BODIPY® 493/503 for formulations containing 0.03% (w/v) Tween® 20. Each of the 30,000 dots on the plot represents one silicone oil droplet with adsorbed humAb. The vertical axis reflects fluorescence due to Alexa Fluor® 647; the horizontal axis corresponds to fluorescence from silicone oil stained with BODIPY® 493/503.

FIGURE 2.13. Fluorescence intensity histograms for 30,000 particles are presented for silicone oil emulsion labeled with BODIPY® 493/503 (A, C, E) and humAbs labeled with Alexa Fluor® 647 (B, D, F). Blue, green, orange, purple, and red histograms correspond to 30 minutes, 3 days, 1 week, 2 weeks, and 1 month incubation times, respectively.

FIGURE 2.14. Visual Evidence of bridging flocculation of humAb-coated silicone oil droplets obtained from light microscopy. Samples are formulated with different excipients in 10 mM L-histidine at pH 6.0 containing 0.01% (w/v) sodium azide. (A) No excipients. (B) 140 mM sodium chloride. (C) 240 mM sucrose. (D) 0.03% (w/v) Tween® 20. Each image is at 400X magnification and the scale bar represents a distance of 25  $\mu\text{m}$ .

FIGURE 2.15. Representative contour plot illustrating the activation barrier to flocculation of two particles of different diameter. Colors range from blue to red representing the increase in the activation barrier from small to large values. For particles with a zeta potential of 30 mV, each contour represents an increase of activation energy of ca. 20  $kT$ .

FIGURE 2.16. Example illustrating the creaming of silicone oil emulsion after sufficient incubation time. (A) Prior to incubation. (B) After incubation.

FIGURE 2.17. Examples of visible particles in pharmaceutical formulations. Source: 1.33.

## CHAPTER 3

FIGURE 3.1. Evidence of protein adsorption verified using light scattering and fluorescence of labeled silicone oil and humAb. Each of the 30,000 dots on the plot represents one silicone oil droplet with adsorbed humAb. (A) Side-scattered light intensity is plotted versus the fluorescence intensity of humAb labeled with Alexa Fluor® 647. (B) Side-scattered light intensity is plotted versus forward-scattered light intensity.

FIGURE 3.2. Evidence of bridging flocculation of humAb-coated silicone oil microdroplets interpreted as shifts in side-scattered light intensity in plots of side- versus forward-scattered light intensity. Each of the 30,000 dots on the plot represents one silicone oil droplet with adsorbed humAb for different excipient conditions in 10 mM L-histidine at pH 6.0 containing 0.01% (w/v) sodium azide. (A) No excipients. (B) 140 mM sodium chloride. (C) 240 mM sucrose. (D) 0.03% (w/v) Tween® 20. Blue and red dots correspond to 30 minutes and 1 month incubation times, respectively.

## CHAPTER 4

FIGURE 4.1. Zeta potential of native humAbs. Data for humAb 1, humAb 2, and humAb 3 are labeled accordingly. For each protein, there are four bars representing different excipient conditions: ▨ 10 mM L-histidine at pH 6.0 containing 0.01% (w/v) sodium azide, ▩ 10 mM L-histidine at pH 6.0 containing 0.01% (w/v) sodium azide and 0.03% (w/v) Tween® 20, ▪ 10 mM L-histidine at pH 6.0 containing 0.01% (w/v) sodium azide and 0.03% (w/v) Tween® 80, ▫ 10 mM L-histidine at pH 6.0 containing 0.01% (w/v) sodium azide and 0.03% (w/v) poloxamer 188. Data represents the arithmetic mean of three replicate samples. Error bars represent the standard error of the mean.

FIGURE 4.2. Zeta potential of silicone oil emulsion in buffer containing humAb 1 and 0.03% (w/v) surfactant. (A) Tween® 20. (B) Tween® 80. (C) poloxamer 188. For each plot, there are two sets of data: □ No protein present, ○ Protein present. Symbols represent the arithmetic mean of three

replicate samples. Error bars represent the standard error of the mean.

FIGURE 4.3. Zeta potential of silicone oil emulsion in buffer containing humAb 2 and 0.03% (w/v) surfactant. (A) Tween® 20. (B) Tween® 80. (C) poloxamer 188. For each plot, there are two sets of data: □ No protein present, O Protein present. Symbols represent the arithmetic mean of three replicate samples. Error bars represent the standard error of the mean.

FIGURE 4.4. Zeta potential of silicone oil emulsion in buffer containing humAb 3 and 0.03% (w/v) surfactant. (A) Tween® 20. (B) Tween® 80. (C) poloxamer 188. For each plot, there are two sets of data: □ No protein present, O Protein present. Symbols represent the arithmetic mean of three replicate samples. Error bars represent the standard error of the mean.

## CHAPTER 5

FIGURE 5.1. Example of visible particles that can form after protein is incubated with silicone oil emulsion. Visible particles were observed after incubation of humAb 1 in 10 mM L-histidine at pH 6.0 containing 0.01% (w/v) sodium azide and 0.03% (w/v) Tween® 80 for 72 hours.

“All the world is a laboratory to the inquiring mind.”

~Martin H. Fischer

# CHAPTER 1: MOTIVATION AND BACKGROUND LITERATURE

## 1.1 INTRODUCTION

Therapeutic protein products are becoming more reputable and widespread in the pharmaceutical industry. In general, protein drugs are more effective at lower concentrations with less side effects than small molecule drugs.<sup>1,40</sup> Many protein drugs are formulated as a liquid. In the development of these formulations, stresses imposed during production, processing, shipping, storage, and delivery to patients can result in the formation of sub-visible and/or visible particles.

Pharmaceutical proteins are ubiquitously exposed to potentially hazardous interfaces. Interface-induced protein damage or aggregation can elicit deleterious effects by reducing drug efficacy, increasing anti-drug immunogenicity, and shortening shelf-life. Also, it is estimated that major pharmaceutical companies spend between \$800 million and \$1.2 billion in research and development to bring a new drug to the market. For these reasons, there is a growing need to understand the behavior of proteins at interfaces, making this an area of research that is actively being pursued.

## 1.2 ANTIBODY STRUCTURE, FUNCTION, INSTABILITY, AND THERAPEUTIC POTENTIAL

### 1.2.1 Structure

Antibodies are immunoglobulins. A single immunoglobulin is roughly Y-shaped and consists of a variable (V) region and a constant (C) region<sup>1,22,1,40</sup> (Figure



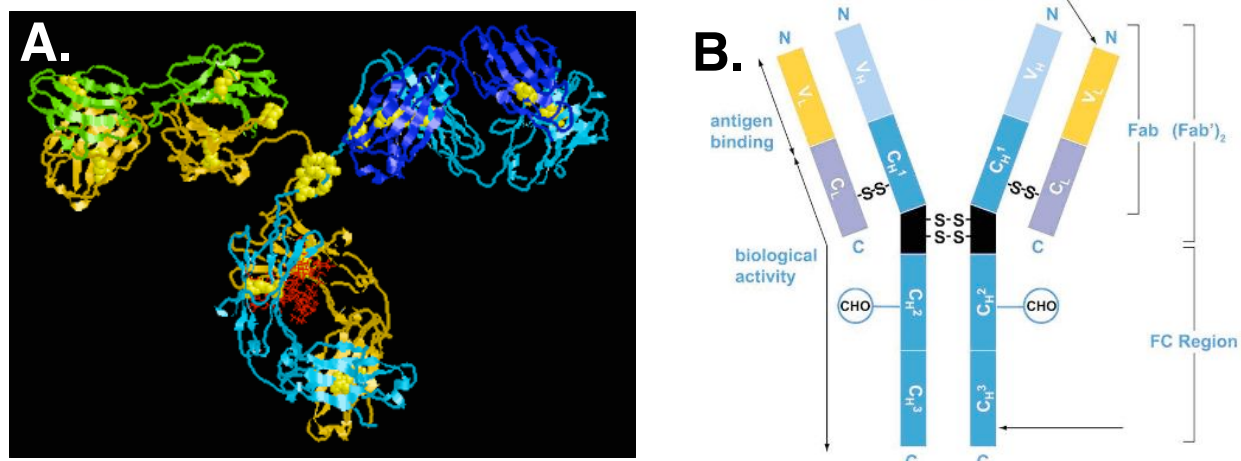


FIGURE 1.1. Representative images of an IgG. (A) Ribbon Model. Light chains are green and dark blue, heavy chains are light blue and orange, disulfide bonds are yellow, and oligosaccharide is red. (B) Y-shape Model. Different regions are labeled. Sources 1.41, 1.42.

1.1). The variable region is found at the top of the Y and is also called the Fab region.<sup>1.22,1.40</sup> The constant region is found at the stem of the Y and is also called the Fc region.<sup>1.22,1.40</sup> There are five different classes of immunoglobulins: IgA, IgD, IgE, IgG, and IgM. These classes of immunoglobulins differ in their constant regions which are denoted  $\alpha$ ,  $\delta$ ,  $\epsilon$ ,  $\gamma$ , and  $\mu$ , respectively<sup>1.22, 1.40</sup>. The variable regions can be divided into three hypervariable (HV) regions and four framework (FR) regions.<sup>1.22, 1.40</sup> Immunoglobulins can exist as monomers (IgD, IgE, IgG), dimers (IgA), or pentamers (IgM).<sup>1.22,1.40</sup> Since IgGs are the most abundant and widely used immunoglobulins used as protein therapeutics and are the focus of this work, these immunoglobulins will be discussed in more detail in the following sections.

IgGs consist of two identical heavy (H) chains approximately 50 kDa and two identical light (L) chains approximately 25 kDa such that the overall molecular weight of the molecule is roughly 150 kDa.<sup>1.22,1.40</sup> In general, there are a total of four

disulfide bonds linking heavy and light chains and four intrachain disulfide bonds residing in each domain of the heavy and light chains.<sup>1.22,1.40</sup> IgGs can further be classified based on their relative abundance in human plasma.<sup>1.22,1.40</sup> These IgGs are referred to as IgG1, IgG2, IgG3, and IgG4 with different heavy chains denoted  $\gamma 1$ ,  $\gamma 2$ ,  $\gamma 3$ , and  $\gamma 4$ , respectively.<sup>1.22,1.40</sup> In addition, there are two types of light chains denoted  $\kappa$  and  $\lambda$ .<sup>1.22,1.40</sup> The ratio of  $\kappa:\lambda$  is species-dependent.<sup>1.40</sup>

Antibodies are glycosylated. In IgGs, there is one oligosaccharide that is N-linked to a conserved Asn 297.<sup>1.40</sup> Also, there are often other areas on the immunoglobulin that are glycosylated. Due to differences in cell lines, bioreactor conditions, and downstream processing, purified antibodies have different glycosylation patterns.<sup>1.40</sup> In addition, terminal processing and instabilities during processing result in a heterogeneous antibody population.<sup>1.40</sup>

The major type of secondary structure in IgGs is  $\beta$ -sheets.<sup>1.40</sup> These structures comprise roughly 70% of the molecule.<sup>1.40</sup> Only a small portion of IgG tertiary structure has been identified. This structure is maintained by disulfide bonds and non-covalent interactions.<sup>1.40</sup>

### 1.2.2 Function

There are two functional areas in IgGs located at the Fab and Fc regions. The Fab region serves as an antigen-binding site.<sup>1.40</sup> More specifically, the exact antigen-binding sites are located in the hypervariable regions with participation of the framework regions<sup>1.40</sup>. Antigen-binding is proposed to occur by an induced-fit

mechanism wherein 5-10 residues are thought to contribute significantly to the binding energy<sup>1.40</sup>. The functionality in the variable region is independent of the constant region.<sup>1.40</sup> The Fc region has three main effector functions<sup>1.40</sup>: (1) It is recognized by receptors on immune effector cells thereby initiating antibody-dependent cell cytotoxicities (ADCC), (2) It binds to complement to recruit activated phagocytes, and (3) It aids in its transportation to different parts of the body. Unlike the Fab region, the functionality of the constant region is affected by the variable region.<sup>1.40</sup> In addition, proper glycosylation is important in the functionality of an antibody.<sup>1.40</sup> Glycosylation can affect the conformation of the antibody thereby affecting antigen binding, influence the immunogenicity of the antibody to the body once administered to patients, and affect its degradation rate.<sup>1.40</sup>

In the development of early antibody therapies, antibodies were made in mice. As a result, an adverse side-effect of these antibody drugs was the production of human anti-mouse antibodies (HAMA).<sup>1.40</sup> To try to minimize this unwanted immune response, chimeric antibodies that are 60-70% human made from mouse variable regions and human constant regions were developed.<sup>1.40</sup> These antibodies still elicited the formation of human anti-chimeric antibodies (HACA).<sup>1.40</sup> Again, to lessen to observed immune response in patients, humanized antibodies that are 90-95% human were developed by replacing murine hypervariable regions with human hypervariable regions.<sup>1.40</sup> Humanized antibodies have nearly the same immunogenic potential as completely human antibodies, but can still elicit the formation of human anti-human antibodies (HAHA).<sup>1.40</sup>

### 1.2.3 Instability

In general, antibodies are stable proteins under normal storage conditions.<sup>1.40</sup> However, like all proteins, antibodies are susceptible to physical and chemical degradation that can result in impaired protein functionality.

Physical instabilities of antibodies can occur via denaturation and aggregation.<sup>1.40</sup> Denaturation can occur as a result of temperature shifts and shearing forces.<sup>1.40</sup> Similarly, aggregation rate depends on protein concentration, viscosity, ionic strength, pH, and temperature.<sup>1.40</sup> Both denaturation and aggregation may occur as a result of agitation, long-term storage, multiple freeze-thaw cycles, and lyophilization.<sup>1.40</sup> In addition, exposure of antibodies to interfaces, like other proteins, results in surface adsorption which decreases the concentration of protein in solution and may result in surface-induced denaturation and/or aggregation<sup>1.3-1.4,1.7-1.9,1.13,1.15,1.18-1.20,1.23-1.24,1.26-1.27,1.32,1.34-1.37</sup>.

Chemical instabilities of antibodies can occur via numerous pathways. These instabilities include cross-linking resulting from disulfide bond formation or exchange, deamidation, isomerization, oxidation, formation of acidic or basic species, C-terminal clipping, fragmentation, and/or the formation of protein-sugar adducts via the Maillard reaction<sup>1.40</sup>. The mechanisms by which said instabilities may occur can be attributed to storage conditions, dosage form, pH conditions, amino acid sequence, steric effects, temperature shifts, or freeze-thaw conditions.<sup>1.40</sup>

#### 1.2.4 Therapeutic Potential

Antibodies can act as agonists or antagonists to potentially control major pathways in cancer, infectious diseases, allergy, autoimmune diseases, and inflammation.<sup>1.40</sup> Currently, there are more than 23 monoclonal drug products on the market including humanized monoclonal antibody drug products such as Avastin®, Campath®, Herceptin®, Humira®, Lucentis®, Mylotarg®, Raptiva®, Synagis®, Tysabri®, Xolair®, and Zenapax®.<sup>1.40</sup> Antibody and antibody derivatives constitute 20% of biopharmaceutical products currently being developed.<sup>1.40</sup> However, development of commercially viable antibody drug products is difficult. Despite having similar molecular weights, isoelectric points, and structures, the behavior of antibodies cannot be generalized.

In addition to liquid and lyophilized antibody formulations, advanced formulations have been attempted. Spray-dried formulations have been tested and limited success has been achieved due to the high propensity of proteins to aggregate.<sup>1.40</sup> Stabilization of antibodies and antibody fragments via mutagenesis and chemical modification has had some success.<sup>1.40</sup> There have been studies that saw noticeable increases in antibody stability.<sup>1.40</sup> However, some studies have showed that chemical modification of antibodies resulted in increased clearance rates and reduced biodistribution.<sup>1.40</sup> PEGylation of antibodies has also been attempted and may be useful in some applications.<sup>1.40</sup> However, this can reduce drug efficacy and can elicit an unwanted immune response.<sup>1.40</sup>

## 1.3 PHARMACEUTICAL EXCIPIENTS

### 1.3.1 Definition of ‘Excipient’

Historically, there have been several formal definitions of ‘excipient.’ Today, the International Pharmaceutical Excipients Council (IPEC) defines ‘excipient’ as any substance contained in the finished pharmaceutical dosage form other than the active drug or prodrug.<sup>1,10</sup>

### 1.3.2 Excipient Selection and Formulation Design

Selection of suitable excipients to use in pharmaceutical formulations can be a daunting task. Excipients should be chemically stable, be non-reactive with the drug and other excipients, possess low toxicity in the human body, have low process and equipment sensitivity, have pleasing organoleptic properties, be well characterized, and be well accepted by regulatory agencies.<sup>1,10,1,28</sup> The number of excipients that adhere to the aforementioned list of requirements is limited making selection of new excipients a challenging process. However, because some drugs have non-ideal physiochemical, permeation, and pharmacokinetic properties, new excipients or new applications of existing excipients have been developed.<sup>1,10</sup> To date, there have been very few new excipients of completely new chemical identity introduced to the market because of the economic strain associated with toxicological screening.<sup>1,10,1,28</sup>

The type of formulation and excipients used in a pharmaceutical product undergo extensive screening experiments to assess the conditions that a particular

protein drug will be stable for the longest period of time. Experiments may be conducted under ‘accelerated’ conditions to allow the behavior of a protein drug to be assessed for a shorter period of time. Once pre-formulation studies are performed to determine possible stabilization strategies, the typical order of experiments conducted to design the optimal formulation is listed as follows<sup>1,28</sup>:

- (1) Obtain the stability profile of the protein solution containing no formulation excipients under ‘stressed’ conditions. Typical stresses include agitation and temperature.
- (2) Obtain the stability profile of the same protein solutions with the same stresses in the presence of excipient(s). Select possible candidates that are the most stable protein formulations.
- (3) Optimize the protein stability of candidate formulations.
- (4) Perform real-time long-term protein stability studies of the optimized candidate formulations at a larger scale.

Aqueous formulations are preferred due to ease manufacturing and administration. Lyophilized formulations are chosen if the shelf-life of an aqueous solution is too low.<sup>1,28</sup> The shelf-life of an economically viable protein therapeutic product ranges from 18-24 months.

### 1.3.3 Excipient-Excipient and Drug-Excipient Interactions

Excipient-excipient interactions and drug-excipient interactions can be favorable or unfavorable depending on the delivery strategy of the formulation.

TABLE 1.1. Class and purpose of common pharmaceutical excipients.  
Sources: 1.10, 1.28.

Class	Purpose
Buffer	pH buffer
Salt	Tonicity modifier, solubilizer
Sugar	Protein-stabilizer, bulking agent, glass former
Polyol	Tonicity modifier, bulking agent
Amino Acid	Tonicity modifier, bulking agent, stabilizer
Polymer	Bulking agent, glass former
Surfactant	Solubilizer, stabilizer, aggregation inhibitor
Preservative	Antimicrobial

These interactions can be classified as physical or chemical. Excipient-excipient and drug-excipient interactions can influence several different phenomena including adsorption, complexation, chemical reactions, pH shifts, and eutectic formation.<sup>1,10,</sup>

1.28

#### 1.3.4 Classes of Excipients used in Pharmaceutical Formulations

There are several classes of excipients commonly utilized in pharmaceutical formulations including salts, sugars, polyols, amino acids, polymers, surfactants, and preservatives (see Table 1.1).<sup>1,10,1.28</sup> The purpose of these excipients are to modulate solution tonicity, enhance protein stability, increase protein solubility, serve as a bulking agent, aid in the formation of a glassy state during lyophilization, or prevent microbial growth.<sup>1,10,1.28</sup>



## 1.4 PROTEIN ADSORPTION TO INTERFACES

Proteins have been shown to be surface-active at various interfaces.<sup>1.1,1.3-1.9,1.13,1.15,1.17-1.21,1.23-1.24,1.26,1.32,1.34-1.36,1.38</sup> More specifically, protein adsorption has been observed at the solid-liquid interface<sup>1.4,1.6-1.8,1.20-1.21,1.36</sup>, the air-liquid interface<sup>1.1,1.3,1.5,1.14,1.17,1.26,1.34</sup>, and the liquid-liquid interface.<sup>1.18,1.23-1.24,1.35</sup> While protein adsorption at solid substrates can be similar to that at fluid-fluid interfaces, there are differences. At the fluid-fluid interface, proteins can penetrate into the non-aqueous phase, diffuse faster, and undergo faster orientational and conformational reorganization.<sup>1.15</sup> Nearly all protein adsorption studies are characterized by non-ideal behavior.<sup>1.15</sup> This is due to enthalpic and entropic contributions to the surface free energy resulting from protein intermolecular interactions and intramolecular rearrangements.<sup>1.15</sup>

The dynamics of protein adsorption at oil-water interface was investigated by Beverung et al. by monitoring the change in interfacial surface tension as a function of time using several model proteins.<sup>1.9</sup> It was found that the kinetics of adsorption can be divided into three distinct regimes<sup>1.9</sup>:

- (1) An initial induction period that depends on diffusion of protein to an interface and the affinity that protein has towards that interface. Only a small change in interfacial tension is observed. Conformational rearrangement begins during this period. This regime is only observed for very dilute protein solutions.

(2) A period where the surface becomes saturated with adsorbed protein.

There is continued conformational rearrangement. An increase in the number of interfacial contacts per protein causes a steep decline in interfacial tension.

(3) The last period begins as a full monolayer is formed. Continued relaxation of the adsorbed protein layer and the onset of multilayer formation occurs in this regime.

The phenomenology discussed thus far is relevant for an ensemble of protein molecules. Recently, techniques based on single-molecule total internal reflection fluorescence microscopy (TIRFM) have been developed to obtain more information about how protein adsorbs to interfaces.<sup>1,21,1.38</sup> Honciuc et al. found that adsorption of individual surfactant molecules is an activated process that involves a competitive exchange between surfactant and surface-bound solvent molecules.<sup>1,21</sup> Walder et al. was able to identify multiple populations of fluorescently-labeled protein molecules that adsorb to the oil-water interface.<sup>1,38</sup> For each population, the hydrodynamic radius, surface residence time, and the surface diffusion coefficient were determined. It was found that larger objects had longer surface residence times and smaller surface diffusion coefficients.

## 1.5 PROTEIN AGGREGATION PATHWAYS

Protein aggregation continues to be a problem in the commercialization of protein drug products. Aggregation can be classified as intrinsic or extrinsic.<sup>1.39</sup> Intrinsic protein aggregation results from changes in protein primary, secondary, tertiary, or quaternary structure.<sup>1.39</sup> Extrinsic protein aggregation is influenced by the local environment of a protein during processing, storage, etc.<sup>1.39</sup> There are several mechanisms/pathways by which protein aggregation can occur<sup>1.39</sup>:

- (1) Aggregation through unfolding intermediates and unfolded states.
- (2) Aggregation through protein self-association or chemical linkages.
- (3) Aggregation through chemical degradations.

Aggregation can be reversible or irreversible.<sup>1.14,1.39</sup> The reversibility of protein aggregation depends on the time scale at which aggregation occurs and the size of protein aggregates that are formed.<sup>1.39</sup> Aggregate morphology (i.e. fibrils, particulates, skin, gels, or combinations of these) depends on these factors as well as pH, density of surface charge, and the degree of structural disruption.<sup>1.39</sup>

There are several major stresses that may cause protein aggregation (see Table 1.2).<sup>1.39</sup> These stresses must overcome an electrostatic activation barrier to aggregation.<sup>1.14</sup> The kinetics of protein aggregation for energy barriers greater than 10-20 kT are extremely slow.<sup>1.14</sup> If the energy barrier is overcome, partial/complete unfolding of protein, chemical degradation, shear, or disruption of hydration layers can occur leading to aggregation.<sup>1.39-1.40</sup> Temperature shifts<sup>1.39-1.40</sup>, light or

TABLE 1.2. Factors enhancing protein aggregation. Source: 1.39.

Factor	Potential Effects
Temperature	-Partial/complete protein unfolding, protein-protein association, and chemical degradation
Light/Irradiation	-Chemical degradation, direct crosslinking of proteins
Container/Closure Systems	-Surface protein adsorption, partial protein unfolding, and release of stability-influencing leachables
pH	-Partial/complete protein unfolding and alteration of colloidal stability
Buffering agent and Concentration	-Variable effects depending on specificity and strength ion-protein interactions and solution ionic strength
Ionic Strength	-Variable effects depending on charge screening, ion-protein interactions, and interference with protein-protein interactions
Excipients	-Variable effects depending on excipient type/purpose and concentration
Protein Concentration	-High concentrations increase kinetics of protein-protein interactions and affects protein solubility
Fermentation/Expression	-Variable effects depending on expression of host system and fermentation/expression conditions
Refolding	-Variable effects depending on refolding conditions, temperature, and protein concentration
Purification	-Variable effects depending on purification conditions
Freeze-thawing	-Ice-protein interactions, interfacial adsorption and unfolding, cryoconcentration, cold denaturation, and pH and ionic strength changes
Shaking	-Air-liquid interfacial adsorption and unfolding
Shearing	-Expose hydrophobic patches of protein
Pressurization	-Pressures > 100 MPa
Drying	-Loss of hydration layers disrupts protein structure

irradiation<sup>1.39</sup>, container/closure systems<sup>1.20,1.24,1.39-1.40</sup>, and leachables<sup>1.6,1.39</sup> can induce protein aggregation. Solution conditions including pH<sup>1.31,1.39-1.40</sup>, buffering agents,<sup>1.39-1.40</sup> protein concentration<sup>1.39-1.40</sup>, solution ionic strength<sup>1.31,1.39-1.40</sup>, and formulation excipients may influence protein aggregation.<sup>1.28,1.39-1.40</sup> Various processing steps may cause protein aggregation. These processing steps include

fermentation/expression, refolding, purification, freeze-thawing, shaking, shearing, pressurization, and drying.<sup>1.39</sup> Since proteins are structurally diverse, the relative effect of said factors on protein aggregation is protein-dependent.<sup>1.39</sup> What may be a stable formulation for one protein may be unstable for another protein. For this reason, there is no universal strategy to prevent or inhibit protein aggregation.<sup>1.39</sup>

## 1.6 CONFORMATIONAL STABILITY OF THERAPEUTIC PROTEINS EXPOSED TO INTERFACES

Proteins can undergo orientational and conformational rearrangement at interfaces.<sup>1.15</sup> Proteins that adsorb to hydrophobic surfaces and undergo appreciable conformational changes are referred to as “soft.”<sup>1.15,1.19</sup> Conversely, proteins that experience little structural change are referred to as “hard.”<sup>1.15,1.19</sup> Proteins tend to adsorb more extensively and irreversibly at hydrophobic surfaces than hydrophilic surfaces.<sup>1.15</sup> At hydrophobic interfaces, a greater degree of protein unfolding leads to displacement of vicinal solvent molecules and the formation of strong interfacial hydrophobic interactions.<sup>1.15</sup>

Protein conformational stability is highly surface and protein dependent.<sup>1.4, 1.13-1.14,1.26</sup> Upon adsorption, proteins can become “harder” or “softer.” Bee et al. found using front-face fluorescence quenching that HSA adsorbed to Alhydrogel® vaccine adjuvant particles became more structurally rigid.<sup>1.4</sup> In the same study, Förster Resonance Energy Transfer (FRET) was used to determine that adsorbed HSA reoriented on the surface of adjuvant but did not unfold.<sup>1.4</sup> Several studies have

been conducted to probe protein conformation at the air-water interface.<sup>1.26,1.32</sup> Using Infrared Reflection-Absorption Spectroscopy (IRRAS), Martin et al. and Schladitz et al. were able to identify changes in protein secondary structure upon adsorption.<sup>1.26,1.32</sup> It was found that some proteins underwent no change in secondary structure, some lost secondary structure, and some gained secondary structure as a result of surface-induced protein aggregation.<sup>1.26,1.32</sup>

Protein denaturation and aggregation at an interface can occur with or without applied stresses.<sup>1.13,1.26,1.32</sup> Soluble aggregates in bulk solution induced by protein adsorption to surfaces have been observed.<sup>1.1,1.5-1.7,1.17,1.34,1.36</sup> Tyagi et al. and Bee et al. showed that stainless steel micro- and nanoparticles served as heterogeneous nucleation sites for soluble homogeneous protein aggregate formation.<sup>1.6-1.7,1.36</sup> The results from Bee et al. suggested that aggregates observed in solution form after adsorption of protein multilayers.<sup>1.7</sup> Insoluble aggregates have been observed as a result agitation of the air-water interface<sup>1.1,1.17,1.34</sup> and the teflon-water interface.<sup>1.34</sup> Bee demonstrated that insoluble protein aggregates formed after compression of the air-water interface.<sup>1.5</sup> It was found that the rate of aggregate formation increased with increasing interfacial compression.<sup>1.5</sup> Bee also showed using air bubble tensiometry that relaxation of the adsorbed protein layer following compression of the air-water interface could be attributed to protein aggregation.<sup>1.3</sup> In addition, Fesinmeyer et al. and Bam et al. found that agitation-induced aggregation at the air-water interface was enhanced by anion binding<sup>1.17</sup> and reduced by Tween® 20<sup>1.1</sup>, respectively. Sluzky et al. concluded that perturbation of the air-water interface

coupled with surface activity at the teflon-water interface resulted in protein aggregation.<sup>1.34</sup>

Aggregation induced by protein adsorption to an interface is protein- and surface-dependent.<sup>1.1,1.3,1.5-1.8,1.17-1.18,1.20,1.23-1.24,1.34-1.36</sup> Numerous studies have found that protein adsorbed to an interface without forming soluble or insoluble protein aggregates in solution.<sup>1.6,1.8,1.18,1.20,1.23-1.24,1.35</sup> Bee et al. and Hoehne et al. showed that monoclonal antibodies adsorbed to glass<sup>1.6,1.20</sup>, cellulose<sup>1.6</sup>, Fe<sub>2</sub>O<sub>3</sub><sup>1.6</sup>, and tungsten<sup>1.8</sup> microparticles without forming homogeneous protein aggregates. The same finding was observed by Ludwig et al. and Gabrielson studying protein interactions with silicone oil emulsion.<sup>1.18, 1.24</sup>

## 1.7 PROBLEMS ASSOCIATED WITH PERTURBED PROTEIN CONFORMATION AND AGGREGATES

The main problems associated with the processing and storage of therapeutic protein formulations are loss of drug activity<sup>1.27,1.37</sup> or induction of an unwanted immune response.<sup>1.2,1.25,1.30</sup> The root-cause of these problems may be associated with changes in protein conformation or protein aggregation. As was previously discussed, non-native denatured or aggregated protein may result from interactions with various interfaces as well as factors such as temperature<sup>1.39-1.40</sup>, pH<sup>1.31,1.39-1.40</sup>, ionic strength<sup>1.31,1.39-1.40</sup>, processing<sup>1.39</sup>, etc. (see Table 1.2).

Loss of drug activity can jeopardize the proper treatment of a patient. Exposure of a protein drugs to contaminants such as steel<sup>1.6-1.7,1.36</sup>, tungsten<sup>1.8</sup>,

glass<sup>1.6,1.20</sup>, or silicone oil emulsion<sup>1.23-1.24,1.35</sup> can be problematic, as previously discussed. However, even common equipment used routinely in hospitals can pose problems. Studies have shown that silicone rubber tubing decreased interleukin-2 activity by 97%<sup>1.37</sup> and PVC infusion bags decreased the activity of Factor VIII by 42%.<sup>1.27</sup>

Another problem associated with protein therapeutics is the potential to induce unwanted immune responses.<sup>1.2,1.25,1.30</sup> Currently, while there are many standard assays to detect immune responses of protein drugs in patients, there is no way to predict how a patient will respond to a drug. There is a complex interplay between an individual's ability to mount an immune response versus that individual's ability to tolerate certain antigens.<sup>1.2</sup> At the moment, much more clinical data needs to be collected to know if it's even possible to predict or eliminate unwanted immunogenicity of drug products. To make this task more difficult, proteins can partially unfold or aggregate before and after delivery to a patient. Maas et al. performed a study that showed that misfolded proteins enhance protein immunogenicity.<sup>1.25</sup> Also, it has been shown that protein aggregates tend to be more potent than monomeric protein at eliciting responses from the immune system.<sup>1.30</sup> Factors influencing enhanced immune responses of protein aggregates include molecular weight, solubility, product origin, the presence of immunomodulatory contaminants, the presence of neoepitopes, heterogeneity in glycosylation patterns, and PEGylation.<sup>1.30</sup> The severity of a patient's immune response to a drug product is variable. Possible outcomes of unwanted immune responses include decreased drug



efficacy, generation of cross-reactive antibodies, anaphylactic shock, and injection site reactions.<sup>1,2, 1.25,1.3</sup>

## 1.8 THESIS OBJECTIVES

Pharmaceutical companies aim to develop safe, effective, and convenient delivery devices. The global market share of injectable drugs, representing about 24% of all routes of drug administration, is growing 10% annually.<sup>1.16</sup> Due to the conveniences offered as a means of storage prior to drug delivery to patients as well as compatibility with auto-injection devices that minimize handling procedures, 2.2 billion prefilled syringes were sold in 2007.<sup>1.29</sup> Silicone oil is a lubricant used in prefilled syringes to aid in plunger depression. Therapeutic proteins can be exposed to the silicone oil-water interface for the entire 18-24 shelf-life of a protein drug product. Currently, there is a dearth of published studies that aim to understand protein interactions with silicone oil contamination in pharmaceutical formulations.

Like previous studies, silicone oil emulsion was utilized in this study. In a typical 1 mL syringe, the maximum surface area of silicone oil that protein can interact with is roughly 10 cm<sup>2</sup>.<sup>1.24</sup> In addition, for a 1 mL syringe lubricated with less than 1.5 mg of silicone oil, about 30-40  $\mu$ g of silicone oil can be expelled in one drug dose.<sup>1.11-1.12</sup> Industrially relevant silicone oil concentrations and surface areas cannot be analyzed using conventional techniques. To overcome this, a silicone oil emulsion with a suitable concentration and total surface area was prepared in-house to be able to qualitatively and quantitatively assess protein-silicone oil interactions.

The overall goal of this work was to assess humanized monoclonal antibody interactions with silicone oil emulsion in the presence of 5 common pharmaceutical formulation excipients: Sodium chloride, sucrose, Tween® 20, Tween® 80, and poloxamer 188. In Chapter 2, it will be shown that human monoclonal antibodies adsorb to the silicone oil-water interface, may undergo conformational changes once adsorbed, and reduce the colloidal stability of silicone oil emulsion in formulations containing different excipients. In Chapter 3, the detection of protein adsorption and assessment of colloidal stability will be verified using a complementary technique. In Chapter 4, the competitive adsorption of protein and surfactant to this interface will be assessed. In addition, the formation of a protein-surfactant complex will be considered. Lastly, in Chapter 5, final conclusions will be summarized and future recommendations will be proposed.

## 1.9 REFERENCES

- 1.1 Bam, N.B., Cleland, J.L., Yang, J., Manning, M.C., Carpenter, J.F., Kelley, R.F., Randolph, T.W. (1998). "Tween Protects Recombinant Human Growth Hormone Against Agitation-Induced Damage Via Hydrophobic Interactions." J Pharm Sci. 87: 1554-1559.
- 1.2 Barbosa, M.D.F.S., Celis, E. (2007). "Immunogenicity of Protein Therapeutics and the Interplay between Tolerance and Antibody Responses." Drug Discovery Today. 12(15-16): 674-681.
- 1.3 Bee, J.S. (2009). "Bubble Tensiometry and Langmuir Trough Studies of a Monoclonal Antibody Adsorbed at the Air-Water Interface. In Effect of Interfaces and Shear on Therapeutic Protein Stability." Ph.D. Thesis: 237-254.

- 1.4 Bee, J.S. (2009). "Front-Face Fluorescence Quenching and FRET Techniques to Probe the Structure of a Protein Antigen Adsorbed to Vaccine Adjuvant. In Effect of Interfaces and Shear on Therapeutic Protein Stability." Ph.D. Thesis: 237-254.
- 1.5 Bee, J.S. 2009. "Interface Oscillations Provide Insight Into Protein Aggregate Particle Formation at the Air-Water Interface. In Effect of Interfaces and Shear on Therapeutic Protein Stability." Ph.D. Thesis: 200-236.
- 1.6 Bee, J.S., Chiu, D., Sawicki, S., Stevenson, J.L., Chatterjee, K., Freund, E., Carpenter, J.F., Randolph, T.W. (2009). "Monoclonal Antibody Interactions with Micro- and Nanoparticles: Adsorption, Aggregation, and Accelerated Stress Studies." J Pharm Sci. 98: 3218-3238.
- 1.7 Bee, J.S., Davis, M., Freund, E., Carpenter, J.F., Randolph, T.W. (2010). "Aggregation of Monoclonal Antibody Induced by Adsorption to Stainless Steel." Biotechnology and Bioengineering. 105(1): 121-129.
- 1.8 Bee, J.S., Nelson, S., Freund, E., Carpenter, J.F., Randolph T.W. (2009). "Precipitation of a Monoclonal Antibody by Soluble Tungsten." J Pharm Sci. 98: 3290-3301.
- 1.9 Beverung, C.J., Radke, C.J., Blanch, H.W. (1999). "Protein Adsorption at the Oil/Water Interface: Characterization of Adsorption Kinetics by Dynamic Interfacial Tension Measurements." Biophysical Chem. 81: 59-80.
- 1.10 Chang, D., Chang, R.K. (2007). "Review of Current Issues in Pharmaceutical Excipients." Pharmaceutical Technology. [Epub].
- 1.11 Chantelau, E.A., Berger, M. (1985). "Pollution of Insulin with Silicone Oil, a Hazard of Disposable Plastic Syringes." Lancet. 1: 1459.
- 1.12 Collier, F.C., Dawson, A.D. (1985). "Insulin syringes and Silicone Oil." Lancet. 2: 611.
- 1.13 de Jongh H.H.J., Wierenga, P.A. (2006). "Assessing the Extent of Protein Intermolecular Interactions at Air-Water Interfaces Using Spectroscopic Techniques." Biopolymers. 82: 384-389.
- 1.14 de Young, L.R., Fink, A.L., Dill, K.A. (1993). "Aggregation of Globular Proteins." Acc Chem Res. 26: 614-620.

- 1.15 Dickinson, E. (1999). "Adsorbed Protein Layers at Fluid Interfaces: Interactions, Structure, and Surface Rheology." Colloids and Surfaces B: Biointerfaces. 15: 161-176.
- 1.16 Eakins, M.N. (2008). "Offering a New Choice in Glass Pre-fillable Syringes." East Sussex, United Kingdom: ONdrugDelivery. pp 7-10.
- 1.17 Fesinmeyer, R.M., Hogan, S., Saluja, A., Brych, S.R., Kras, E., Narhi, L.O., Brems, D.N., Gokarn, Y.R. (2009). "Effect of Ions on Agitation- and Temperature-Induced Aggregation Reactions." Pharmaceutical Research. 26(4): 903-913.
- 1.18 Gabrielson, J. (2006). "Irreversible Association of Monoclonal Antibody with Silicone Oil in Aqueous Formulation Containing Sucrose and Surfactants. In Monoclonal Antibody Aggregation in Therapeutic Formulation: Size and Shape-Distribution Analysis." Ph.D. Thesis: 100-124.
- 1.19 Gajraj, A., Ofoli, R.Y. (2000). "Quantitative Technique for Investigating Macromolecular Adsorption and Interactions at the Liquid-Liquid Interface." Langmuir. 16: 4279-4285.
- 1.20 Hoehne, M., Samuel, F., Dong, A., Wurth, C., Mahler, H., Carpenter, J.F., Randolph, T.W. (2010). "Adsorption of Monoclonal Antibodies to Glass Microparticles". J Pharm Sci. 1: 1-10.
- 1.21 Honciuc, A., Baptiste, D., Campbell, I.P., Schwartz, D.K. (2009). "Solvent Dependence of the Activation Energy of Attachment Determined by Single Molecule Observations of Surfactant Adsorption." Langmuir. 25(13): 7389-7392.
- 1.22 Janeway, C.A., Travers, P.A., Walport, M. (2001). Immunobiology. New York: Garland Publishing.
- 1.23 Jones, L.S., Kaufmann, A., Middaugh, C.R. (2005). "Silicone Oil Induced Aggregation of Proteins." J Pharm Sci. 94: 918-927.
- 1.24 Ludwig, D.B., Carpenter, J.F., Hamel, J., Randolph, T.W. (2009). "Protein Adsorption and Excipient Effects on Kinetic Stability of Silicone Oil Emulsions." J Pharm Sci. 99: 1721-1733.
- 1.25 Maas, C., Hermeling, S., Bouma, B., Jiskoot, W., Gebbink, M.F.B.G. (2007). "A Role for Protein Misfolding in Immunogenicity of Biopharmaceuticals." J Biological Chemistry. 282(4): 2229-2236.

- 1.26 Martin, A.H., Meinders, M.B.J., Bos, M.A., Stuart, M.A.C., van Vliet, T. (2003). "Conformational Aspects of Proteins at the Air/Water Interface Studied by Infrared Reflection-Absorption Spectroscopy." Langmuir. 19: 2922-2928.
- 1.27 Mcleod, A.G., Walker, I.R., Zheng, S., Hayward, C.P.M. (2000). "Loss of Factor VIII Activity During Storage in PVC Containers due to Adsorption." Haemophilia. 6: 89.
- 1.28 Pifferi, G., Restani, P. (2003). "The Safety of Pharmaceutical Excipients." Il Farmaco. 58: 541-550.
- 1.29 Romacker, M., Schoenknecht, T., Forster, R. (2008). "The Rise of Prefilled Syringes from Niche Product to Primary Container of Choice: A Short History. East Sussex, United Kingdom: ONdrugDelivery. pp 4-5.
- 1.30 Rosenberg, A.S. (2006). "Effects of Protein Aggregates: An Immunologic Perspective." The AAPS Journal. 8(3): E501-E507.
- 1.31 Sahin, E., Adeola, A.O., Perkins, M.D., Roberts, C.J. (2010). "Comparative Effects of pH and Ionic Strength on Protein-Protein Interactions, Unfolding, and Aggregation for IgG1 Antibodies." J Pharma Sci. 99(12): 4830-4848.
- 1.32 Schladitz, C., Vieira, E.P., Hermel, H., Mohwald, H. (1999). "Amyloid- $\beta$ -Sheet Formation at the Air-Water Interface." Biophysical Journal. 77: 3305-3310.
- 1.33 Seneviratne, A.K. (2010). "Visible Particles in Protein Therapeutics: Physical Nature, Origin, Detection, and Solutions." 2010 AAPS National Biotechnology Conference, May 16-19, San Francisco.
- 1.34 Sluzky, V., Tamada, J.A., Klibanov, A.M., Langer, R. (1991). "Kinetics of Insulin Aggregation in Aqueous Solutions Upon Agitation in the Presence of Hydrophobic Surfaces." Applied Biological Sciences. 88: 9377-9381.
- 1.35 Thirumangalathu, R., Krishnan, S., Speed Ricci, M., Brems, D.N., Randolph, T.W., Carpenter, J.F. (2009). Silicone Oil- and Agitation-Induced Aggregation of a Monoclonal Antibody in Aqueous Solution. J Pharm Sci. 98: 3167-3181.
- 1.36 Tyagi, A.K., Randolph, T.W., Dong, A., Maloney, K.M., Hitscherich, C., Carpenter, J.F. (2009). "IgG Particle Formation during Filling Pump Operation: A Case Study of Heterogeneous Nucleation on Stainless Steel Nanoparticles." J Pharm Sci. 98: 94-104.

- 1.37 Tzannis, S.T., Hrushesky, W.J.M., Wood, P.A., Przybycien, T.M. (1997). "Adsorption of a Formulated Protein on a Drug Delivery Device Surface." J Colloid Interface Sci. 189: 216-228.
- 1.38 Walder, R., Schwartz, D.K. (2010). "Single Molecule Observations of Multiple Populations at the Oil-Water Interface." Langmuir. 26(16): 13364-13367.
- 1.39 Wang, W., Nema, S., Teagarden, D. (2010). "Protein Aggregation: Pathways and Influencing Factors." International J Pharmaceutics. 390: 89-99.
- 1.40 Wang, W., Singh, S., Zeng, D.L., King, K., Nema, S. (2007). "Antibody Structure, Instability, and Formulation." J Pharma Sci. 96(1): 1-26.
- 1.41 2005. Mimetibody.com. Online posting. December 15, 2010 <<http://mimetibody.com>>.
- 1.42 2010. abcam. Online posting. December 15, 2010 <<http://www.abcam.com/ps/CMS/Images/abstructure.jpg>>.

## CHAPTER 2: EXCIPIENT EFFECTS OF HUMANIZED MONOCLONAL ANTIBODY INTERACTIONS WITH SILICONE OIL EMULSION

### 2.1 INTRODUCTION

Therapeutic proteins are a growing class of drug products. A convenient strategy to deliver these drugs to patients is to administer them in a liquid formulation using prefilled glass syringes. In order to provide smooth plunger action and enhance compatibility with autoinjector devices, glass syringes typically must be lubricated by application of silicone oil to the syringe barrels. Because prefilled syringes act as both the delivery device and as a storage container, proteins formulated in prefilled syringes may be exposed to the silicone oil-water interface for the entire 18-24 month shelf-life.

Silicone oil contamination in insulin formulations was first documented twenty-five years ago in reports that found that contamination up to 0.25 mg/mL of silicone oil in a 10 mL insulin vial was possible when a standard filling procedure for siliconized syringes was followed.<sup>2,9,2,10</sup> More recently, several studies have been conducted to assess the behavior of proteins exposed to silicone oil. Jones et al. showed that silicone oil emulsions induced aggregation of ribonuclease A, lysozyme, bovine serum albumin, and concanavalin A.<sup>2,30</sup> Similarly, Thirumangalathu et al. found that an IgG1 antibody aggregated in the presence of silicone oil emulsion when agitated.<sup>2,49</sup> Ludwig et al. examined the effects of adsorption of BSA, lysozyme, abatacept, and trastuzumab to the silicone oil-water interface by

assessing the kinetic stability of silicone oil emulsions in the presence of excipients.<sup>2,33</sup> In a comparability study, Lubiniecke et al. observed that a monoclonal antibody drug product exhibited greater levels of particles >10  $\mu\text{m}$ , particles >25  $\mu\text{m}$ , and turbidity levels after storage in prefilled glass syringes as compared to storage in glass vials.<sup>2,32</sup> Despite these efforts, the interaction of proteins with the silicone oil-water interface still remains poorly understood.

In this work, we examined the adsorption of three human IgG1 monoclonal antibodies to the surfaces of silicone oil microdroplets in the presence of various excipients. In order to better resolve effects of silicone oil-water interfaces, an “accelerated” approach was chosen wherein proteins were exposed to silicone oil microdroplets in emulsions that presented roughly 100 to 1000 times the interfacial area to which proteins may be exposed within a prefilled syringe.

Protein-silicone oil interactions were assessed in the presence of three common pharmaceutical formulation excipients: sodium chloride, sucrose, and Tween® 20. Sodium chloride increases the ionic strength in solution, which serves to reduce electrostatic interactions via charge shielding.<sup>2,7,2,28</sup> Sucrose is a preferentially excluded co-solute that increases native protein conformational stability.<sup>2,48</sup> Lastly, Tween® 20 is a surfactant that is anticipated to compete with proteins for adsorption sites at silicone oil-water interfaces.<sup>2,17,2,33-2,34</sup> The goals of this work were to compare the behavior of three humanized monoclonal antibodies at the silicone oil-water interface, to determine whether silicone oil emulsion induces



homogeneous protein aggregation in solution, and to observe how different formulation excipients affect the colloidal stability of silicone oil emulsions.

## 2.2 MATERIALS AND METHODS

### 2.2.1 Proteins

Three recombinant humanized monoclonal antibodies (referred to as humAb 1, humAb 2, and humAb 3; these are the same antibodies whose adsorption behavior on glass microparticle surfaces was described previously<sup>2,26</sup> were manufactured and provided by F. Hoffmann-La Roche Ltd. (Basel, Switzerland). humAb 1 and humAb 2 are humanized IgG from Chinese hamster ovary (CHO) cells and humAb 3 is humanized IgG from mouse cells. Each humAb is glycosylated. humAb 1 and humAb 2 were provided as frozen liquid formations of 89.1 mg/mL and 10.26 mg/mL, respectively, and stored at -80°C. humAb 3 was provided as a liquid formulation of 10.30 mg/mL and stored at 2-8°C. humAb 1, humAb 2, and humAb 3 were formulated in 20 mM L-histidine at pH 5.5, 20 mM L-histidine/histidine-HCl at pH 6.0 containing 240 mM trehalose and 0.02% (w/v) Tween® 20, and 25 mM sodium acetate at pH 6.0 containing 125 mM sodium chloride, respectively. Additional information about each humAb is summarized in Table 2.1.

### 2.2.2 Buffer Conditions

Each humAb was dialyzed into 10 mM L-histidine at pH 6.0 containing 0.01% (w/v) sodium azide (hereafter denoted as “buffer”) using 10,000 MWCO Pierce Slide-

TABLE 2.1. Summary of some physical properties of each humAb

	Molecular Weight (Da)	Extinction Coefficient at 280 nm (cm <sup>2</sup> /mg)	Isoelectric Point (Calculated)
humAb 1	146,243	1.40	9.0-10.0
humAb 2	145,996	1.49	8.8-8.9
humAb 3	152,942	1.57	9.3

A-Lyzer cassettes (Thermo Scientific, Rockford, IL). Using the appropriate extinction coefficient at 280 nm (see Table 2.1), protein concentrations were determined using a PerkinElmer Lambda 35 spectrophotometer (Wellesley, MA). The final concentration of protein in the stock solutions was adjusted to 5 mg/mL after dilution using buffer. Three excipient conditions were studied. These buffers contained 140 mM sodium chloride, 240 mM sucrose, or 0.03% (w/v) Tween® 20. All buffers were prepared using distilled deionized water and filtered using 0.22  $\mu$ m pore-size filters (Millipore Corp., Billerica, MA). All chemicals used were reagent grade or higher quality.

### 2.2.3 Preparation of Silicone Oil Emulsion

0.5-1.0% (v/v) silicone oil in water emulsions of medical grade 1000 cSt silicone oil (Dow Corning 360, Midland, MI) were prepared using a combination of mechanical mixing and high-pressure homogenization.<sup>2,33</sup> A 100 mL suspension of 5% (v/v) silicone oil in water was prepared by mixing silicone oil and water in a stainless steel cylinder at room temperature using a 20 mm shaft rotor/stator (The

VirTis Co., Warminster, PA, Virtisshear Mechanical Homogenizer) for 15 minutes at 5000 rpm. Immediately following mixing, the suspension was passed eight times through a high-pressure homogenizer (Avestin Inc., Ottawa, Ontario, Canada, Emulsiflex C5 Homogenizer) operating such that the pressure oscillated from 20-40 kpsi. The final silicone oil emulsion was collected and stored in a 125 mL glass bottle. The difference between the initial and final silicone oil concentrations in emulsion was due to phase separation in the sample chamber prior to passage through the homogenizer.

#### 2.2.4 Concentration of Silicone Oil in Emulsion

The concentration of silicone oil suspended in the emulsions was determined using a combination of liquid-liquid extraction and infrared absorbance.<sup>2,33</sup> A 1 mL aliquot of a 1:1 mixture of silicone oil emulsion and 0.5 M sodium chloride was added to 1 mL of n-hexane in a glass test tube. This mixture was mixed for 1 minute by vortexing and centrifuged at 1500g for 1 hour. The efficiency of extraction of silicone oil from water to n-hexane was improved by increasing the ionic strength of the aqueous phase (data not shown). Silicone oil has a characteristic absorbance at 1260  $\text{cm}^{-1}$  due to its Si-CH<sub>3</sub> moieties.<sup>2,23</sup> The infrared absorbance at 1260  $\text{cm}^{-1}$  of silicone oil in n-hexane was measured using a Bomem MB154S (Quebec, QC, Canada) Fourier Transform Infrared (FT-IR) Spectrometer equipped with a Pike MIRacle™ (Madison, WI) attenuated total reflection sampling accessory containing a ZnSe crystal plate. The area of the peak at 1260  $\text{cm}^{-1}$  was determined by

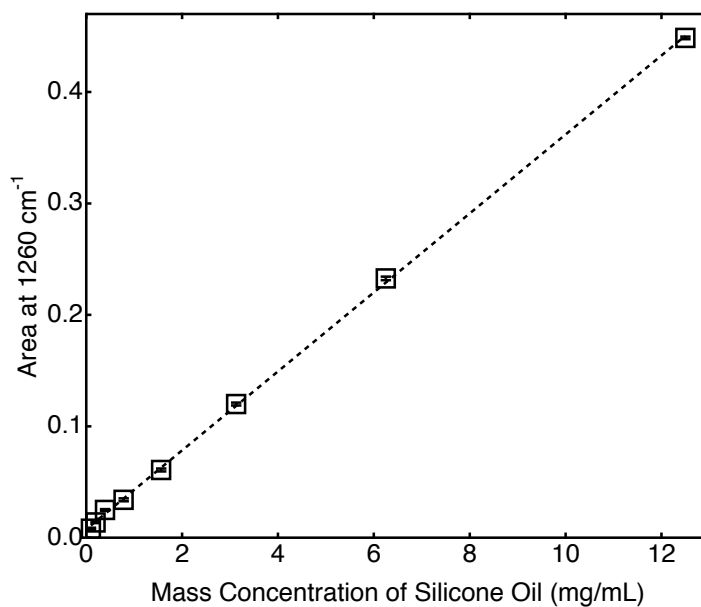


FIGURE 2.1. Standard curve showing the area of the peak at  $1260\text{ cm}^{-1}$  as a function of mass concentration of silicone oil in n-hexane. The area of the peak at  $1260\text{ cm}^{-1}$  was determined from  $1245\text{ cm}^{-1}$  to  $1275\text{ cm}^{-1}$ . This area was determined for silicone oil concentrations of 12.5, 6.25, 3.13, 1.56, 0.781, 0.391, 0.195, 0.0977 mg/mL in n-hexane. The dotted line is a linear fit of the data. The equation of this line is  $y = 0.036x$  with an  $R^2$  value of 0.99. Data represents the arithmetic mean of three replicate samples. Error bars represent the standard error of the mean.

integrating the signal from  $1245\text{ cm}^{-1}$  to  $1275\text{ cm}^{-1}$ . In order to determine the concentration of silicone oil in n-hexane from the area under the peak at  $1260\text{ cm}^{-1}$ , a standard curve was constructed. The area under the peak at  $1260\text{ cm}^{-1}$  (y-axis) for known concentrations of silicone oil in n-hexane (x-axis) was plotted and fitted to the line  $y = 0.036x$  with  $R^2 = 0.99$  (Figure 2.1).

### 2.2.5 Particle Size Distribution of Silicone Oil Emulsion

The particle size distribution of silicone oil droplets in emulsion was measured by laser diffraction analysis using a Beckman Coulter LS230 (Fullerton, CA). Scattering of silicone oil droplets assumed to be spheres was assessed using a

refractive index of silicone oil of 1.4046 provided by the manufacturer.<sup>2,55</sup> The particle size distributions obtained were reported as a number or surface area percent versus particle diameter.

The total surface area of silicone oil in emulsion was determined from the particle size distribution obtained from the aforementioned analysis. The total number of particles per volume analyzed,  $N$ , was determined from mass balance according to Equation 1.

$$N \sum_i^b \left( \frac{4}{3} \pi r_i^3 n_i \right) = V \quad (1)$$

where  $b$  is the number of bins describing the size distribution,  $r_i$  is the radius of a silicone oil droplet in bin  $i$ ,  $n_i$  is the number percent in bin  $i$ , and  $V$  is the volume of silicone oil analyzed determined using the mass concentration of silicone oil in emulsion and a density of silicone oil of 0.972 g/mL (supplied by the manufacturer).<sup>2,55</sup> The total number of particles per volume analyzed was typically on the order of  $10^{11}$  droplets. Using this value, the surface area of particles in each bin was calculated and summed over all bins to yield the total surface area of silicone oil droplets in emulsion per volume of solution.

### 2.2.6 Silicone Oil-Induced humAb Loss from Solution

Samples were prepared by mixing silicone oil emulsion, 2 mg/mL stock humAb solution, and 6X buffer (in that order) in 15 mL polypropylene falcon tubes. Control samples containing water instead of silicone oil emulsion were also

prepared. The final humAb concentration in each sample was 0.2 mg/mL in buffer. Samples and control samples were incubated statically at room temperature ( $23^{\circ}\text{C} \pm 2^{\circ}\text{C}$ ) for 30 minutes, 3 days, 1 week, 2 weeks, or 1 month. After each incubation period, 0.35 mL of sample and control were centrifuged at 18,000g for 15 minutes to separate silicone oil and protein adsorbed to silicone oil droplets from the aqueous supernate. The absorbance of protein at 280 nm in the supernate was measured using size exclusion high-performance liquid chromatography (SE-HPLC). SE-HPLC analysis was conducted using a Beckman Coulter System Gold equipped with 126 pump (Beckman Coulter Inc., Fullerton, CA), a Waters 717 Plus autosampler (Waters Corp., Milford, MA), and 168 UV detector (Beckman Coulter Inc., Fullerton, CA). Studies were conducted using a TSK-GEL G3000SW<sub>XL</sub> column (TOSOH Biosciences, Montgomeryville, PA). The mobile phase was a 0.2 M potassium phosphate buffer at pH 7.0 containing 0.25 M KCl and 0.01% (w/v) sodium azide that ran at a flow rate of 0.5 mL/min. 75  $\mu\text{L}$  of sample was injected per run. The absorbance of eluate from the column was used to determine the mass of humAb eluted using the appropriate extinction coefficient (see Table 2.1). To determine the mass of humAb lost from solution, the mass of humAb eluted from samples containing silicone oil emulsion was subtracted from the mass of humAb eluted from samples containing no silicone oil. These values were normalized by the dividing by the initial silicone oil surface area per volume of the emulsion.

### 2.2.7 humAb Conformation at the Silicone Oil-Water Interface

Tertiary structure of humAb molecules adsorbed to silicone oil-water interfaces was probed using tryptophan fluorescence quenching. Tryptophan residues of adsorbed protein were excited at 295 nm using an SLM-Aminco Spectrofluorometer (SLM-Aminco, Urbana, IL) in front-face geometry using a custom-built cuvette holder rotated 53° from the excitation beam. Samples were prepared by mixing 9 mL of silicone oil emulsion with appropriate amounts of 5 mg/mL stock humAb solution and 4X buffer (in that order) in 15 mL polypropylene falcon tubes such that the amount of protein not adsorbed to the silicone oil-water interface was minimized. Samples were incubated statically for at least 2 hours at room temperature ( $23^{\circ}\text{C} \pm 2^{\circ}\text{C}$ ). Freshly prepared 7.6 M acrylamide solution was used as a quenching agent. Spectra were recorded after each addition of acrylamide. A total of four aliquots of acrylamide were added to each sample until the final acrylamide concentration was approximately 0.25 M. Fluorescence intensities were recorded from 300 nm to 380 nm at a scan rate of 0.95 nm/s. Spectra were recorded at room temperature ( $23^{\circ}\text{C} \pm 2^{\circ}\text{C}$ ). Tryptophan emission fluorescence was monitored at 328 nm. Raw fluorescence intensities were corrected for dilution after addition of each aliquot of acrylamide and the inner-filter effect resulting from absorption of acrylamide at 295 nm. The relationship between corrected fluorescence intensity values and acrylamide concentration was assessed using the Stern-Volmer equation<sup>2.18-2.19</sup>:

$$\frac{F_o}{F} = 1 + K_{SV}[Q] \quad (2)$$

where  $F_o$  is the initial fluorescence intensity,  $F$  is the fluorescence intensity at a particular quencher concentration,  $[Q]$  is the quencher concentration, and  $K_{SV}$  is the Stern-Volmer constant. This fit was linear ( $R^2$  values ranging from 0.992 to 0.998) through five points for acrylamide concentrations ranging from 0 to 0.25 M. Blank corrections were made by subtracting the spectra of corresponding humAb-free samples.

### 2.2.8 Colloidal Stability

The colloidal stability of humAbs and silicone oil emulsions were assessed using laser Doppler velocimetry. A Malvern Zetasizer Nano ZS (Worcestershire, United Kingdom) was used to measure the electrophoretic mobility of protein and silicone oil dispersions in an applied electric field. The zeta potential was calculated from Henry's equation using the Smoluchowski approximation valid at ionic strengths greater than 1 mM<sup>2,20</sup>:

$$\mu_e = \frac{2\varepsilon k_s \zeta}{3\eta} \quad (3)$$

$\mu_e$  is the electrophoretic mobility,  $\varepsilon$  is the dielectric constant of the solution,  $k_s = 1.5$  is a model-based constant,  $\eta$  is the solution viscosity, and  $\zeta$  is the zeta potential. The viscosity of solution was assumed to be that of water for all buffer conditions except when the formulation contained sucrose. Viscosities for sucrose solutions were



obtained from ISCO tables.<sup>2,25</sup> Samples were prepared by mixing silicone oil emulsion, 2 mg/mL protein, and 6X buffer (in that order) in 1.5 mL polypropylene microcentrifuge tubes. The final protein concentration in each sample was 0.2 mg/mL in buffer. Samples were incubated statically at room temperature ( $23^{\circ}\text{C} \pm 2^{\circ}\text{C}$ ) for 30 minutes, 3 days, 1 week, 2 weeks, or 1 month. After incubation, a 20:1 dilution of silicone oil emulsion in the appropriate buffer was prepared and 0.8 mL of diluted sample was analyzed using a disposable capillary zeta potential cell equipped with gold electrodes (Malvern Instruments Ltd., Worcestershire, United Kingdom).

To investigate the effect of electrostatics in particle interactions, Derjaguin-Landau-Verwey-Overbeek (DLVO) theory was invoked. The total interaction potential between two spheres of unequal radii encompassing both van der Waals attractive forces and electrostatic double layer repulsive forces is given as<sup>2,6,2,27</sup>:

$$W(D) = \frac{\epsilon r_1 r_2 (\psi_1^2 + \psi_2^2)}{4(r_1 + r_2)} \left[ \frac{2\psi_1 \psi_2}{\psi_1^2 + \psi_2^2} \ln\left(\frac{1 + e^{-\kappa D}}{1 - e^{-\kappa D}}\right) + \ln(1 - e^{-2\kappa D}) \right] - \frac{A_H r_1 r_2}{6(r_1 + r_2)D} \quad (4)$$

where  $\epsilon$  is the dielectric constant of the dispersant phase,  $r$  is the particle radius,  $\psi$  is the surface potential,  $\kappa$  is the inverse Debye length,  $D$  is the interparticle separation distance, and  $A_H$  is the Hamaker constant which is approximately  $5 kT$  for proteins.<sup>2,37</sup> For the analysis in this study, the zeta potential was substituted for the surface potential.

### 2.2.9 Fluorescence-Activated Particle Analysis

humAbs were fluorescently labeled with Alexa Fluor® 647 (Invitrogen Corp., Carlsbad, CA). Alexa Fluor® 647 is a bright and photostable dye with absorption and fluorescence maxima of approximately 650 nm and 668 nm, respectively.<sup>2,56</sup> In addition, Alexa Fluor® 647 is pH insensitive between 4 and 10 and resistant to quenching at high degrees of substitution.<sup>2,56</sup> Each humAb was dialyzed into phosphate-buffered saline (PBS) and diluted to 2 mg/mL. A 0.5 mL aliquot of 2 mg/mL humAb solution in PBS was incubated with Alexa Fluor® 647 dye for 1 hour with gentle stirring. Alexa Fluor® 647 dye has a succinimidyl ester moiety that reacts efficiently with primary amines of a protein.<sup>2,56</sup> For this reason, conjugation cannot proceed in buffer containing L-histidine. Immediately after the labeling reaction, labeled humAb was separated from unreacted dye molecules using a 30,000 MW size-exclusion resin (Invitrogen Corp., Carlsbad, CA) in PBS at pH 7.2 containing 2 mM sodium azide. The concentration of labeled humAb was determined using Equation 5:

$$c_{protein} = \frac{(A_{280} - CF \cdot A_{650})DF}{\epsilon_{protein}} \quad (5)$$

where  $A_{280}$  is the absorbance at 280 nm,  $A_{650}$  is the absorbance at 650 nm,  $\epsilon_{protein}$  is the extinction coefficient at 280 nm (see Table 2.1),  $CF = 0.03$  is a correction factor that accounts for the contribution of Alexa Fluor® 647 to the absorbance at 280 nm, and  $DF$  is a dilution factor. The degree of labeling was determined using Equation 6:

$$DOL = \frac{A_{650}DF}{\varepsilon_{dye}c_{protein}} \quad (6)$$

where  $\varepsilon_{dye} = 239,000 \text{ cm}^{-1} \text{ M}^{-1}$  is the molar extinction coefficient of Alexa Fluor® 647 dye. The degree of labeling for humAb 1, humAb 2, and humAb 3 was  $6.96 \pm 0.01$ ,  $7.18 \pm 0.01$ , and  $7.98 \pm 0.01$  moles of dye per mole of protein, respectively. Prior to use, labeled humAb was dialyzed into 10 mM L-histidine at pH 6.0 containing 0.01% (w/v) sodium azide and stored protected from ambient light.

Silicone oil was stained with 4,4-difluoro-1,3,5,7,8-pentamethyl-4-bora-3a,4a-diaza-s-indacene (BODIPY® 493/503).<sup>2,34</sup> BODIPY® 493/503 was chosen because it is a nonpolar, electrically neutral molecule that is highly soluble in silicone oil.<sup>2,34</sup> This dye has absorption and fluorescence maxima of approximately 488 nm and 515 nm, respectively.<sup>2,57</sup> BODIPY® 493/503 was dissolved in 2 mL of dimethylsulfoxide (DMSO) at a concentration of 2.5 mg/mL. A 10 mL aliquot of silicone oil was dissolved in 40 mL of dichloromethane (DCM). After complete dissolution of BODIPY® 493/503 and silicone oil into their respective solvents, 800  $\mu\text{L}$  of BODIPY® 493/503-DMSO solution was added to the silicone oil-DCM solution and mixed for 1 hour at room temperature. Immediately following mixing, DMSO and DCM were removed using a Laborota 4000eco rotary evaporator (Heidolph-Brinkmann, Elk Grove Village, IL). About 80% percent of labeled silicone oil was recovered.

Emulsions of labeled silicone oil were created as described above. Samples were prepared by mixing labeled silicone oil emulsion, 0.1 mg/mL labeled protein, and 6X buffer (in that order) in 2 mL polypropylene microcentrifuge tubes. The final protein concentration in each sample was 0.01 mg/mL in buffer. Samples were incubated statically at room temperature ( $23^{\circ}\text{C} \pm 2^{\circ}\text{C}$ ) for 30 minutes, 3 days, 1 week, 2 weeks, or 1 month. After incubation, 200  $\mu\text{L}$  of sample was analyzed using a BD FACSCalibur<sup>TM</sup> instrument (Becton Dickinson and Co. Biosciences, San Jose, CA) equipped with a 488 nm blue argon laser, 635 nm red diode laser, four fluorescence detectors (FL1 530/30, FL2 585/42, FL3 670LP, and FL4 661/16), and 488 nm forward and 90° side light scattering detectors. The fluorescence intensities of Alexa Fluor® 647 and BODIPY® 493/503 for 30,000 particles were plotted. The data were fit to Equation 7:

$$I_{AF-647} = A(\Gamma)I_{BODIPY}^v \quad (7)$$

where  $I_{AF-647}$  is the fluorescence intensity of protein labeled with Alexa Fluor® 647,  $I_{BODIPY}$  is the fluorescence intensity of silicone oil droplets labeled with BODIPY® 493/503,  $A(\Gamma)$  is a constant, and  $v$  is a scaling exponent. Sheath fluid matching the formulation buffer was used to dilute samples.

### 2.2.10 Light Microscopy

Silicone oil emulsion stability in the presence of humAbs was assessed visually using light microscopy. Droplets were imaged at 400X using an Eclipse

TE300 inverted optical microscope (Nikon Instruments Inc., Melville, NY) with a SPOT™ RT-KE CCD camera (Sterling Heights, MI). Samples were prepared by mixing silicone oil emulsion, 2 mg/mL protein, and 6X buffer (in that order) in 2 mL polypropylene microcentrifuge tubes. The final protein concentration in each sample was 0.2 mg/mL in buffer. Samples were incubated statically at room temperature ( $23^{\circ}\text{C} \pm 2^{\circ}\text{C}$ ) for 1 month.

#### 2.2.11 Statistical Analysis

In this work, averaged values are reported with standard errors about the mean. Also, student's t-test was used to obtain a p-value that was used to assess statistically significant differences observed between data sets. A p-value less than 0.05 indicated that data sets were statistically different.

## 2.3 RESULTS

#### 2.3.1 Characterization of Silicone Oil Emulsion

From analysis of the peak at  $1260\text{ cm}^{-1}$  using ATR-FTIR, the mass concentration of silicone oil in the emulsion was found to be  $6.90 \pm 0.82\text{ mg/mL}$ , or  $0.71 \pm 0.08\%$  (v/v).

Silicone oil emulsion particle size distributions were assessed as both number- and surface area-weighted distributions (Figure 2.2). The majority of silicone oil droplets were about  $0.1\text{ }\mu\text{m}$  in diameter (Figure 2.2A). A small minority of larger droplets were present as was evident from the surface area-weighted particle size

distribution. This distribution exhibited a bimodal distribution with maxima at roughly  $0.1\ \mu\text{m}$  and  $1.7\ \mu\text{m}$  (Figure 2.2B). Analysis of these particle size distributions revealed that 1 mL of silicone oil emulsion had a total surface area of  $330 \pm 40\ \text{cm}^2$ .

### 2.3.2 Silicone Oil-Induced humAb Loss from Solution

After 1 month of static incubation at room temperature, SE-HPLC analysis of samples containing humAbs 1-3 and silicone oil emulsion provided no evidence that soluble protein aggregates ( $< 1,000\ \text{kDa}$ ) formed as a result of protein-silicone oil interactions under static conditions. No aggregate peaks were observed in any of the chromatograms obtained (Figure 2.3). Accordingly, after a rapid initial loss of protein from solution due to adsorption to silicone oil droplets, there was no

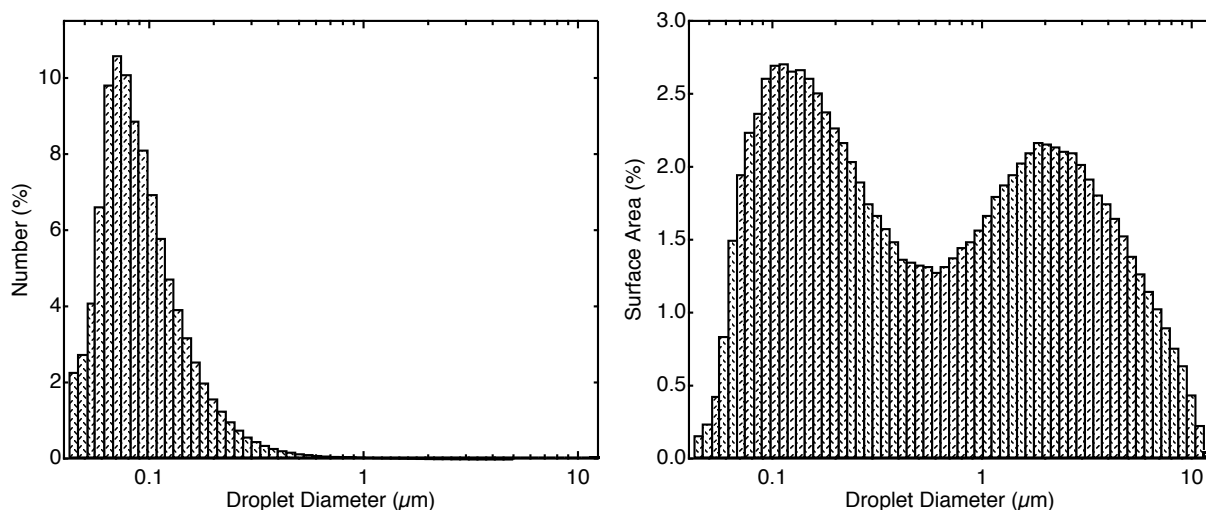


FIGURE 2.2. Representative particle size distributions of silicone oil emulsion prepared in water. Droplet diameters are grouped into bins and represented as a percent of the total number of droplets analyzed. (A) Percent number particle size distribution. (B) Percent surface area particle size distribution.

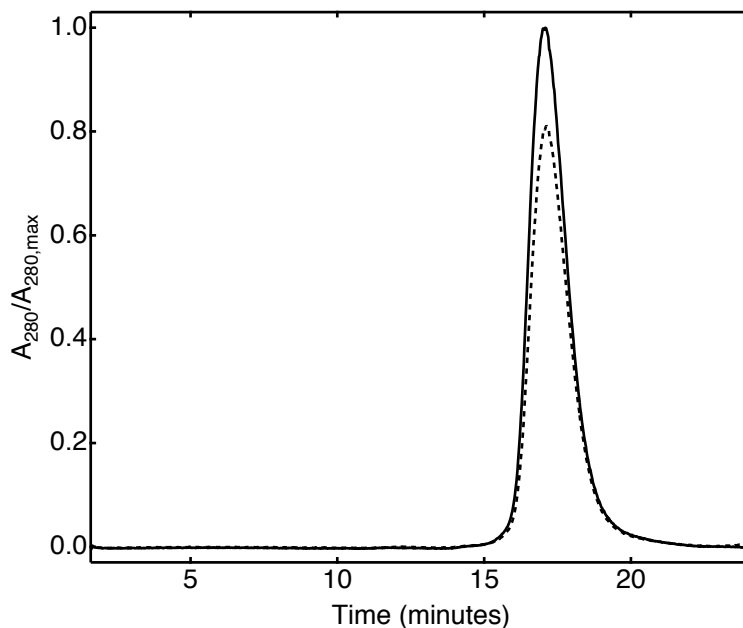


FIGURE 2.3. Representative chromatograms from SE-HPLC. A control that was not incubated with silicone oil emulsion is represented by the solid line. A sample that was incubated with silicone oil emulsion is represented by the dashed line. There is a peak at roughly 17 minutes that corresponds to native humAb monomers. The formation of small homogeneous protein aggregates would appear at times before the monomer peak.

noticeable decrease in the mass of monomeric protein with time. In addition, there was no visible evidence of the formation of insoluble protein aggregates. In the absence of formulation excipients, silicone oil-induced protein loss from solution varied for each humAb such that humAb 1 < humAb 3 < humAb 2 (Figure 2.4). These differences were statistically significant ( $p < 0.05$ ). Although the amount of protein lost from solution varied for the three humAbs investigated, the same trend in the presence of different formulation excipients was exhibited. For formulations containing sodium chloride, the silicone oil-induced protein loss from solution was greater than for formulations containing no excipients. This difference was statistically significant for humAb 1 and humAb 3 ( $p < 0.05$ ) but not statistically

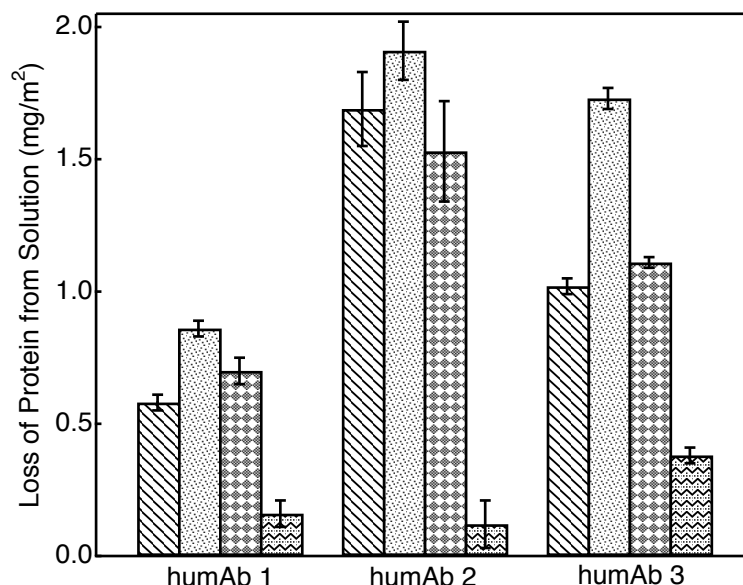


FIGURE 2.4. Loss of protein from solution after incubation of humAbs with silicone oil emulsion for 72 hours. Data for humAb 1, humAb 2, and humAb 3 are labeled accordingly. For each protein, there are four bars representing different excipient conditions: 10 mM L-histidine at pH 6.0 containing 0.01% (w/v) sodium azide, 10 mM L-histidine at pH 6.0 containing 0.01% (w/v) sodium azide and 140 mM sodium chloride, 10 mM L-histidine at pH 6.0 containing 0.01% (w/v) sodium azide and 240 mM sucrose, 10 mM L-histidine at pH 6.0 containing 0.01% (w/v) sodium azide and 0.03% (w/v) Tween® 20. Data represents the arithmetic mean of three replicate samples. Error bars represent the standard error of the mean.

significant for humAb 2 ( $p > 0.05$ ). For formulations containing sucrose, differences from values obtained for formulations containing no excipients were not statistically significant for humAbs 1-3 ( $p > 0.05$ ). Lastly, for formulations containing Tween® 20, silicone oil-induced protein loss from solution was less than that of formulations containing no excipients. These differences were statistically significant for humAbs 1-3 ( $p < 0.05$ ).

### 2.3.3 humAb Conformation at the Silicone Oil-Water Interface

Over the range of acrylamide concentrations tested, Stern-Volmer plots for each of the proteins were linear, with a  $R^2$  value of ca. 0.99 (Figure 2.5). Front-face



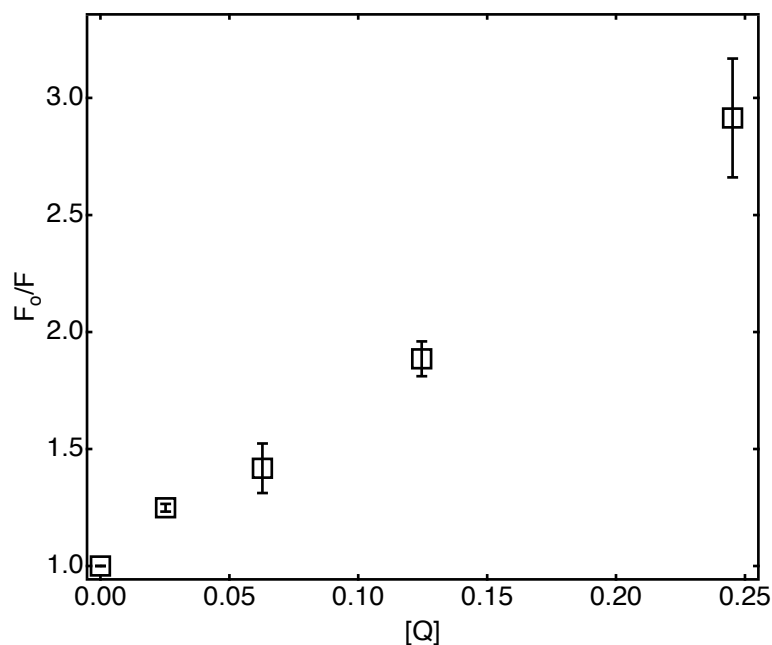


FIGURE 2.5. Representative Stern-Volmer plot obtained from front-face fluorescence quenching. These plots were linear with an  $R^2$  of ca. 0.99. Data represents the arithmetic mean of three replicate samples. Error bars represent the standard error of the mean.

fluorescence quenching revealed that protein adsorbed to the silicone oil-water interface had increased tryptophan exposure to acrylamide, perhaps indicative of conformationally perturbed protein (Figure 2.6). In formulations containing humAb 1 and humAb 2, differences between Stern-Volmer constants of adsorbed protein and unfolded protein were not statistically significant ( $p > 0.05$ ). However, this difference for humAb 3 was statistically significant ( $p < 0.05$ ). For each humAb, there was not a statistically significant difference between formulations containing sodium chloride or sucrose and formulations containing no excipients ( $p > 0.05$ ).

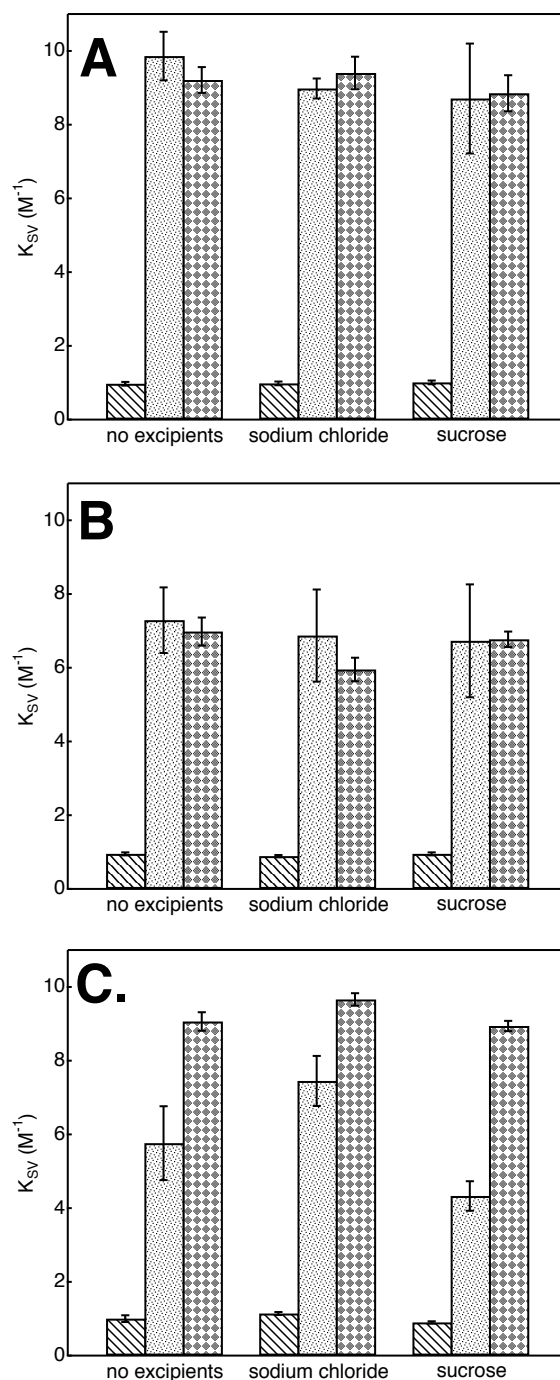


FIGURE 2.6. Measured Stern-Volmer constants after incubation of humAbs with silicone oil emulsion for at least 2 hours. (A) humAb 1. (B) humAb 2. (C) humAb 3. Data for each protein in 10 mM L-histidine at pH 6.0 containing 0.01% (w/v) sodium azide in the presence of no excipients, 140 mM sodium chloride, or 240 mM sucrose are labeled accordingly. For each protein, there are three bars representing different states of the protein: native protein, protein adsorbed to silicone oil, unfolded protein in 9.5 M urea. Data represents the arithmetic mean of three replicate samples. Error bars represent the standard error of the mean.

### 2.3.4 Colloidal Stability of humAbs

The zeta potentials of native humAbs 1-3 were statistically different from one another ( $p < 0.05$ ). In addition, the zeta potentials of humAbs 1-3 were dependent on the presence of excipients (Figure 2.7). In formulations containing sodium chloride, the zeta potentials of humAb 1 and 3 were statistically different than those in formulations containing no excipients ( $p < 0.05$ ). However, this difference was not statistically significant for humAb 2 formulations ( $p > 0.05$ ). In formulations containing sucrose, the zeta potential of each humAb was not statistically different than in formulations containing no excipients ( $p > 0.05$ ).

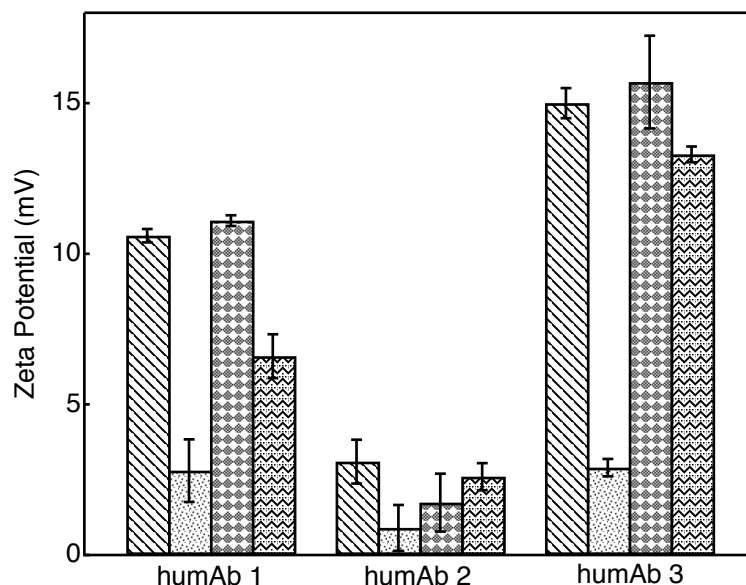


FIGURE 2.7. Zeta potential of native humAbs. Data for humAb 1, humAb 2, and humAb 3 are labeled accordingly. For each protein, there are four bars representing different excipient conditions: 10 mM L-histidine at pH 6.0, containing 0.01% (w/v) sodium azide, 10 mM L-histidine at pH 6.0 containing 0.01% (w/v) sodium azide and 140 mM sodium chloride, 10 mM L-histidine at pH 6.0 containing 0.01% (w/v) sodium azide and 240 mM sucrose, 10 mM L-histidine at pH 6.0 containing 0.01% (w/v) sodium azide and 0.03% (w/v) Tween® 20. Data represents the arithmetic mean of three replicate samples. Error bars represent the standard error of the mean.

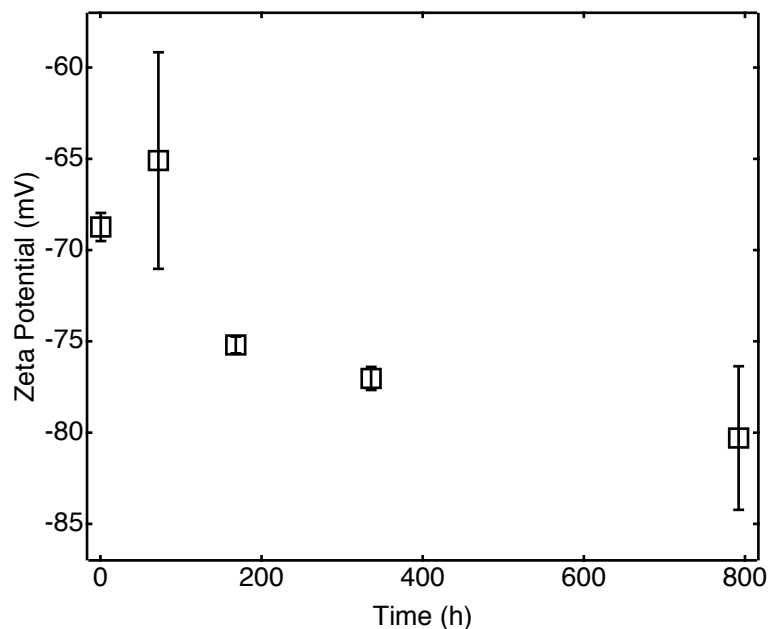


FIGURE 2.8. Zeta potential of silicone oil in emulsion in water plotted versus incubation time. Data represents the arithmetic mean of three replicate samples. Error bars represent the standard error of the mean.

Lastly, in formulations containing Tween® 20, the zeta potential of humAb 1 was statistically different compared to formulations containing no excipients ( $p < 0.05$ ), but the difference was not significant for humAb 2 and humAb 3 ( $p > 0.05$ ).

### 2.3.5 Colloidal Stability of Silicone Oil Emulsion

The average zeta potential of silicone oil droplets in water was  $-73.3 \pm 2.6$  mV and did not change significantly ( $p > 0.05$ ) over a one-month incubation period (Figure 2.8). The zeta potential of humAb-free silicone oil droplets in emulsion was dependent on the presence of excipients (Figure 2.9A). In formulations containing no excipients or sucrose, there appeared to be a slight decrease in the zeta potential to more negative values at longer incubation times. However, this difference was not statistically significant ( $p > 0.05$ ). Conversely, in formulations containing

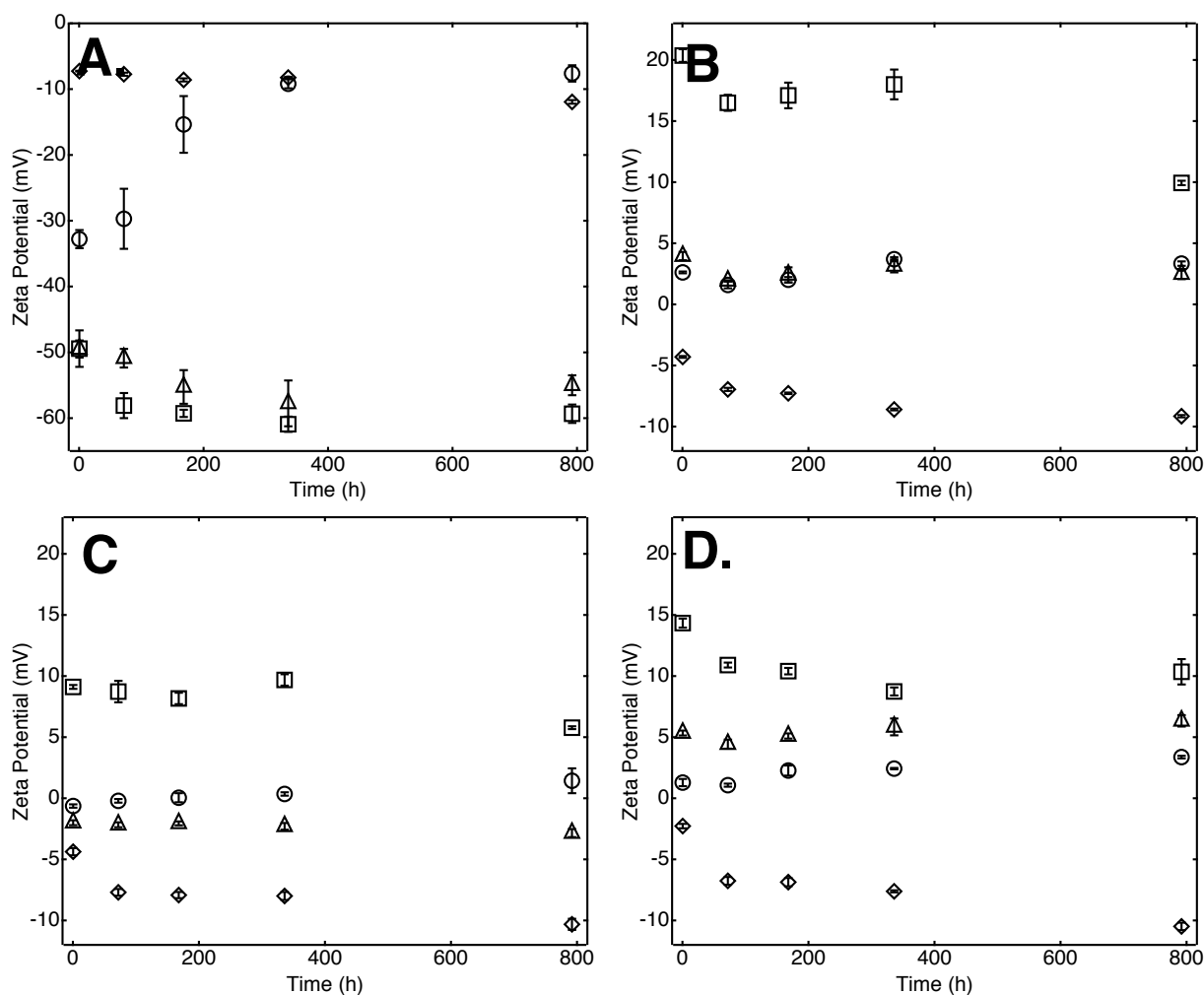


FIGURE 2.9. Zeta potential of humAb-coated silicone oil droplets plotted versus incubation time. (A) No protein. (B) humAb 1. (C) humAb 2. (D) humAb 3. For each case, there are four data sets representing different excipient conditions in 10 mM L-histidine at pH 6.0 containing 0.01% (w/v) sodium azide:  $\square$  No excipients,  $\circ$  140 mM sodium chloride,  $\Delta$  240 mM sucrose,  $\diamond$  0.03% (w/v) Tween  $\text{\textcircled{R}}$  20. Symbols represent the arithmetic mean of three replicate samples. Error bars represent the standard error of the mean.

sodium chloride, the zeta potential increased with increasing incubation time, approaching a value of zero after 1 month. Lastly, formulations containing Tween $\text{\textcircled{R}}$  20, the average zeta potential over a 1 month period was  $-8.75 \pm 0.83$  mV.

Immediately following humAb adsorption to the silicone oil-water interface, the zeta potential of silicone oil droplets in emulsion changed drastically for all formulations (Figure 2.9B-D). In formulations containing no excipients, there was a reversal in the sign of the measured zeta potentials from negative to positive. Differences in these values for formulations containing humAbs 1-3 were statistically significant ( $p < 0.05$ ). Over a period of 1 month, the zeta potential of silicone oil droplets decreased with time. This decrease was statistically significant for each humAb formulation ( $p < 0.05$ ). In formulations containing sodium chloride or sucrose, the measured zeta potential was significantly lower than in formulations containing no excipients with no clear change with incubation time. Similarly, the zeta potential of silicone oil droplets in formulations containing Tween® 20 were lower than in formulations containing no excipients. However, there was a decrease in the zeta potential of silicone oil droplets with time such that after 1 month of incubation the zeta potential approached that of humAb-free solutions. The difference between the zeta potentials of silicone oil droplets formulated with humAbs 1-3 and Tween® 20 incubated for 1 month and the same formulations incubated without humAbs 1-3 was not statistically significant ( $p > 0.05$ ).

### 2.3.6 Fluorescence-Activated Particle Analysis

Fluorescence-activated particle analysis can differentiate between protein particles without silicone oil and protein adsorbed to the surface of silicone microdroplets.<sup>2,34</sup> In the current study, there was no evidence that protein

aggregates  $> 0.2 \mu\text{m}$  formed as a result of protein-silicone oil interactions (Figure 2.10). Such protein-only particulates, had they been present, would have appeared as a population in the upper left quadrant in Figure 2.10.

After 30 minutes of incubation, the scaling exponent (Figure 2.11) ranged from 0.60 to 0.68 in all formulations examined. This value increased with incubation time over the course of a one-month storage period, with the largest incremental change occurring between 30 minutes and 72 hours. This change was greatest in formulations containing sodium chloride. In formulations containing no excipients or sucrose, the largest incremental changes during this period were similar. After 1

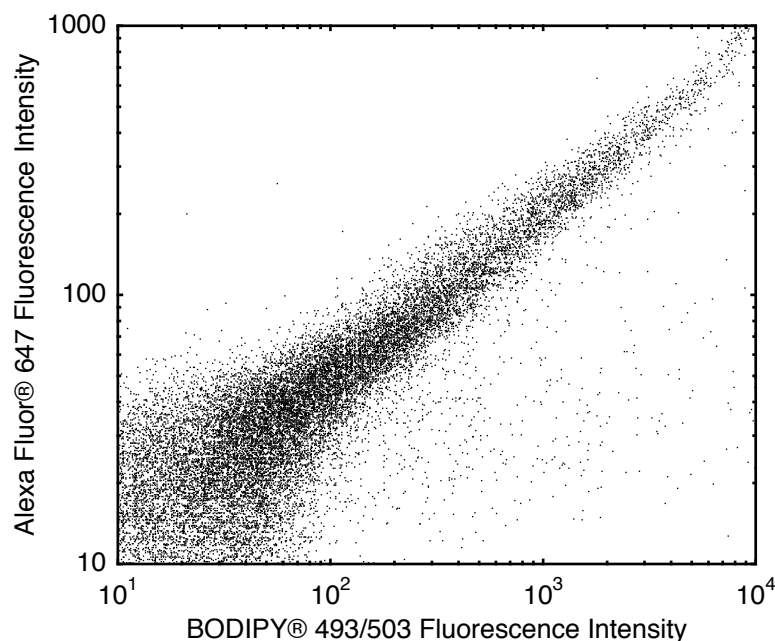


FIGURE 2.10. Representative plot of the fluorescence intensity of humAb labeled with Alexa Fluor® 647 versus the fluorescence intensity of silicone oil emulsion labeled with BODIPY® 493/503. Each of the 30,000 dots on the plot represents one silicone oil droplet with adsorbed humAb. The vertical axis reflects fluorescence due to Alexa Fluor® 647; the horizontal axis corresponds to fluorescence from silicone oil stained with BODIPY® 493/503.

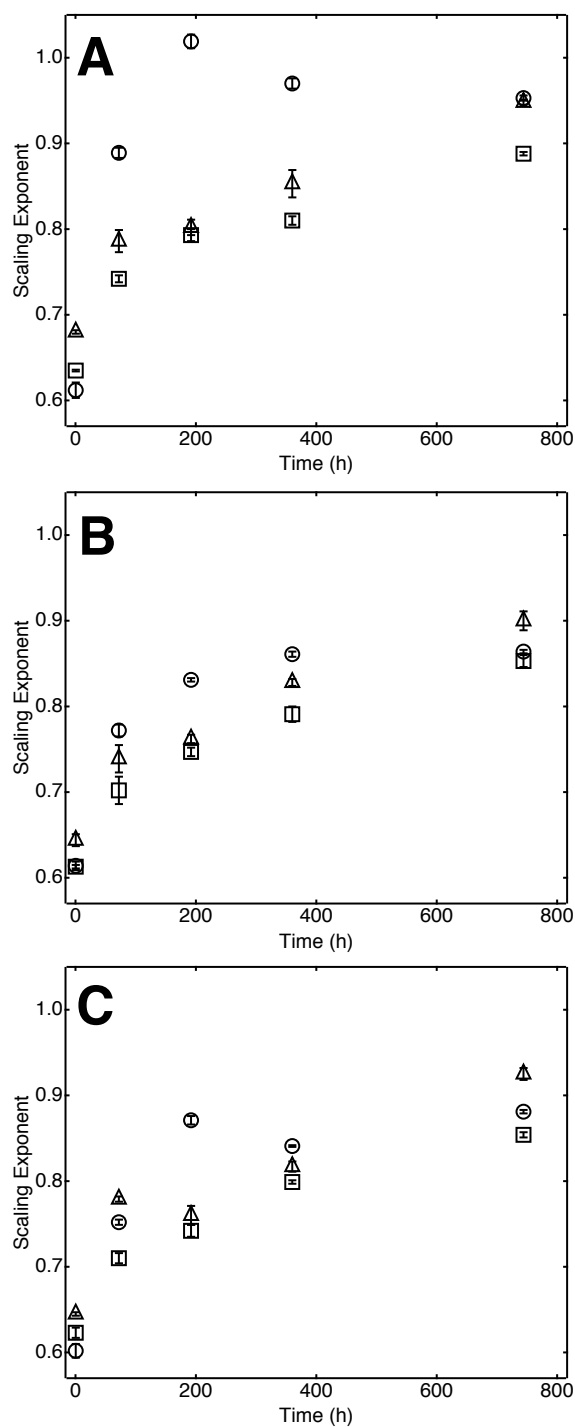


FIGURE 2.11. Scaling exponents determined from fluorescence-activated particle analysis plotted versus incubation time. (A) humAb 1. (B) humAb 2. (C) humAb 3. For each protein, there are three data sets representing different excipient conditions in 10 mM L-histidine at pH 6.0 containing 0.01% (w/v) sodium azide: □ No excipients, ○ 140 mM sodium chloride, △ 240 mM sucrose. Symbols represent the arithmetic mean of three replicate samples. Error bars represent the standard error of the mean.



month of incubation, the scaling exponent was statistically different than the value determined after 30 minutes ( $p < 0.05$ ) in all formulations. This experiment was also performed with humAb formulations containing Tween® 20. However, due to the low levels of protein adsorbed to silicone oil droplets under these conditions, Alexa Fluor® 647 fluorescence was below meaningful detection limits (Figure 2.12).

Histograms of BODIPY® 493/503 and Alexa Fluor® 647 fluorescence intensities were plotted for each time point (Figure 2.13). These histograms serve as particle size distributions. It was observed that the fraction of particles with

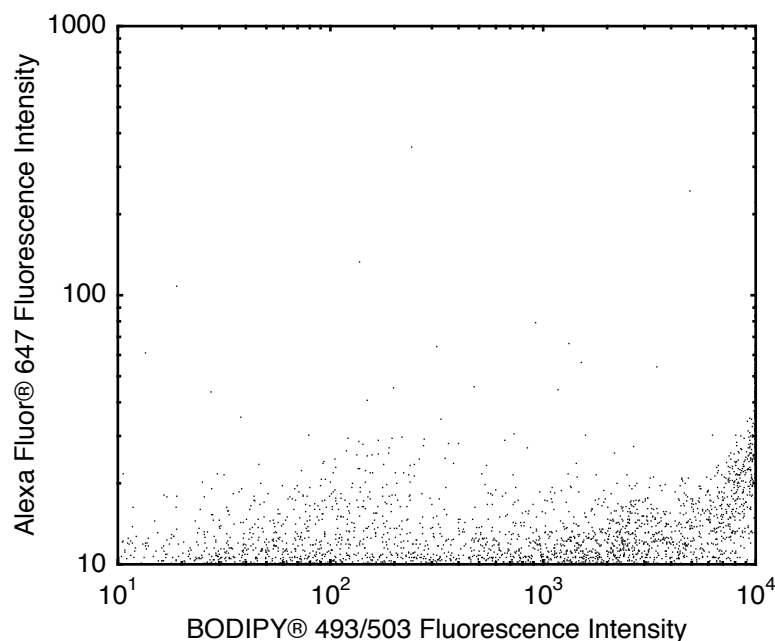


FIGURE 2.12. Representative plot of the fluorescence intensity of humAb labeled with Alexa Fluor® 647 versus the fluorescence intensity of silicone oil emulsion labeled with BODIPY® 493/503 for formulations containing 0.03% (w/v) Tween® 20. Each of the 30,000 dots on the plot represents one silicone oil droplet with adsorbed humAb. The vertical axis reflects fluorescence due to Alexa Fluor® 647; the horizontal axis corresponds to fluorescence from silicone oil stained with BODIPY® 493/503.

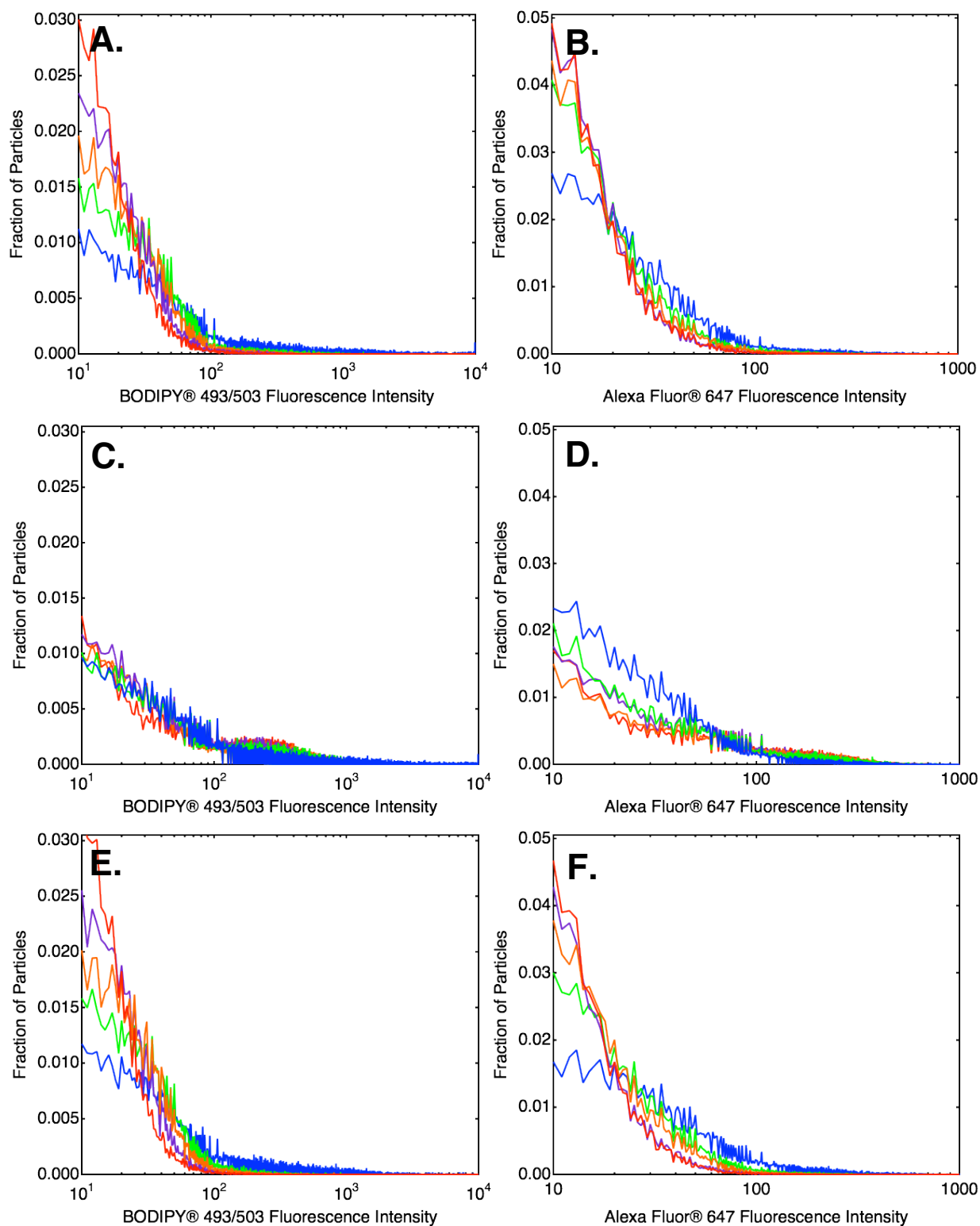


FIGURE 2.13. Fluorescence intensity histograms for 30,000 particles are presented for silicone oil emulsion labeled with BODIPY® 493/503 (A, C, E) and humAbs labeled with Alexa Fluor® 647 (B, D, F). Blue, green, orange, purple, and red histograms correspond to 30 minutes, 3 days, 1 week, 2 weeks, and 1 month incubation times, respectively.

fluorescence intensities between 10 and 100 increased with increasing incubation time in formulations containing no excipients or sucrose. In formulations containing sodium chloride, there was an increase in fraction of particles with fluorescence intensities between 100 and 1000 with incubation time. These observations were consistent in formulations containing humAbs 1-3.

### 2.3.7 Light Microscopy to Inspect Silicone Oil Droplet Flocculation

Light microscope images of silicone oil emulsion incubated for 1 month with humAb 1-3 revealed that bridging flocculation of droplets had occurred (Figure 2.14). In formulations containing no excipients or sucrose, there were relatively few, small flocs formed. Identification of flocs was even more difficult in formulations containing Tween® 20. Conversely, in formulations containing sodium chloride, large flocs were easily observed.

## 2.4 DISCUSSION

### 2.4.1 Characterization of Stock Silicone Oil Emulsion

Plunger depression in 1 mL prefilled syringes lubricated with silicone oil can expel 30-40 ppm of dilute silicone oil emulsion into solution.<sup>2,9,2,10</sup> The 0.5-1.0% silicone oil emulsion used in this study was roughly 100X the concentration of silicone oil emulsion that can be expelled by a typical 1 mL prefilled syringe, allowing the use of conventional analytical techniques to monitor processes like adsorption and aggregation in an “accelerated” approach.

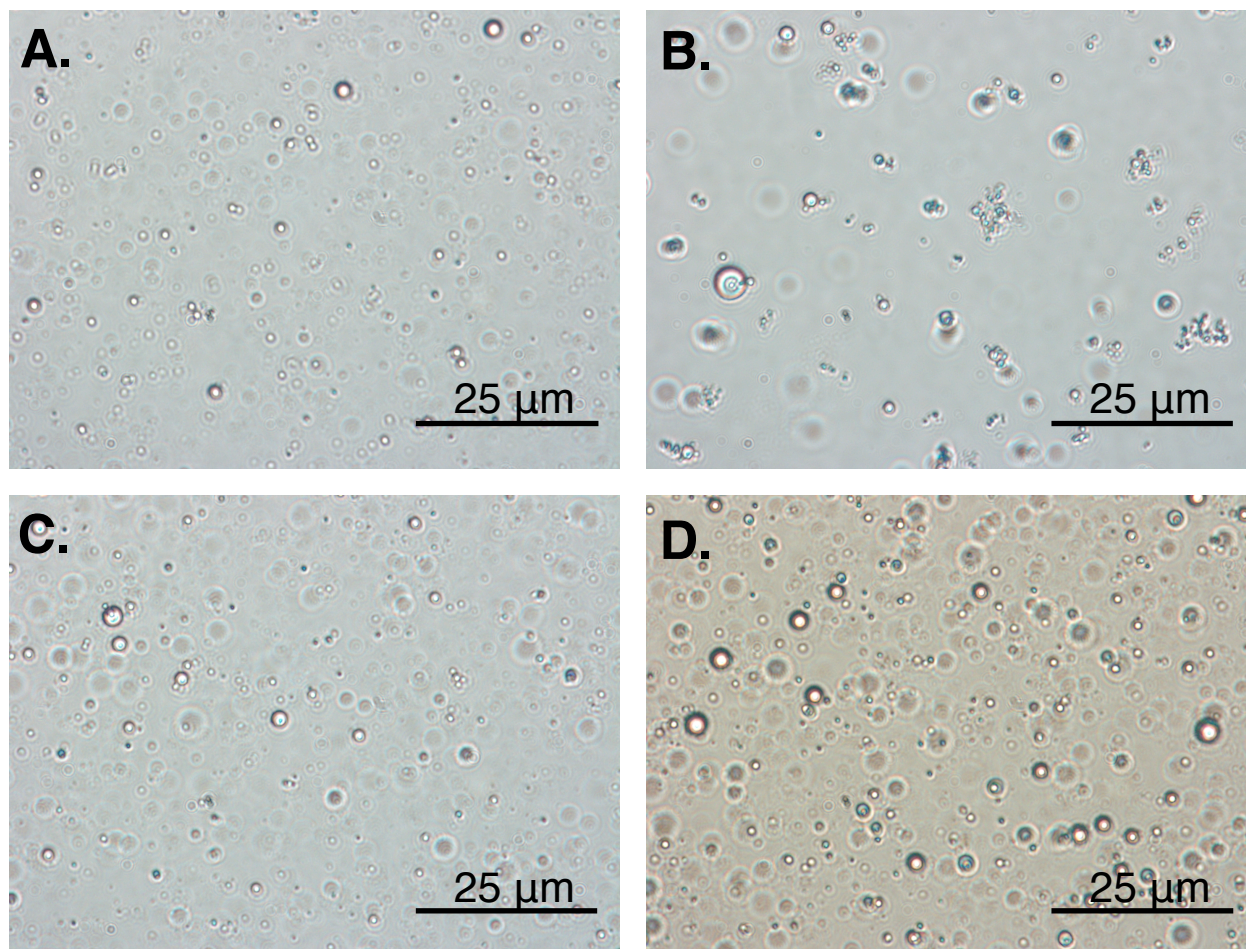


FIGURE 2.14. Visual Evidence of bridging flocculation of humAb-coated silicone oil droplets obtained from light microscopy. Samples are formulated with different excipients in 10 mM L-histidine at pH 6.0 containing 0.01% (w/v) sodium azide. (A) No excipients. (B) 140 mM sodium chloride. (C) 240 mM sucrose. (D) 0.03% (w/v) Tween® 20. Each image is at 400X magnification and the scale bar represents a distance of 25  $\mu\text{m}$ .

#### 2.4.2 Silicone Oil-Induced humAb Loss from Solution

Since there was no observable evidence that silicone oil-induced protein loss from solution could have resulted from protein aggregation, it is reasonable to assume that the values obtained reflect the amount of protein adsorbed to the silicone oil-water interface. These surface loading values ranged from 0.1-2.0  $\text{mg}/\text{m}^2$  and were not consistent with multilayer formation. The data suggested that

addition of sodium chloride resulted in increased protein adsorption to silicone oil, likely due to increased screening of charges that reduced protein-protein repulsive forces at the interface. Conversely, the data suggested that in the presence of Tween® 20, less protein adsorbed to silicone oil than in the absence of formulation excipients. Tween® 20 most likely competed with protein for adsorption sites at the interface.<sup>2,17,2,40</sup> If this was the case, then the results showed that Tween® 20 preferentially adsorbed to the silicone oil-water interface instead of humAb 1-3. However, in the presence of sucrose, there was seemingly no difference in surface coverage compared to formulations containing no excipients. This behavior was consistent for each humAb.

This study used three humanized monoclonal antibodies with similar hydrodynamic radii, isoelectric points, and molecular weights (see Table 2.1). Interestingly, based on the silicone oil-induced protein loss from solution calculated in the absence of formulation excipients, the amount of each humAb that adsorbed varied. The amount that adsorbed was not limited by the amount of protein added, since roughly four times as much protein remained free in solution as adsorbed to silicone oil microdroplets. In all cases, the amount of protein adsorbed was less than the amount that could theoretically adsorb in a hexagonally close-packed monolayer (about 2.5 mg/m<sup>2</sup>)<sup>2,3</sup>, and the amount of protein adsorbed represented only about 20% or less of the total protein in each sample.

There are several potential, non-exclusive explanations for why humAbs 1-3 exhibit differences in adsorption to the silicone oil-water interface. First, humAbs

1-3 may adsorb to the interface in different preferential orientations. Second, nearest-neighbor interactions between humAbs 1-3 may differ. Third, differences in silicone oil-induced conformational changes at the interface may have resulted in different protein-silicone oil interfacial contact areas for humAbs 1-3. However, there is insufficient information at this time to determine which mechanism(s) are responsible for differences in silicone oil interactions between humAbs 1-3.

#### 2.4.3 humAb Conformation at the Silicone Oil-Water Interface

humAbs 1-3 have 9, 11, and 13 tryptophan residues, respectively. At distances less than about 3Å, acrylamide dynamically quenches tryptophan fluorescence emission.<sup>2,47</sup> The Stern-Volmer constant reflects the accessibility of acrylamide to these residues in humAbs 1-3. Stern-Volmer constants showed that acrylamide accessibility to tryptophan was essentially equivalent for humAbs unfolded in urea or adsorbed at the silicone oil-water interface, and substantially greater than that for folded, native protein in solution. Addition of sucrose or sodium chloride to the formulation did not affect the value of the Stern-Volmer constant. Sodium chloride increased humAb packing at the silicone oil-water interface, but this did not influence tryptophan exposure to solvent. Sucrose is used to enhance the conformational stability of protein in solution through preferential hydration.<sup>2,48</sup> Stern-Volmer constants for humAbs 1-3 adsorbed to silicone oil/water interfaces were not affected by the addition of sucrose, suggesting that stabilization of

humAbs 1-3 in the bulk solution did not block the apparent change in conformation that lead to enhanced acrylamide accessibility to tryptophan residues.

Each of the three humAbs used in this work adsorbed to the silicone oil-water interface. Previous work with these same humAbs showed that these proteins also adsorbed to glass microparticles, with similar dependence of the surface loading values on formulation excipients.<sup>2,26</sup> Behavior of proteins at the solid-liquid interface is expected to differ from their behavior at fluid-fluid interfaces.<sup>2,17</sup> Specifically, at fluid interfaces, proteins can penetrate into the non-aqueous phase and diffuse faster at the surface, and more orientational and conformational changes occur at fluid interfaces than at solid interfaces.<sup>2,17</sup> Comparison of Stern-Volmer constants for humAbs 1-3 adsorbed to silicone oil from the current work with previously reported Stern-Volmer constants for humAbs 1-3 adsorbed to glass<sup>2,26</sup> suggests that humAbs 1-3 retain substantially native-like structure when adsorbed to glass but may unfold at the silicone oil-water interface.

#### 2.4.4 Colloidal Stability of humAbs

The zeta potentials of humAbs 1-3 were excipient-dependent. In formulations containing sodium chloride, zeta potentials were drastically reduced as result of increased charge shielding. Addition of sucrose had no effect on zeta potentials of humAbs1-3. Small decreases in zeta potential were seen in the presence of Tween® 20. The reasons for these decreases are not clear.

For humAbs 1-3, under all conditions, the measured zeta potentials of the proteins in the absence of silicone oil were less than 20 mV. These dispersions were colloidally unstable, but aggregation in the absence of silicone oil was not observed over the time period studied.

#### 2.4.5 Colloidal Stability of Silicone Oil Emulsion

Silicone oil droplets in pure water were negatively charged. The reason that emulsions were negatively charged is currently unknown. One possibility is that hydroxide ions adsorb to the interface.<sup>2,35</sup> Stock silicone oil emulsions were colloidally stable for at least 1 month at room temperature (see Figure 2.8). From Equation 4, the electrostatic energy barrier for droplet coalescence plotted in Figure 2.15 was approximately 150  $kT$  and 3500  $kT$  for 0.1  $\mu\text{m}$  and 2  $\mu\text{m}$  droplets, respectively.

Upon adsorption of humAbs 1-3, silicone oil emulsions were colloidally destabilized for all formulations examined. In formulations containing sodium chloride, near-zero zeta potentials of silicone oil droplets were observed, likely the result of increased charge shielding. Interestingly, the same effect was observed in formulations containing sucrose. The reason for this unexpected result is unknown. Lastly, in formulations containing Tween® 20, decreasing zeta potential values that approached those for humAb-free solutions suggested that surfactant preferentially adsorbed to the silicone oil-water interface, displacing adsorbed humAb.



For two droplets of unequal radii, the electrostatic activation energy barrier to flocculation was estimated using Equation 4. Figure 2.15 shows that this energy barrier is expected to increase with particle diameter. Each line represents the same incremental increase in the activation energy barrier to flocculation. For every formulation investigated excluding formulations containing sodium chloride, the Debye length was about 8.6 nm. At a zeta potential of 30 mV, each line represents an incremental increase of about  $20 kT$ . For lower zeta potentials, the incremental change decreases whereas at higher zeta potentials it increases. However, at zeta potentials less than approximately 12 mV, the activation energy barrier to flocculation falls to zero. Similarly, in formulation buffer containing sodium

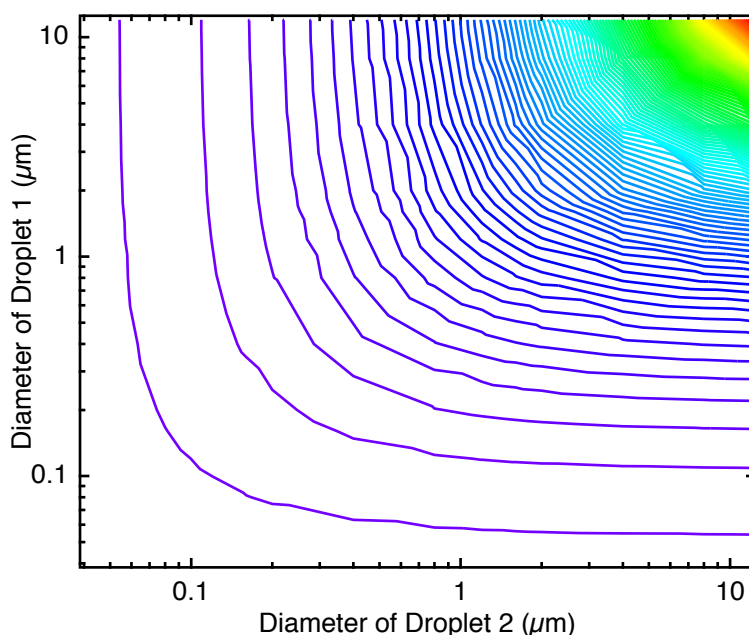


FIGURE 2.15. Representative contour plot illustrating the activation barrier to flocculation of two particles of different diameter. Colors range from blue to red representing the increase in the activation barrier from small to large values. For particles with a zeta potential of 30 mV, each contour represents an increase of activation energy of ca.  $20 kT$ .

chloride, where the Debye length was about 1.1 nm, there was no activation energy barrier to flocculation at the zeta potentials obtained in this work.

#### 2.4.6 Fluorescence-Activated Particle Analysis

The amount of humAb adsorbed to the silicone oil-water interface was proportional to the interfacial surface area present. For spherical droplets coated uniformly with protein, a log-log plot of the fluorescence intensities of BODIPY® 493/503-labeled silicone oil and Alexa Fluor® 647-labeled humAb on the x- and y-axis, respectively, should yield a slope equal to  $2/3$ . This slope is equal to the scaling exponent presented in Equation 7. Indeed, after 30 minutes of incubation, fluorescence-activated particle analysis yielded values of the scaling exponent close to this value for each excipient condition for humAbs 1-3 (Figure 2.11). However, the scaling exponent value increased with incubation time, suggesting that bridging flocculation between droplets was occurring.

To deduce whether bridging flocculation was occurring in solution, the particle size distributions in each formulation were assessed (Figure 2.13). In all formulations excluding formulations containing sodium chloride, it was found that the fraction of droplets with the highest fluorescence intensities ranging from 100-1000 decreased with time. Under static conditions, it seems unlikely that large droplets would fragment into smaller droplets. Instead, from visual inspection, it seems more likely that these droplets collided and stuck to the container walls. Because this technique can detect particles  $> 0.2 \mu\text{m}$ , the observed increase in the

fraction of small particles with time can be attributed to the formation of flocs by bridging flocculation. Individual particles that were initially too small to be detected may have flocculated resulting in flocs large enough to be detected. In formulations containing sodium chloride, there was an increase in the fraction of particles at fluorescence intensities ranging from 100-1000. These results suggest that larger flocs formed in the presence of sodium chloride than in the other excipient conditions which implies that floc size is related to the solution ionic strength. Unfortunately, in formulations containing Tween® 20, due to low humAb surface coverages, this kind of analysis could not be conducted.

humAb-coated silicone oil emulsions were colloiddally unstable, and evidence suggests that bridging flocculation occurred in silicone oil emulsions. However, no protein aggregates were detected in using SE-HPLC or fluorescence-activated particle analysis. Silicone oil emulsions have been shown to phase separate under static conditions due to density differences between silicone oil and water (Figure 2.16).<sup>2,33</sup> Silicone oil is less dense than water to which it is suspended. As a result, silicone oil droplets rose in solution. As the local concentration of droplets at the top of the container increased, bridging flocculation occurred. Assuming diffusion-limited growth, the rate of floc formation should be proportional to the square of the number concentration of droplets.<sup>2,24</sup> As expected, increases in the scaling exponent indicated that bridging flocculation had occurred at the fastest rate between 30 minutes and 3 days. After 1 month of incubation, this rate decreased because either the number concentration of droplets decreased appreciably and/or flocs formed

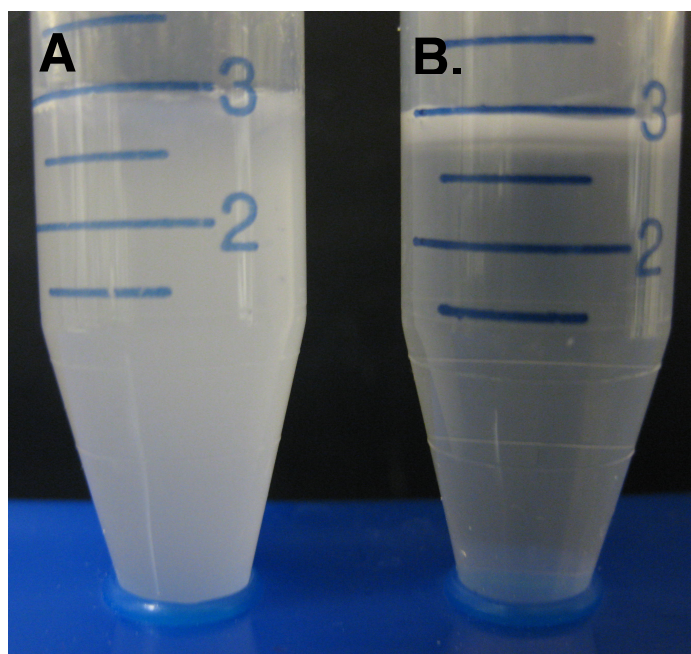


FIGURE 2.16. Example illustrating the creaming of silicone oil emulsion after sufficient incubation time. (A) Prior to incubation. (B) After incubation.

were so large that the electrostatic activation barrier to flocculation was too large for continued floc growth.

#### 2.4.7 Light Microscopy to Inspect Silicone Oil Droplet Flocculation

In accordance with Ludwig et al., silicone oil emulsion formulation with Tween® 20 did not seem to flocculate (Figure 2.14).<sup>2,33</sup> In both the excipient-free formulation and formulations containing sucrose, one can see small flocs by light microscopy, whereas in formulations containing sodium chloride one can see large flocs. From visual inspection, the number concentration of droplets correlates inversely with the size of flocs formed. Conditions in which the largest flocs had formed had the lowest number concentration of silicone oil droplets whereas

conditions with much smaller flocs had a higher number concentration of silicone oil droplets.

We speculate that a similar flocculation phenomenon might be operative in some actual therapeutic protein formulations, where visible particles may sometimes appear over the course of the therapeutic protein's shelf life. Small droplets of silicone oil, colloiddally destabilized by adsorption of protein, may flocculate into larger, visible assemblies. The appearance of such visible particles may not reflect ongoing protein aggregation.

## 2.5 CONCLUSION

This study sought to identify if the presence of silicone oil in pharmaceutical formulations alone was enough to induce homogeneous humAb aggregation. From this study, it was not. It was found that humAbs adsorb to the silicone oil-water interface. Silicone oil droplets were colloiddally destabilized by humAb adsorption and flocculated. Flocculation can result in the formation of visible particles (Figure 2.17). Visible particles and even sub-visible particles can result in lowered drug efficacy, unwanted immune responses, and shortened shelf-lives. Pharmaceutical companies strive to avoid these problems through stringent quality assurance and control protocols. According to USP <788>, a sterile injectable solution should be free of visual particulate matter.<sup>2,39</sup> With that being said, formulations with visual particulates are likely to be discarded. Financially, this poses a serious problem that

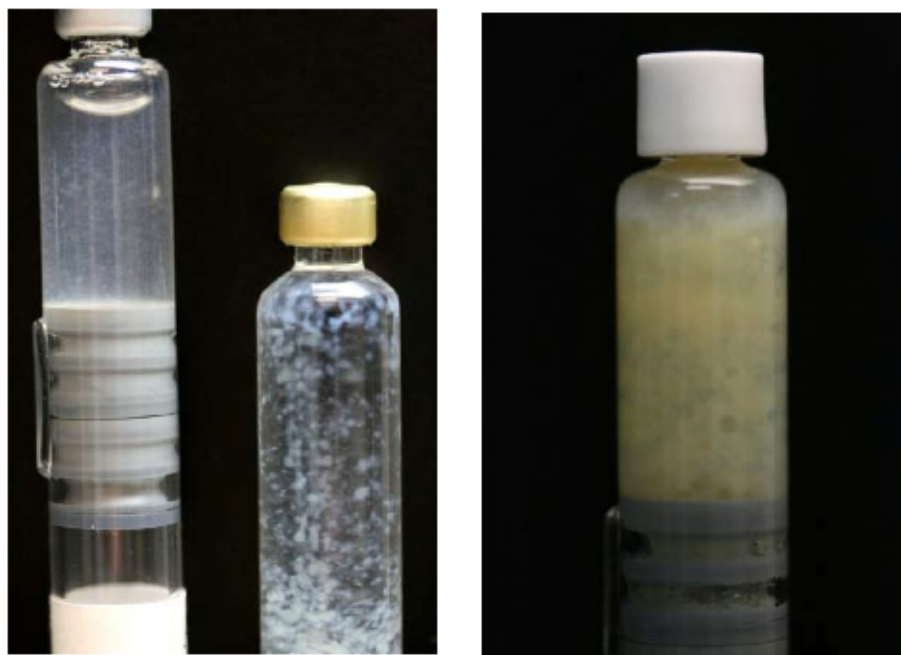


FIGURE 2.17. Examples of visible particles in pharmaceutical formulations. Source: 1.33.

needs to be avoided through continued research and development advances that aim to understand how protein therapeutics behave with respect to the container/closure system, microparticle contaminants, or leachables under various stresses.

## 2.6 REFERENCES

- 2.1 Bam, N.B., Cleland, J.L., Yang, J., Manning, M.C., Carpenter, J.F., Kelley, R.F., Randolph, T.W. (1998). "Tween Protects Recombinant Human Growth Hormone Against Agitation-Induced Damage Via Hydrophobic Interactions." J Pharm Sci. 87: 1554-1559.
- 2.2 Bee, J.S. (2009). "Front-Face Fluorescence Quenching and FRET Techniques to Probe the Structure of a Protein Antigen Adsorbed to Vaccine Adjuvant. In Effect of Interfaces and Shear on Therapeutic Protein Stability." Ph.D. Thesis: 237-254.
- 2.3 Bee, J.S., Chiu, D., Sawicki, S., Stevenson, J.L., Chatterjee, K., Freund, E., Carpenter, J.F., Randolph, T.W. (2009). "Monoclonal Antibody Interactions

- with Micro- and Nanoparticles: Adsorption, Aggregation, and Accelerated Stress Studies.” J Pharm Sci. 98: 3218-3238.
- 2.4 Bee, J.S., Davis, M., Freund, E., Carpenter, J.F., Randolph, T.W. (2010). “Aggregation of Monoclonal Antibody Induced by Adsorption to Stainless Steel.” Biotechnology and Bioengineering. 105(1): 121-129.
- 2.5 Bee, J.S., Nelson, S., Freund, E., Carpenter, J.F., Randolph T.W. (2009). “Precipitation of a Monoclonal Antibody by Soluble Tungsten.” J Pharm Sci. 98: 3290-3301.
- 2.6 Bhattacharjee, S., Elimelech, M., Borkovec, M. (1998). “DLVO Interaction between Colloidal Particles: Beyond Derjaguin’s Approximation.” CCACAA. 71(4): 883-903.
- 2.7 Butt, H.J., Graf, K., Kappl, M. (2003). Physics and Chemistry of Interfaces. 1st Edition. Wiley.
- 2.8 Carpenter, J.F., Randolph, T.W., Jiskoot, W., Crommelin, D.J.A., Middaugh, C.R., Winter, G. (2010). “Potential Inaccurate Quantitation and Sizing of Protein Aggregates by Size Exclusion Chromatography: Essential Need to Use Orthogonal Methods to Assure the Quality of Therapeutic Protein Products.” J Pharma Sci. 99: 2200-2208.
- 2.9 Chantelau, E.A., Berger, M. (1985). “Pollution of Insulin with Silicone Oil, a Hazard of Disposable Plastic Syringes.” Lancet. 1: 1459.
- 2.10 Chantelau, E., M. Berger, Bohlken, B. (1986). "Silicone Oil Released From Disposable Insulin Syringes." Diabetes Care 9(6): 672-673.
- 2.11 Chi, E.Y., Krishnan, S., Kendrick, B.S., Chang, B.S., Carpenter, J.F., Randolph, T.W. (2003). “Roles of Conformational Stability and Colloidal Stability in the Aggregation of Recombinant Human Granulocyte Colony-Stimulating Factor.” Protein Science. 12: 903-913.
- 2.12 Chi, E.Y., Weickmann, J., Carpenter, J.F., Manning, M.C., Randolph, T.W. (2005). “Heterogeneous Nucleation-Controlled Particulate Formation of Recombinant Human Platelet-Activating Factor Acetylhydrolase in Pharmaceutical Formulation.” J Pharma Sci. 94: 256-274.
- 2.13 Cleland, J.L., Powell, M.F., Shire, S.J. (1993). “The Development of Stable Protein Formulations: A Closer Look at Protein Aggregation, Deamidation, and Oxidation.” Crit Rev Ther Drug Carrier Syst. 10: 307-377.

- 2.14 Collier, F.C., Dawson, A.D. (1985). "Insulin syringes and Silicone Oil." Lancet. 2: 611.
- 2.15 de Jongh H.H.J., Wierenga, P.A. (2006). "Assessing the Extent of Protein Intermolecular Interactions at Air-Water Interfaces Using Spectroscopic Techniques." Biopolymers. 82: 384-389.
- 2.16 de Young, L.R., Fink, A.L., Dill, K.A. (1993). "Aggregation of Globular Proteins." Acc Chem Res. 26: 614-620.
- 2.17 Dickinson, E. (1999). "Adsorbed Protein Layers at Fluid Interfaces: Interactions, Structure, and Surface Rheology." Colloids and Surfaces B: Biointerfaces. 15: 161-176.
- 2.18 Eftink, M.R., Ghiron, C.A. (1977). "Exposure of Tryptophanyl Residues and Protein Dynamics. Biochemistry. 16: 5546-5551.
- 2.19 Eftink, M.R., Ghiron, C.A. (1981). "Fluorescence Quenching Studies with Proteins. Anal Biochem. 114: 199-227.
- 2.20 Faude, A., Zacher, D., Muller, E., Bottinger, H. (2007) "Fast Determination of Conditions for Maximum Dynamic Capacity in Cation-Exchange Chromatography of Human Monoclonal Antibodies. J Chromatogr A. 1161: 29-35.
- 2.21 Fesinmeyer, R.M., Hogan, S., Saluja, A., Brych, S.R., Kras, E., Narhi, L.O., Brems, D.N., Gokarn, Y.R. (2009). "Effect of Ions on Agitation- and Temperature-Induced Aggregation Reactions." Pharmaceutical Research. 26(4): 903-913.
- 2.22 Gabrielson, J. (2006). "Irreversible Association of Monoclonal Antibody with Silicone Oil in Aqueous Formulation Containing Sucrose and Surfactants. In Monoclonal Antibody Aggregation in Therapeutic Formulation: Size and Shape-Distribution Analysis." Ph.D. Thesis: 100-124.
- 2.23 Groza, A., A. Surmeian, et al. (2005). "Infrared spectral investigation of organosilicon compounds under corona charge injection in air at atmospheric pressure." Journal of Optoelectronics and Advanced Materials 7(5): 2545-2548.
- 2.24 Harrison, R.G., Todd, P., Rudge, S.R., Petrides, D.P. (2003). Bioseparations Science and Engineering. New York: Oxford University Press.



- 2.25 Hoffman, G. (1977) Iscotables, 7th Edition. Lincoln, Neb., ISCO.
- 2.26 Hoehne, M., Samuel, F., Dong, A., Wurth, C., Mahler, H., Carpenter, J.F., Randolph, T.W. (2010). "Adsorption of Monoclonal Antibodies to Glass Microparticles". J Pharm Sci. 1: 1-10.
- 2.27 Hogg, R., Healy, T.W., Fuerstenau, D.W. (1966). "Mutual Coagulation of Colloidal Dispersions." Trans. Faraday Soc. 62: 1638-1651.
- 2.28 Israelachvili, J.N. (1992). Intermolecular and Surface Forces, 2nd Edition. New York: Academic Press.
- 2.29 Jakupi, P., Halvorsen, Leaist, D.G. (2004). "Thermodynamic Interpretation of the 'Excluded-Volume Effect' in Coupled Diffusion." J Phys Chem B. 108: 7978-7985.
- 2.30 Jones, L.S., Kaufmann, A., Middaugh, C.R. (2005). "Silicone Oil Induced Aggregation of Proteins." J Pharm Sci. 94: 918-927.
- 2.31 Kerwin, B.A. (2008). "Polysorbates 20 and 80 Used in the Formulation of Protein Biotherapeutics: Structure and Degradation Pathways." J Pharma Sci. 97(8): 2924-2935.
- 2.32 Lubiniecki, A., D. B. Volkin, et al. "Comparability assessments of process and product changes made during development of two different monoclonal antibodies." Biologicals. In Press, Corrected Proof.
- 2.33 Ludwig, D.B., Carpenter, J.F., Hamel, J., Randolph, T.W. (2009). "Protein Adsorption and Excipient Effects on Kinetic Stability of Silicone Oil Emulsions." J Pharm Sci. 99: 1721-1733.
- 2.34 Ludwig, D.B., Trotter, J.T., Gabrielson, J.P., Carpenter, J.F., Randolph, T.W. (2010) "Flow Cytometry: A Promising Technique for the Study of Silicone Oil-Induced Particulate Formation in Protein Formulations." J Pharm Sci. 99(4): 1721-1733.
- 2.35 Marinova, K. G., R. G. Alargova, Denkov, N.D., Velev, O.D., Petsev, D.N., Ivanov, I.B., Borwankar, R.P. (1996). "Charging of oil-water interfaces due to spontaneous adsorption of hydroxyl ions." Langmuir 12(8): 2045-2051.
- 2.36 Martin, A.H., Meinders, M.B.J., Bos, M.A., Stuart, M.A.C., van Vliet, T. (2003). "Conformational Aspects of Proteins at the Air/Water Interface

- Studied by Infrared Reflection-Absorption Spectroscopy.” Langmuir. 19: 2922-2928.
- 2.37 Moon, Y.U., Curtis, R.A., Anderson, C.O., Blanch, H.W., Prausnitz, J.M. (2000). “Protein-Protein Interactions in Aqueous Ammonium Sulfate Solutions. Lysozyme and Bovine Serum Albumin (BSA).” J Solution Chem. 29(8): 699-717.
  - 2.38 Pace, N.C., Trevino, S., Prabhakaran, E., Scholtz, J.M. (2004). “Protein Structure, Stability, and Solubility in Water and Other Solvents.” Phil Trans R Soc Lond B. 359: 1225-1235.
  - 2.39 Pharmacopedia US. (2006). <788> Particulate Matter in Injections. USF-NF, 24th edition.
  - 2.40 Randolph, T.W., Jones, L.S. (2002). “Surfactant-Protein Interactions.” Pharm Biotechnology. 13: 159-175.
  - 2.41 Rosenberg, A.S. (2006). “Effects of Protein Aggregates: An Immunologic Perspective.” The AAPS Journal. 8(3): E501-E507.
  - 2.42 Sahin, E., Adeola, A.O., Perkins, M.D., Roberts, C.J. (2010). “Comparative Effects of pH and Ionic Strength on Protein-Protein Interactions, Unfolding, and Aggregation for IgG1 Antibodies.” J Pharma Sci. 99(12): 4830-4848.
  - 2.43 Salinas, B.A., Sathish, H.A., Bishop, S.M., Harn, N., Carpenter, J.F., Randolph, T.W. (2010). Understanding and Modulating Opalescence and Viscosity in a Monoclonal Antibody Formulation.” J Pharma Sci. 99: 82-93.
  - 2.44 Schladitz, C., Vieira, E.P., Hermel, H., Mohwald, H. (1999). “Amyloid- $\beta$ -Sheet Formation at the Air-Water Interface.” Biophysical Journal. 77: 3305-3310.
  - 2.45 Sharma, B. (2007). “Immunogenicity of Therapeutic Proteins. Part 2: Impact of Container Closures.” Biotechnology Advances. 25: 318-324.
  - 2.46 Sluzky, V., Tamada, J.A., Klibanov, A.M., Langer, R. (1991). “Kinetics of Insulin Aggregation in Aqueous Solutions Upon Agitation in the Presence of Hydrophobic Surfaces.” Applied Biological Sciences. 88: 9377-9381.
  - 2.47 Strambini, G.B., Gonnelli, M. (2010). “Fluorescence Quenching of Buried Trp Residues by Acrylamide Does Not Require Penetration of the Protein Fold.” J Phys Chem B. 114: 1089-1093.

- 2.48 Timasheff, S.N. (1992). "Water as Ligand: Preferential Binding and Exclusion of Denaturants in Protein Unfolding." Biochemistry. 31: 9857-9864.
- 2.49 Thirumangalathu, R., Krishnan, S., Speed Ricci, M., Brems, D.N., Randolph, T.W., Carpenter, J.F. (2009). Silicone Oil- and Agitation-Induced Aggregation of a Monoclonal Antibody in Aqueous Solution. J Pharm Sci. 98: 3167-3181.
- 2.50 Tyagi, A.K., Randolph, T.W., Dong, A., Maloney, K.M., Hitscherich, C., Carpenter, J.F. (2009). "IgG Particle Formation during Filling Pump Operation: A Case Study of Heterogeneous Nucleation on Stainless Steel Nanoparticles." J Pharm Sci. 98: 94-104.
- 2.51 Walstra, P. (1996). Emulsion Stability. In: Bercher P, editor. Encyclopedia of Emulsion Technology. New York: Marcel Dekker. 4: 1-62.
- 2.52 Wang, W., Nema, S., Teagarden, D. (2010). "Protein Aggregation: Pathways and Influencing Factors." International J Pharmaceutics. 390: 89-99.
- 2.53 Wang, W., Singh, S., Zeng, D.L., King, K., Nema, S. (2007). "Antibody Structure, Instability, and Formulation." J Pharma Sci. 96(1): 1-26.
- 2.54 Yeung, A., Moran, K., Masliyah, J., Czarnecki, J. (2003). "Shear-Induced Coalescence of Emulsified Oil Drops." J Colloid and Interface Sci. 265: 439-443.
- 2.55 2010. DOW CORNING 360 Medical Fluid [product information]. Dow Corning Corporation.
- 2.56 2010. "Fluorophores and Their Amine-Reactive Derivatives: Alexa Fluor Dyes Spanning the Visible and Infrared Spectrum." Molecular Probes: The Handbook. Life Technologies.
- 2.57 2010. "Probes for Lipids and Membranes." Molecular Probes: The Handbook. Life Technologies.

## CHAPTER 3: LIGHT SCATTERING ANALYSIS OF HUMANIZED MONOCLONAL ANTIBODY INTERACTIONS WITH SILICONE OIL EMULSION

### 3.1 INTRODUCTION

Flow cytometry is used routinely as a diagnostic tool in clinical and research practice. This technique is capable of measuring the properties of individual particles through a process called hydrodynamic focusing.<sup>3.2,3.4</sup> For particles ranging from 0.2 to 150  $\mu\text{m}$  in size, laser light incident upon a particle can either excite fluorophores associated with the particle or scatter.<sup>3.2,3.4</sup> Accordingly, most commercial flow cytometry instruments are equipped to detect the fluorescence at various wavelengths as well as both forward- and side-scattered light.

A useful principle of flow cytometry is the concept of ‘gating’ whereby one can selectively analyze particles of interest and eliminate results generated by unwanted particles.<sup>3.2,3.4</sup> In typical applications of flow cytometry, heterogeneous cell populations are analyzed.<sup>3.2,3.4</sup> For this reason, flow cytometry and fluorescence-activated cell sorting (FACS) are often used interchangeably. Cells types can be sorted based on size. Cell size is directly proportional to the forward-scattered light intensity.<sup>3.2,3.4</sup> Also, cell types can be sorted based on differences in granularity or surface topology. Cells with extensive internal compartmentalization or irregular surface topologies (e.g. surface roughness, unusual shapes, etc.) tend to have higher side-scattered light intensities.<sup>3.2,3.4</sup>

Fluorescence coupled with light scattering has made flow cytometry a versatile tool. The list of developed fluorescence-activated applications of flow cytometry is growing. This list includes but is not limited to DNA copy number variation analysis (Flow-FISH), protein expression and localization analysis, intracellular antigen level determination (e.g. cytokines, secondary mediators, etc.), enzyme activity determination, cell membrane potential determination, and immunophenotyping.<sup>3,2,3,4</sup>

A nonconventional application of flow cytometry was described in Chapter 2 and called 'Fluorescence-Activated Particle Analysis.' The ability to identify protein adsorption to silicone oil and bridging flocculation of silicone oil emulsion occurring in a protein formulation is realized in this work. The value of flow cytometry used in this context may grow to be a valuable tool used by the pharmaceutical industry in formulation development. However, this application of flow cytometry is still in its infancy. Only one study to date published by Ludwig et al. has utilized this technique in such as fashion.<sup>3,3</sup> To build upon the core concept of 'Fluorescence-Activated Particle Analysis' first introduced by Ludwig et al.<sup>3,3</sup> and developed further in Chapter 2 of this work, this chapter discusses the potential of light scattering analysis as a complementary tool to identify protein adsorption and bridging flocculation phenomena occurring in pharmaceutical formulations containing particulate contaminants such as silicone oil emulsion.

## 3.2 MATERIALS AND METHODS

### 3.2.1 Materials

In this analysis, the humAbs described in section 2.2.1 were used in the buffer conditions listed in section 2.2.2. Silicone oil emulsion was prepared and characterized as previously mentioned in sections 2.2.3 and 2.2.4-2.2.5, respectively.

### 3.2.2 Light Scattering Analysis

The humAbs and silicone oil emulsion used in this study were fluorescently labeled with Alexa Fluor® 647 and BODIPY® 493/503, respectively, as previously described in section 2.2.9. Samples were prepared by mixing labeled silicone oil emulsion, 0.1 mg/mL labeled protein, and 6X buffer in that order in 2 mL polypropylene microcentrifuge tubes. The final protein concentration in each sample was 0.01 mg/mL. Samples were incubated statically at room temperature ( $23^{\circ}\text{C} \pm 2^{\circ}\text{C}$ ) for 30 minutes, 3 days, 1 week, 2 weeks, and 1 month. After incubation, 200  $\mu\text{L}$  of sample was analyzed using a BD FACSCalibur™ instrument (Becton Dickinson and Co. Biosciences, San Jose, CA) equipped with a 488 nm blue argon laser, 635 nm red diode laser, four fluorescence detectors (FL1 530/30, FL2 585/42, FL3 670LP, and FL4 661/16), and 488 nm forward and  $90^{\circ}$  side light scattering detectors. The forward- and side-scattered light intensities for 30,000 particles were detected. Also, the fluorescence intensities of Alexa Fluor® 647 and BODIPY® 493/503 for these particles were detected.

### 3.3 RESULTS

#### 3.3.1 humAb Adsorption to the Silicone Oil-Water Interface

The adsorption of humAbs to the silicone oil-water interface was verified by measuring the intensity of forward and side light scattering as well as the fluorescence of labeled silicone oil and protein associated with individual droplets (Figure 3.1). Using silicone oil emulsion fluorescently labeled with BODIPY® 493/503, it was found that the intensity of forward-scattered light was proportional to the fluorescence intensity of BODIPY® 493/503, as expected (data not shown). In addition, using humAbs labeled with Alexa Fluor® 647, it was also found that the intensity of side-scattered light was proportional to the fluorescence intensity of Alexa Fluor® 647 (Figure 3.1A). Relating the two types of light scattering, the

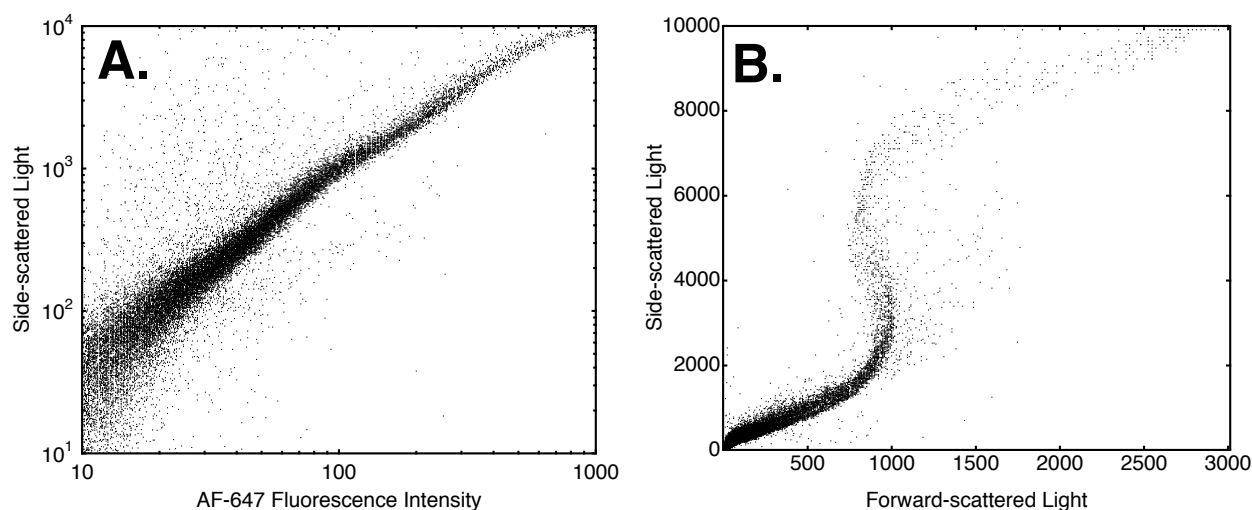


FIGURE 3.1. Evidence of protein adsorption verified using light scattering and fluorescence of labeled silicone oil and humAb. Each of the 30,000 dots on the plot represents one silicone oil droplet with adsorbed humAb. (A) Side-scattered light intensity is plotted versus the fluorescence intensity of humAb labeled with Alexa Fluor® 647. (B) Side-scattered light intensity is plotted versus forward-scattered light intensity.

intensity of side-scattered light was proportional to the intensity of forward-scattered light (Figure 3.1B).

### 3.3.2 Bridging Flocculation of Silicone Oil Emulsion

The intensities of forward- and side-scattered light were plotted on a log-log plot versus one another for different excipient conditions in Figure 3.2. In chapter 2, it was found that the scaling exponent from ‘Fluorescence-Activated Particle Analysis’ increased significantly over the period of 1 month (Figure 2.5). For silicone oil emulsion incubated with humAbs 1-3 for 30 minutes and 1 month, there was a shift to larger side-scattering intensities with time, (Figure 3.2A, 3.2B, 3.2C) especially in the presence of sodium chloride (Figure 3.2B). In the presence of Tween 20, there was no noticeable shift in side-scattered light intensity (Figure 3.2D).

## 3.4 DISCUSSION

### 3.4.1 humAb Adsorption to the Silicone Oil-Water Interface

The intensity of forward-scattered light is proportional to the size of the silicone oil droplet being analyzed.<sup>3,2,3,4</sup> Larger droplets are represented by higher intensities of forward-scattered light whereas smaller droplets are represented by lower intensities. The interpretation of side-scattered light in this system is more complicated. Larger droplets have larger surface areas to adsorb more protein than smaller droplets. For larger droplets with more adsorbed protein, there was a higher side-scattered light intensity. Consequently, the side-scattered light intensity



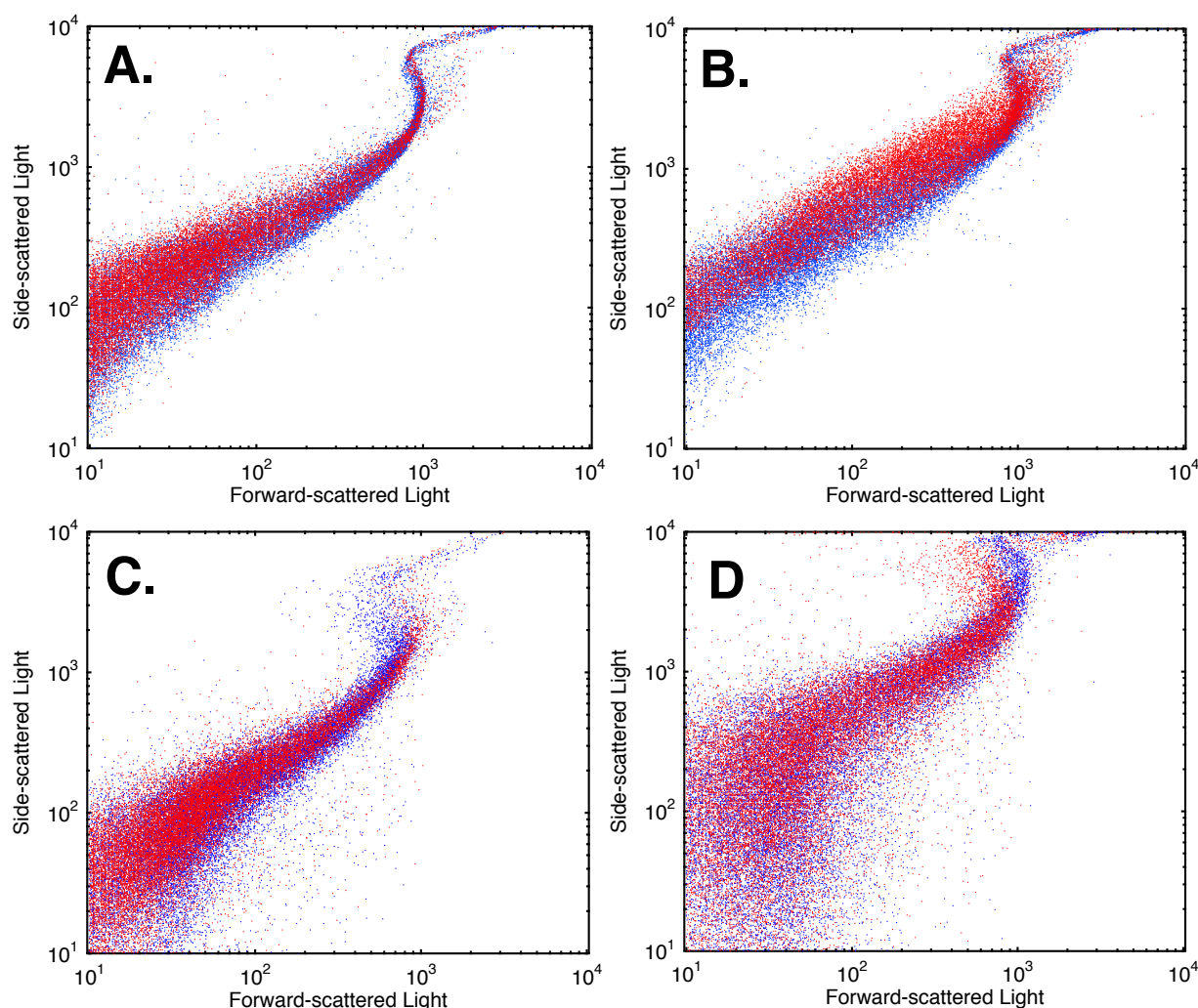


FIGURE 3.2. Evidence of bridging flocculation of humAb-coated silicone oil microdroplets interpreted as shifts in side-scattered light intensity in plots of side- versus forward-scattered light intensity. Each of the 30,000 dots on the plot represents one silicone oil droplet with adsorbed humAb for different excipient conditions in 10 mM L-histidine at pH 6.0 containing 0.01% (w/v) sodium azide. (A) No excipients. (B) 140 mM sodium chloride. (C) 240 mM sucrose. (D) 0.03% (w/v) Tween® 20. Blue and red dots correspond to 30 minutes and 1 month incubation times, respectively.

scaled with the forward-scattered light intensity. This scaling is equivalent to the surface area to volume scaling introduced in chapter 2. In that analysis, the fluorescence intensity of labeled silicone oil droplet volume scaled with the fluorescence intensity of labeled protein adsorbed to its surface. This scaling was fit

to Equation 7 using a simple geometric scaling relationship to provide insight about the shape of objects detected. Here, however, there is no analogous interpretation relating forward- and side-scattered light. This plot only serves to verify that adsorption of humAbs 1-3 to silicone oil microdroplets occurs. It does not provide insight into the shape of droplets directly.

Plots of forward- versus side-light scattering intensities revealed an unexpected result. This plot appeared sigmoidal. A majority of droplets analyzed appear in a linear region at smaller particle sizes. This result was expected. However, a small minority of larger droplets had higher side-scattering intensities than initially anticipated. There are two possible explanations to account for this finding. First, there is a small number of large flocs of silicone oil droplets present in solution from the onset of the analysis. As discussed in Chapter 2, the energy barrier to coalescence of large silicone oil droplets is seemingly insurmountable. However, it may be possible to overcome said barrier in the emulsifying process where the large pressures ca. 40 kpsi applied might impart enough energy to induce droplet coalescence. Second, in passing through the BD FACSCalibur™ instrument (Becton Dickinson and Co. Biosciences, San Jose, CA), the shape of large droplets may be distorted. Protein adsorption to the silicone oil-water interface lowers the interfacial surface tension of an individual droplet.<sup>3.1</sup> This drop in interfacial tension might be enough so that at the operating flow rate used the effect of shear might be significant. This distortion effect would be more pronounced for larger

droplets. Fortunately, for a majority of droplets, this effect appears to be negligible making the analysis presented in Chapter 2 valid.

### 3.4.2 Bridging Flocculation of Silicone Oil Emulsion

How does the side-scattered light intensity of two equally sized objects, a single silicone oil droplet and a floc comprised of multiple droplets, compare? The question posed is not trivial. But, it is reasonable to state that the intensity of side-scattered light depends on the geometry of particles analyzed. Based on the results obtained, there appears to be a shift to higher side-scattered light intensities after flocculation has occurred. Assuming that a majority of silicone oil droplets are initially spherical, flocs formed after a 1 month period are most likely non-spherical. The exact shape and size of flocs cannot be determined from this analysis alone. But, the difference in the relative size of flocs formed in the presence of different formulation excipients can be determined (Figure 3.2). The shift in side-scattered light intensity in formulations containing sodium chloride (Figure 3.2B) was greater than in formulations containing no excipients (Figure 3.2A) or sucrose (Figure 3.2C). This most likely means that flocs formed in presence of sodium chloride were larger than those formed in the presence of no excipients or sucrose. This finding was verified using light microscopy (see Figure 2.14). In the presence of Tween® 20, however, there appeared to be no shift in side-scattered light intensity. As droplets coated with Tween® 20 approach one another, flocculation may be prevented by

steric repulsion.<sup>3.5</sup> Hence, there should be no shift in the side-scattered light intensity.

### 3.5 CONCLUSIONS

The use of light scattering of individual silicone oil droplets offers a new means to assess protein adsorption to emulsified droplets and bridging flocculation of these droplets. This method provides qualitative information about these processes that to date have not been discussed in the literature.<sup>3.3</sup> The ability to look at individual objects is very appealing in many applications. Used primarily to sort cells, light scattering analysis has potential to be used in a variety of unexplored capacities as a complementary technique to conventional methodologies.

### 3.6 REFERENCES

- 3.1 Beverung, C.J., Radke, C.J., Blanch, H.W. (1999). "Protein Adsorption at the Oil/Water Interface: Characterization of Adsorption Kinetics by Dynamic Interfacial Tension Measurements." Biophysical Chem. 81: 59-80.
- 3.2 Givan, A.L. (2002). Flow Cytometry: First Principles. 2nd Edition. Wiley.
- 3.3 Ludwig, D.B., Trotter, J.T., Gabrielson, J.P., Carpenter, J.F., Randolph, T.W. (2010) "Flow Cytometry: A Promising Technique for the Study of Silicone Oil-Induced Particulate Formation in Protein Formulations." Anal Biochem. [Epub ahead of print].
- 3.4 Rahman, M., Lane, A., Swindell, A., Bartram, S. (2006). "Introduction to Flow Cytometry: Principles, Data Analysis, Protocols, and Troubleshooting." Oxford, United Kingdom, Serotec Incorporated.
- 3.5 Walstra, P. (1996). Emulsion Stability. In: Bercher P, editor. Encyclopedia of Emulsion Technology. New York: Marcel Dekker. 4: 1-62.

## CHAPTER 4: COMPETITIVE ADSORPTION OF HUMANIZED MONOCLONAL ANTIBODIES AND SURFACTANTS TO THE SILICONE OIL-WATER INTERFACE

### 4.1 INTRODUCTION

Selection of a suitable pharmaceutical formulations for therapeutic protein products is an important process that is vital to the long-term stability and reproducible activity of the drug. Accordingly, the type of buffer and the addition of formulation excipients are chosen to maximize protein stability and maintain proper functionality of the protein. Excipients used in modern pharmaceutical formulations include but are not limited to salts, carbohydrates, polyols, polymers, antioxidants, and surfactants.

Protein-surfactant interactions are important in many biological applications including including drug delivery, cosmetics, and detergent actions.<sup>4.7</sup> This interaction depends on whether the surfactant in question is ionic or non-ionic. Interactions between ionic surfactants and proteins have been studied in the literature using steady state and time resolved fluorescence, dynamic light scattering, electron-spin resonance, deuterium nuclear magnetic resonance (NMR) spectroscopy, excited state protein transfer, and thermodynamic and piezoelectric crystal techniques.<sup>4.7,4.12-4.13</sup> In pharmaceutical formulations, non-ionic surfactants are typically used.<sup>4.1,4.8-4.9,4.11,4.14</sup> Using electron paramagnetic resonance (EPR)<sup>4.1,4.8</sup> and analytical ultracentrifugation (AUC)<sup>4.8</sup>, it has been shown that protein-surfactant complexes form between protein and non-ionic surfactant. While the

formation of a protein-surfactant complex is well established in the literature, the complicated nature of this interaction remains poorly understood.

In the presence of hydrophobic surfaces, both protein and surfactant can adsorb.<sup>4.3-4.4</sup> At high bulk concentrations, small-molecule surfactants reduce the surface tension more than proteins.<sup>4.9</sup> This translates to a greater reduction in the interfacial free energy.<sup>4.9</sup> Therefore, surfactants have a greater thermodynamic affinity for interfaces than proteins.<sup>4.9</sup> For a solution containing protein and surfactant, there is a competition for adsorption sites at an interface. Because surfactants have a higher thermodynamic affinity to adsorb to interfaces than protein, it will preferentially bind to an interface forming a densely packed layer.<sup>4.3-4.4,4.9</sup> A protein can be displaced from an interface by surfactant molecules. Another means by which which protein can be removed from an interface by surfactant involves the formation of a protein-surfactant complex.<sup>4.4</sup> Surfactant molecules can bind to hydrophobic patches on protein surfaces.<sup>4.1,4.8,4.11</sup> This protein-surfactant complex may have a lower thermodynamic affinity for an interface than protein alone. Solubilization of the protein-surfactant complex can result in protein desorption and replacement by individual surfactant molecules.

In therapeutic protein formulations, surfactants serve as stabilizing agents to prevent protein aggregation.<sup>4.9</sup> Surfactants have been shown to adsorb to interfaces to eliminate surface-mediated protein aggregation and to prevent agitation-induced protein aggregation in solution.<sup>4.1,4.8-4.9</sup> In this chapter, the competitive adsorption of surfactant and humanized monoclonal antibodies to the silicone oil-water interface

was assessed using zeta potential measurements. The zeta potentials of protein solutions containing non-ionic surfactants Tween® 20, Tween® 80, and poloxamer 188 were compared as a function of time.

## 4.2 MATERIALS AND METHODS

### 4.2.1 Materials

In this analysis, the humAbs described in section 2.2.1 were used in the buffer conditions listed in section 2.2.2. Silicone oil emulsion was prepared and characterized as previously mentioned in sections 2.2.3 and 2.2.4-2.2.5, respectively.

### 4.2.2 Zeta Potential Analysis

The zeta potential of humAbs and silicone oil emulsion was assessed using laser Doppler velocimetry (LDV) as described in section 2.2.8. A Malvern Zetasizer Nano ZS (Worcestershire, United Kingdom) was used to measure the electrophoretic mobility of protein and silicone oil dispersions in an applied electric field. The zeta potential is calculated using Equation 3. Samples were prepared by mixing silicone oil emulsion, 2 mg/mL protein, and 6X buffer in that order in 1.5 mL polypropylene microcentrifuge tubes. The final protein concentration in each sample was 0.2 mg/mL. Samples were incubated statically at room temperature ( $23^{\circ}\text{C} \pm 2^{\circ}\text{C}$ ) for 30 minutes, 3 days, 1 week, 2 weeks, or 1 month. After incubation, a 20:1 dilution of silicone oil emulsion in the appropriate buffer was prepared and 0.8 mL of diluted

sample was analyzed using a disposable capillary zeta potential cell equipped with gold electrodes (Malvern Instruments Ltd., Worcestershire, United Kingdom).

#### 4.2.3 Statistical Analysis

Average values are reported with standard errors about the mean. Also, student's t-test was used obtain a p-value that was used to compare statistically significant differences observed between data sets. A p-value less than 0.05 indicated that data sets were statistically different.

### 4.3 RESULTS

#### 4.3.1 Zeta Potential of humAbs-surfactant Solutions

The measured zeta potential of native humAbs both with and without surfactant in the formulation are reported in Figure 4.1. For formulations containing surfactant, the measured zeta potential was not statistically different from the case where no surfactant was present in formulations containing humAb 2 and humAb 3 ( $p > 0.05$ ). Conversely, in formulations containing humAb 1, the difference observed in the measured zeta potential between formulations containing no surfactant and formulations containing surfactant was statistically significant ( $p < 0.05$ ). In addition, the difference in the measured zeta potential of humAbs 1-3 in formulations containing different surfactants were not statistically significant for most cases with some exceptions ( $p > 0.05$ ). Formulations of humAb 1 containing



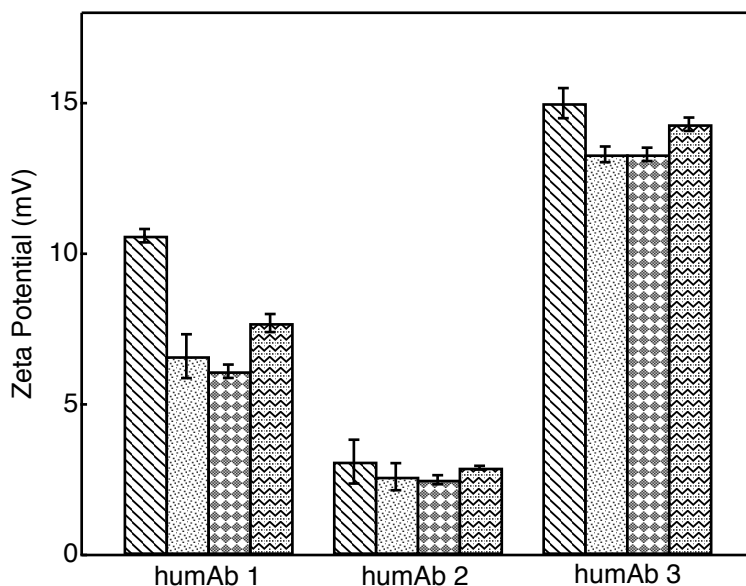


FIGURE 4.1. Zeta potential of native humAbs. Data for humAb 1, humAb 2, and humAb 3 are labeled accordingly. For each protein, there are four bars representing different excipient conditions: 10 mM L-histidine at pH 6.0 containing 0.01% (w/v) sodium azide, 10 mM L-histidine at pH 6.0 containing 0.01% (w/v) sodium azide and 0.03% (w/v) Tween® 20, 10 mM L-histidine at pH 6.0 containing 0.01% (w/v) sodium azide and 0.03% (w/v) Tween® 80, 10 mM L-histidine at pH 6.0 containing 0.01% (w/v) sodium azide and 0.03% (w/v) poloxamer 188. Data represents the arithmetic mean of three replicate samples. Error bars represent the standard error of the mean.

poloxamer 188, humAb 3 containing Tween® 80, and humAb 3 containing poloxamer 188 were statistically different than formulations containing no surfactant ( $p < 0.05$ ).

#### 4.3.2 Competitive Adsorption of humAbs and Surfactants at the Silicone Oil-Water Interface

For formulations containing humAb and surfactant, the zeta potentials of silicone oil emulsion over a 1 month period of time were collected (Figure 4.2, Figure 4.3, Figure 4.4). The behavior observed was consistent for each humAb and was dependent on the identity of the surfactant. In the presence of Tween® 20, the zeta

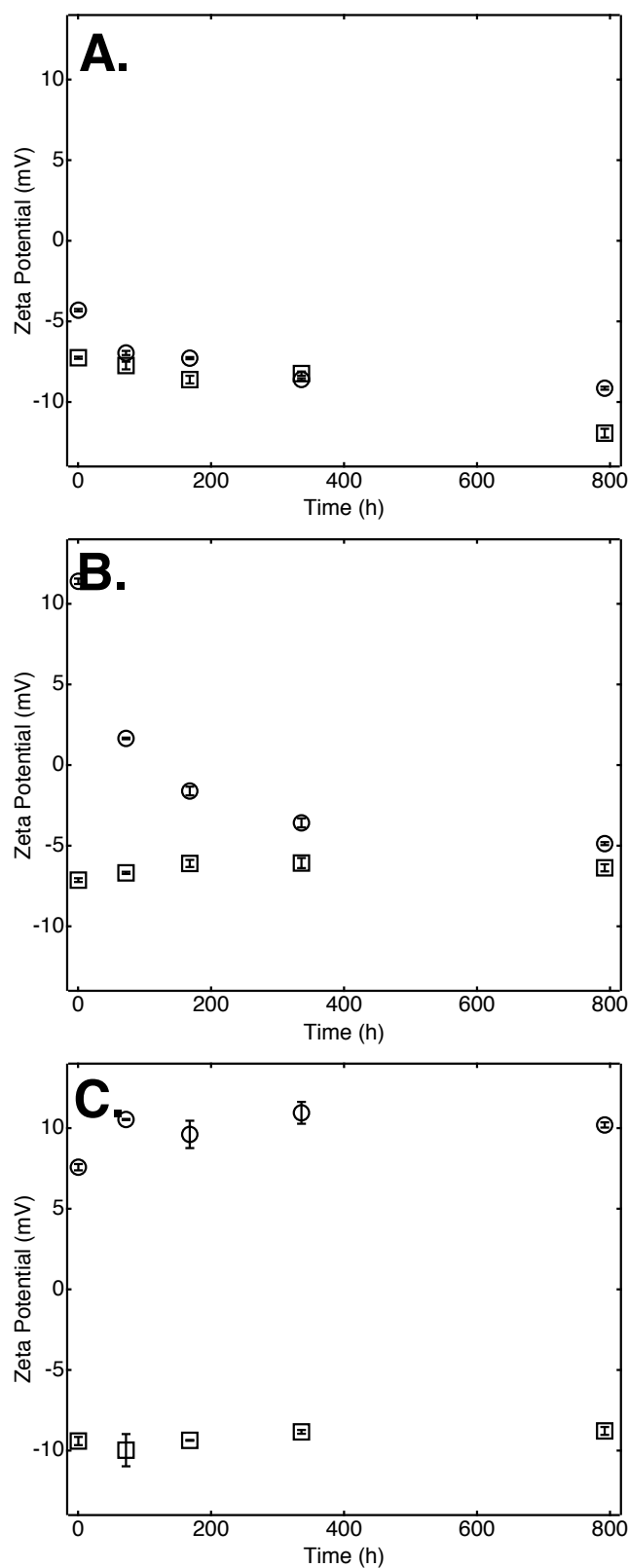


FIGURE 4.2. Zeta potential of silicone oil emulsion in buffer containing humAb 1 and 0.03% (w/v) surfactant. (A) Tween® 20. (B) Tween® 80. (C) poloxamer 188. For each plot, there are two sets of data:  $\square$  No protein present,  $\circ$  Protein present. Symbols represent the arithmetic mean of three replicate samples. Error bars represent the standard error of the mean.

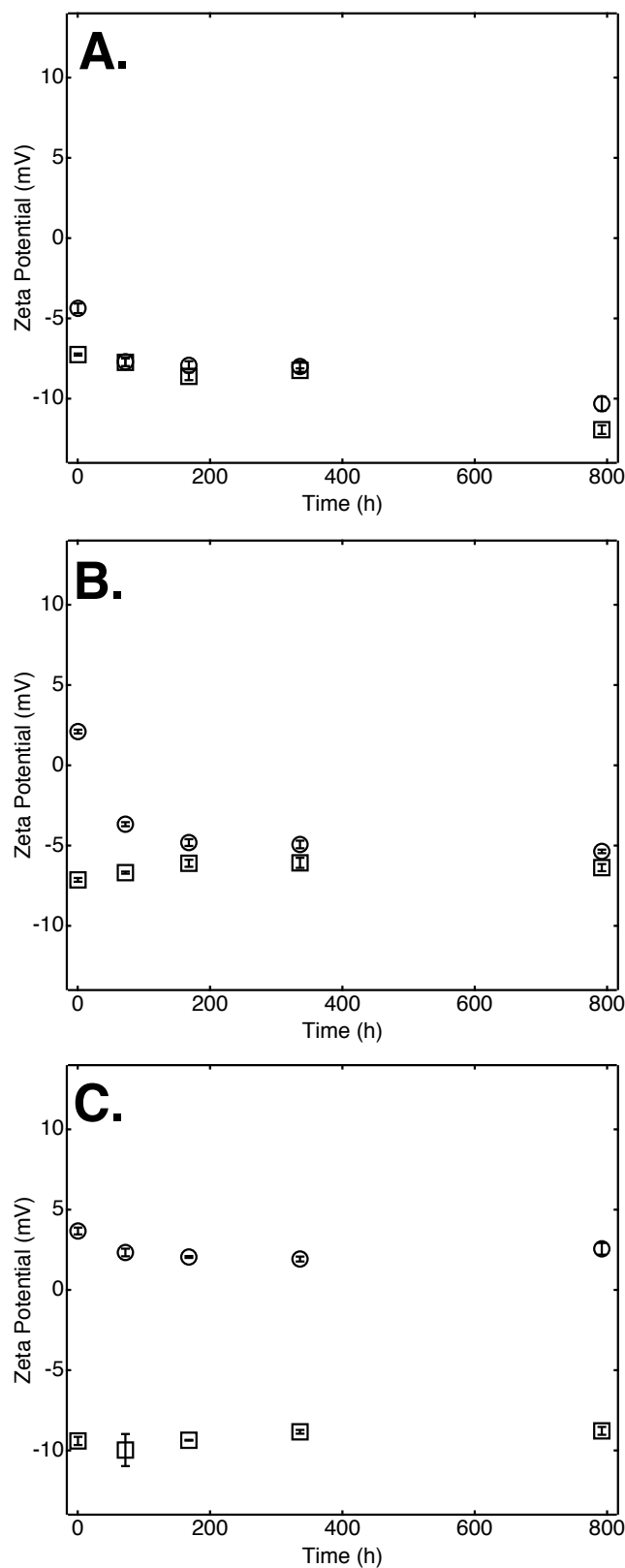


FIGURE 4.3. Zeta potential of silicone oil emulsion in buffer containing humAb 2 and 0.03% (w/v) surfactant. (A) Tween® 20. (B) Tween® 80. (C) poloxamer 188. For each plot, there are two sets of data: □ No protein present, ○ Protein present. Symbols represent the arithmetic mean of three replicate samples. Error bars represent the standard error of the mean.

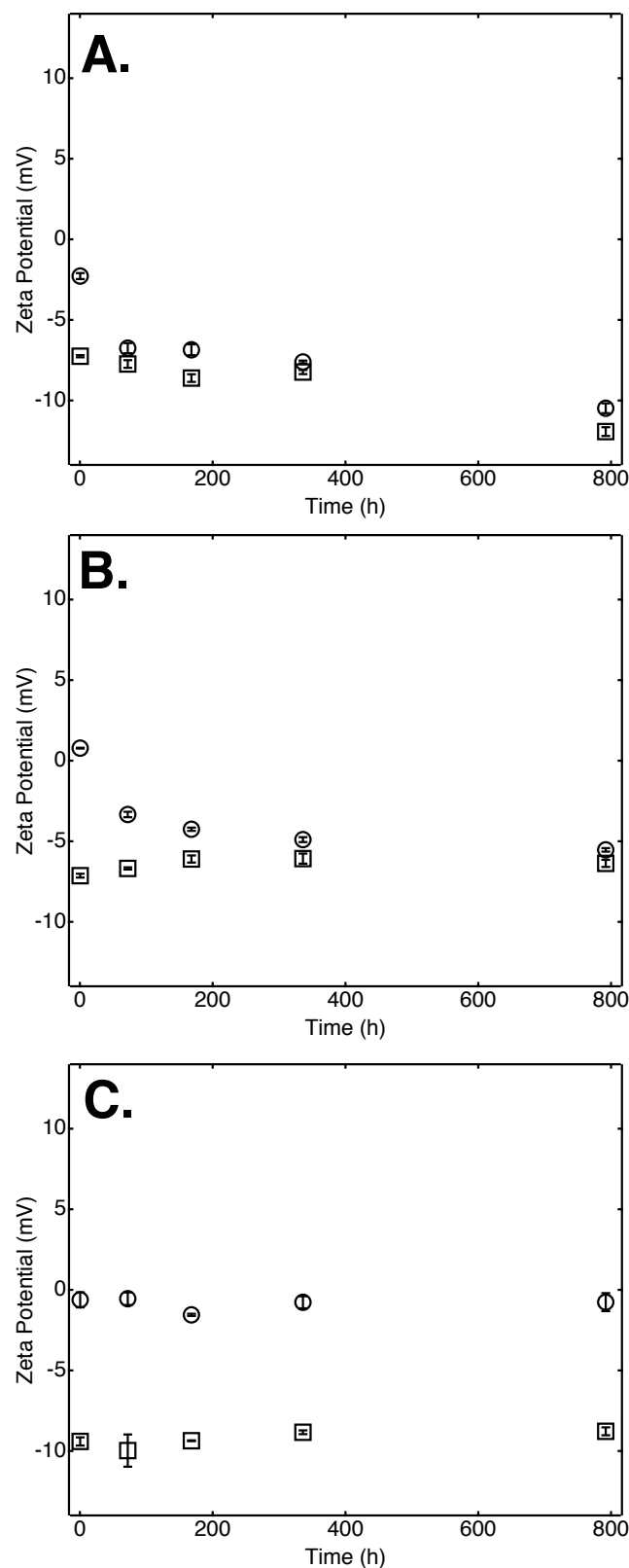


FIGURE 4.4. Zeta potential of silicone oil emulsion in buffer containing humAb 3 and 0.03% (w/v) surfactant. (A) Tween® 20. (B) Tween® 80. (C) poloxamer 188. For each plot, there are two sets of data: □ No protein present, ○ Protein present. Symbols represent the arithmetic mean of three replicate samples. Error bars represent the standard error of the mean.

potential of silicone oil emulsion decreased with time and approached that of a humAb-free solution. Similar behavior was observed for formulations containing Tween® 80. Conversely, the zeta potential remained constant over time for formulations containing poloxamer 188 at a value statistically different than that of a humAb-free solution ( $p < 0.05$ ).

## 4.4 DISCUSSION

### 4.4.1 Zeta Potential of humAb-surfactant Solutions

In the literature, there have been many studies to determine if a protein-surfactant complex forms in solution.<sup>4.1,4.7-4.8,4.11-4.13</sup> The results of these reports depend on the protein and surfactant used. However, in general, surfactants tend to interact with proteins. Accordingly, there was no evidence that this should not be true for the proteins and surfactants used in this study. For formulations containing humAb 1, the differences in the measured zeta potential for formulations containing no surfactant and formulations containing surfactant may represent an indirect piece of evidence that such a protein-surfactant complex formed. Even in formulations containing humAb 3, while the observable differences were statistically insignificant, one cannot rule out the possibility that this interaction may take place. The same argument can be made for formulations containing humAb 2. An interesting note about humAb 2 was that it was originally formulated in a solution containing surfactant then dialyzed into the formulation buffers used in this study (see section 2.2.2). If a protein-surfactant complex formed in the

original formulation and the complex remained in tact during sample preparation, the zeta potential of humAb 2 in the presence of no formulation excipients could represent that of the protein-surfactant complex formed and not pure protein as was originally assumed. If this was the case, this could partially explain why no difference in zeta potential between formulations containing no excipients and formulations containing surfactants was observed.

The aforementioned claims neglected the possibility that it may be the surfactants themselves that are responsible for the decreased zeta potential values. This would depend on whether the concentration of surfactant was above or below the critical micelle concentration (CMC). The CMC of Tween® 20, Tween® 80, and poloxamer 188 are 0.007% (w/v)<sup>4,9</sup>, 0.0017% (w/v)<sup>4,9</sup>, and 0.1% (w/v)<sup>4,15</sup>, respectively. At a concentration of 0.03% (w/v), Tween® 20 and Tween® 80 are formulated above their respective CMC while poloxamer 188 is formulated below its CMC. Above the CMC, the formation of micelles which are comprised of roughly 50-100 surfactant molecules may influence the measured zeta potential.<sup>4,9</sup> In fact, there are statistically significant differences in the measured zeta potential of humAb formulations containing Tween® 20 or Tween® 80 and formulations containing poloxamer 188 ( $p < 0.05$ ). Whether this is due to the presence of micelles, differences in the chemical identity of the surfactants used, binding stoichiometry of surfactants to protein, and/or structural differences in the protein-surfactant complex remains unknown. However, since the measured zeta potential of all humAb formulations containing surfactant are different from that formulations

containing no excipients, it is more likely that a protein-surfactant complex was forming with only minor observable effects caused by micelle formation.

#### 4.4.2 Competitive Adsorption of humAbs and Surfactants at the Silicone Oil-Water Interface

The driving force for the adsorption of protein to fluid-fluid interfaces is the hydrophobic effect and is described by the interfacial free energy.<sup>4.4,4.9</sup> This interfacial free energy is proportional to the interfacial surface tension.<sup>4.2</sup> At increasing surfactant concentrations, the surface tension decreases as a result of surfactant adsorption to the interface. At the CMC, the surface becomes saturated and micelles form in solution. At concentrations in excess of the CMC, the surface tension may be attenuated or may still decrease as a result of additional packing of surfactant at the interface.<sup>4.2,4.9</sup> Experiments were not conducted in this work to verify this claim but this behavior has been observed in similar systems in the literature.

In a solution containing surfactant and protein, there is competition for adsorption sites at an interface. In this work, formulations containing silicone oil emulsion, protein, and surfactant were prepared. Protein was added prior to surfactant in the sample preparation process. As a result, for a brief period of time prior to addition of surfactant to the formulation, protein had no competition for adsorption sites to the silicone oil-water interface. After the addition of surfactant, surfactant adsorption was dependent on its ability to displace adsorbed protein. This competition of protein and surfactant for adsorption sites on silicone oil

droplets was monitored by measuring the zeta potential at the interface. This measurement is not capable of quantifying the amount of protein or surfactant adsorption to the interface like the experiments described in section 2.3.2. However, it serves as a qualitative method to observe the kinetics of adsorption.

Looking specifically at solutions of humAbs 1-3 and 0.03% (w/v) Tween® 20, 0.03% (w/v) Tween® 80, or 0.03% (w/v) poloxamer 188, zeta potential measurements implied that the kinetics of humAb displacement was fastest for Tween® 20 and slowest for poloxamer 188 (Figure 4.2-4). For Tween® 20 and Tween® 80, the concentration of surfactant in the formulation was in excess of each respective CMC. At concentrations in excess of the CMC, the surface tension has been shown to be greater for Tween 80 than Tween 20 at an hydrophobe-aqueous interface.<sup>4,9</sup> Accordingly, it is reasonable to assert that Tween® 20 lowered the interfacial free energy more than Tween® 80 resulting in the the faster displacement kinetics observed. For poloxamer 188, however, the concentration used in this study was less than the CMC. While it appeared as if adsorption of poloxamer 188 had occurred since the measured zeta potential after 30 minutes was less than when no surfactant was present in the formulation (see Figure 2.9), there was no change in the zeta potential to claim that displacement of humAbs from the interface had occurred. But, it is not unreasonable to speculate that this observation may be the result of much slower displacement kinetics. If this is true, then the interfacial free energy in the presence of poloxamer 188 cannot be compared to that of formulations containing Tween® 20 or Tween® 80 in this study. In general, it cannot be



concluded in this analysis whether there is displacement of humAbs or humAb-surfactant complexes from the silicone oil-water interface.

#### 4.5 CONCLUSION

While more direct measurements would provide better insight into the formation of protein-surfactant complexes and protein/surfactant adsorption to interfaces, the use of zeta potential measurements has the ability to provide some useful qualitative insights into said processes. This method alone is capable of making simple comparisons. Used in conjunction with more advanced or complicated techniques, zeta potential measurements can be used to obtain a more complete description of protein-surfactant complexation and protein/surfactant adsorption to interfaces. However, this type of analysis should be used with caution. The complex interplay of different charged species in zeta potential measurements may make this type of analysis too complicated to be useful in some systems.

#### 4.6 REFERENCES

- 4.1 Bam, N.B., Randolph, T.W., Cleland, J.L. (1995). "Stability of Protein Formulations: Investigation of Surfactant Effects by a Novel EPR Spectroscopic Technique." Pharmaceutical Research. 12(1): 2-11.
- 4.2 Beverung, C.J., Radke, C.J., Blanch, H.W. (1999). "Protein Adsorption at the Oil/Water Interface: Characterization of Adsorption Kinetics by Dynamic Interfacial Tension Measurements." Biophysical Chem. 81: 59-80.
- 4.3 Bos, M.A., Vliet, T.V. (2001). "Interfacial Rheological Properties of Adsorbed Protein Layers and Surfactants: A Review." Advances in Colloid and Interface Sci. 91: 437-471.

- 4.4 Chen, J., Dickinson, E. (1995). "Protein/Surfactant Interfacial Interactions Part 3. Competitive Adsorption of Protein + Surfactant in Emulsions. Colloids Surf A Physichem Eng Aspects. 101: 77-85.
- 4.5 Dagleish, D.G., Srinivasan, M., Singh, H. (1995). "Surface Properties of Oil-in-Water Emulsion Droplets Containing Casein and Tween 60." J Agric Food Chem. 43: 2351-2355.
- 4.6 Faude, A., Zacher, D., Muller, E., Bottinger, H. (2007) "Fast Determination of Conditions for Maximum Dynamic Capacity in Cation-Exchange Chromatography of Human Monoclonal Antibodies. J Chromatogr A. 1161: 29-35.
- 4.7 Hazra, P., Chakrabarty, D., Chakraborty, A., Sarkar, N. (2004). "Probing Protein-Surfactant Interaction by Steady State and Time-Resolved Fluorescence Spectroscopy." Biochemical and Biophysical Research Communications. 314: 543-549.
- 4.8 Jones, L.S., Cipolla D., Liu, J., Shire, S.J., Randolph, T.W. (1999). "Investigation of Protein-Surfactant Interactions by Analytical Ultracentrifugation and Electron Paramagnetic Resonance: The Use of Recombinant Human Tissue Factor as an Example." Pharmaceutical Research. 16: 808-812.
- 4.9 Kerwin, B.A. (2008). "Polysorbates 20 and 80 Used in the Formulation of Protein Biotherapeutics: Structure and Degradation Pathways." J Pharma Sci. 97(8): 2924-2935.
- 4.10 Kragel, J., Derkatch, S.R., Miller, R. (2008). "Interfacial Shear Rheology of Protein-Surfactant Layers." Advances in Colloid and Interface Sci. 144: 38-53.
- 4.11 Randolph, T.W., Jones, L.S. (2002). "Surfactant-Protein Interactions." Pharm Biotechnology. 13: 159-175.
- 4.12 Sahu, K., Roy, D., Mondal, S.K., Karmakar, R., Bhattacharyya, K. (2005). "Study of Protein-Surfactant Interaction Using Excited State Proton Transfer." Chemical Physics Letters. 404: 341-345.
- 4.13 Turro, N.J., Lei, X.G. (1995). "Spectroscopic Probe Analysis of Protein-Surfactant Interactions: The BSA/SDS System." Langmuir. 11: 2525-2533.

- 4.14 Wang, W., Wang, Y.J., Wang, D.Q. (2008). "Dual Effects on Tween 80 on Protein Stability." International J Pharmaceutics. 347: 31-38.
- 4.15 Youan, B.B.C., Hussain, A., Nguyen, N.T. (2003). "Evaluation of Sucrose Esters as Alternative Surfactants in Microencapsulation of Protein by the Solvent Evaporation Method." AAPS PharmSci. 5(2): 1-9.

## CHAPTER 5: CONCLUSIONS AND FUTURE RECOMMENDATIONS

### 5.1 FINAL CONCLUSIONS

In this work, the interaction between three humanized monoclonal antibodies with silicone oil emulsion was assessed in the presence of different formulation excipients. Using an ‘accelerated’ approach, with an emulsion concentration nearly 100X that of silicone oil contamination expelled from a syringe, this study sought to identify if homogeneous protein aggregation occurred under static conditions. It was found that static incubation in the presence of silicone oil emulsion was not a sufficient stress to induce aggregation. The presence of different formulation excipients did not affect this result. Protein adsorbed to the silicone oil-water interface and there was evidence that the conformation of protein at the interface was non-native. That analysis could not explain what specifically occurred at the interface, but showed that the presence of different formulation excipients did not influence this conformational change. As a result of protein adsorption to the silicone oil-water interface, emulsion was colloiddally destabilized. In addition, due to creaming of silicone oil emulsion observed with time, the local concentration of emulsion droplets towards the top of the storage container increased. This caused bridging flocculation of these droplets which could yield either be sub-visible or visible particles (Figure 5.1). This finding was startling. If visible particles formed during processing or manufacturing of a commercial therapeutic protein product, the whole protein lot may be discarded. This potential problem is alarming to

pharmaceutical companies because such a loss could financially cripple a start-up company or damage the reputation of a large company. If sub-visible or visible particles are present as a formulation is delivered to a patient, the drug could be ineffective to treat the disease/disorder, mount an unwanted immune response, and/or reduce the advertised shelf-life of the product. Use of a surfactant in a formulation can serve to prevent the aforementioned problems. Surfactant preferentially adsorbed to the silicone oil-water interface. The kinetics of said adsorption seems to be dependent on the surfactant concentration and chemical identity. During the formulation design process, scientists will have to take this into consideration so that the surfactant used in a specific formulation effectively displaces most if not all of adsorbed protein from interfaces associated with the container/closure system, microparticle contaminants, and/or leachables. If a formulation contains the proper surfactant concentration, homogeneous protein aggregation and/or heterogeneous protein-contaminant aggregation can be either be minimized or completely inhibited.

## 5.2 FUTURE RECOMMENDATIONS

The work that has been accomplished is far from complete. More is known about protein interactions with silicone oil than before these experiments were conducted, but these interactions are still not understood at a fundamental level. There are many questions left unanswered. Under what conditions does silicone oil induce homogeneous protein aggregation? What is the mechanism of homogeneous

protein aggregation? How do single protein molecules interact with the silicone oil-water interface at low protein concentrations? What happens when the concentration of protein increases such that protein-protein interactions become important? There are two important directions that need to be traveled to be able to answer some of these questions.

What happens when the silicone oil-water interface is perturbed? In this work, the interface remained static. These experiments need to be repeated for agitated samples. Also, experiments geared towards monitoring the effect of interfacial compression need to be assessed. End-over-end rotation studies and axisymmetric bubble-shape tensiometry are good starting points.

What happens at the molecular level when the concentration of protein is increased from just single molecules to ensembles? Single-molecule total internal reflection fluorescence spectroscopy (TIRFM) can provide insight about the adsorption of single molecules. This technique can identify different protein populations (i.e. monomers, dimers, aggregates) and determine their surface residence times and surface diffusion coefficients. What happens as the concentration increases? How do protein-protein interactions influence the surface residence times and surface diffusion coefficients of different populations? Does protein-protein association give rise to new populations (e.g. aggregates)? If so, work needs to be done to develop methods to complement front-face fluorescence quenching experiments to determine the conformation of adsorbed protein. Methods such as circular dichroism (CD), Förster Resonance Energy Transfer (FRET) and

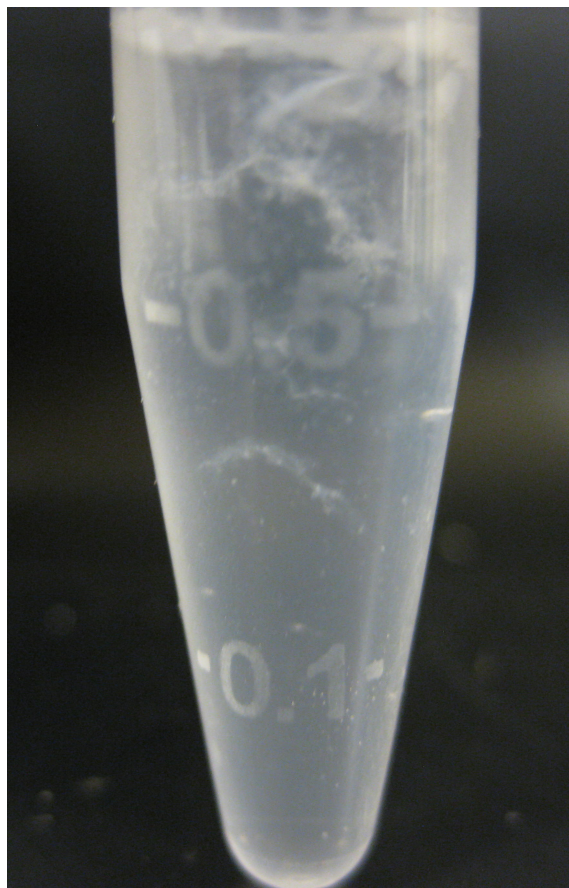


FIGURE 5.1. Example of visible particles that can form after protein is incubated with silicone oil emulsion. Visible particles were observed after incubation of humAb 1 in 10 mM L-histidine at pH 6.0 containing 0.01% (w/v) sodium azide and 0.03% (w/v) Tween® 80 for 72 hours.

hydrogen-deuterium exchange need to be investigated. Lastly, it will be important to understand what happens to the functionality of adsorbed protein. Is there a correlation between protein adsorption and loss of functionality?

While it is unlikely that all questions will be answered if all these types of experiments were conducted, some questions will be answered. At this stage, it is difficult to know exactly what experiments to do without being guided by results. The only way to figure out what the next stage will be is to go into the laboratory and learn more through experimentation.

### 5.3 REFERENCES

- 5.1 Antia, M., Islas, L.D., Boness, D.A., Baneyx, G., Vogel, V. (2006). "Single Molecule Fluorescence Studies of Surface-Adsorbed Fibronectin." Biomaterials. 27: 679-690.
- 5.2 Halling, P.J. (2009). "Estimation of Flattening Coefficient for Absorption and Circular Dichroism Using Simulation." Anal Biochem. 387(1): 76-81.
- 5.3 McMillin, C.R., Walton, A.G. (1974). "A Circular Dichroism Technique for the Study of Adsorbed Protein Structure." J Colloid and Interface Sci. 48(2): 345-349.
- 5.4 Shugar, D. (1952). "The Measurement of Lysozyme Activity and the Ultraviolet Inactivation of Lysozyme." Biochimica et Biophysica Acta. 8: 302-309.
- 5.5 Smith, J.R., Cicerone, M.T., Meuse, C.W. (2009). "Measuring Hydrogen-Deuterium Exchange in Protein Monolayers." Surf Interface Anal. 41: 878-885.
- 5.6 Tilton, R.D., Gast, A.P., Robertson, C.R. (1990). "Surface Diffusion of Interacting Proteins." Biophysical Society. 58: 1321-1326.



## BIBLIOGRAPHY

Antia, M., Islas, L.D., Boness, D.A., Baneyx, G., Vogel, V. (2006). "Single Molecule Fluorescence Studies of Surface-Adsorbed Fibronectin." Biomaterials. 27: 679-690.

Bam, N.B., Cleland, J.L., Yang, J., Manning, M.C., Carpenter, J.F., Kelley, R.F., Randolph, T.W. (1998). "Tween Protects Recombinant Human Growth Hormone Against Agitation-Induced Damage Via Hydrophobic Interactions." J Pharm Sci. 87: 1554-1559.

Bam, N.B., Randolph, T.W., Cleland, J.L. (1995). "Stability of Protein Formulations: Investigation of Surfactant Effects by a Novel EPR Spectroscopic Technique." Pharmaceutical Research. 12(1): 2-11.

Barbosa, M.D.F.S., Celis, E. (2007). "Immunogenicity of Protein Therapeutics and the Interplay between Tolerance and Antibody Responses." Drug Discovery Today. 12(15-16): 674-681.

Bee, J.S. (2009). "Bubble Tensiometry and Langmuir Trough Studies of a Monoclonal Antibody Adsorbed at the Air-Water Interface. In Effect of Interfaces and Shear on Therapeutic Protein Stability." Ph.D. Thesis: 237-254.

Bee, J.S. (2009). "Front-Face Fluorescence Quenching and FRET Techniques to Probe the Structure of a Protein Antigen Adsorbed to Vaccine Adjuvant. In Effect of Interfaces and Shear on Therapeutic Protein Stability." Ph.D. Thesis: 237-254.

Bee, J.S. 2009. "Interface Oscillations Provide Insight Into Protein Aggregate Particle Formation at the Air-Water Interface. In Effect of Interfaces and Shear on Therapeutic Protein Stability." Ph.D. Thesis: 200-236.

Bee, J.S., Chiu, D., Sawicki, S., Stevenson, J.L., Chatterjee, K., Freund, E., Carpenter, J.F., Randolph, T.W. (2009). "Monoclonal Antibody Interactions with Micro- and Nanoparticles: Adsorption, Aggregation, and Accelerated Stress Studies." J Pharm Sci. 98: 3218-3238.

Bee, J.S., Davis, M., Freund, E., Carpenter, J.F., Randolph, T.W. (2010). "Aggregation of Monoclonal Antibody Induced by Adsorption to Stainless Steel." Biotechnology and Bioengineering. 105(1): 121-129.

Bee, J.S., Nelson, S., Freund, E., Carpenter, J.F., Randolph T.W. (2009). "Precipitation of a Monoclonal Antibody by Soluble Tungsten." J Pharm Sci. 98: 3290-3301.

Beverung, C.J., Radke, C.J., Blanch, H.W. (1999). "Protein Adsorption at the Oil/Water Interface: Characterization of Adsorption Kinetics by Dynamic Interfacial Tension Measurements." Biophysical Chem. 81: 59-80.

Bhattacharjee, S., Elimelech, M., Borkovec, M. (1998). "DLVO Interaction between Colloidal Particles: Beyond Derjaguin's Approximation." CCACAA. 71(4): 883-903.

Bos, M.A., Vliet, T.V. (2001). "Interfacial Rheological Properties of Adsorbed Protein Layers and Surfactants: A Review." Advances in Colloid and Interface Sci. 91: 437-471.

Butt, H.J., Graf, K., Kappl, M. (2003). Physics and Chemistry of Interfaces. 1st Edition. Wiley.

Carpenter, J.F., Randolph, T.W., Jiskoot, W., Crommelin, D.J.A., Middaugh, C.R., Winter, G. (2010). "Potential Inaccurate Quantitation and Sizing of Protein Aggregates by Size Exclusion Chromatography: Essential Need to Use Orthogonal Methods to Assure the Quality of Therapeutic Protein Products." J Pharma Sci. 99: 2200-2208.

Chang, D., Chang, R.K. (2007). "Review of Current Issues in Pharmaceutical Excipients." Pharmaceutical Technology. [Epub].

Chantelau, E.A., Berger, M. (1985). "Pollution of Insulin with Silicone Oil, a Hazard of Disposable Plastic Syringes." Lancet. 1: 1459.

Chantelau, E., M. Berger, Bohlken, B. (1986). "Silicone Oil Released From Disposable Insulin Syringes." Diabetes Care 9(6): 672-673.

Chen, J., Dickinson, E. (1995). "Protein/Surfactant Interfacial Interactions Part 3. Competitive Adsorption of Protein + Surfactant in Emulsions. Colloids Surf A Physichem Eng Aspects. 101: 77-85.

Chi, E.Y., Krishnan, S., Kendrick, B.S., Chang, B.S., Carpenter, J.F., Randolph, T.W. (2003). "Roles of Conformational Stability and Colloidal Stability in the Aggregation of Recombinant Human Granulocyte Colony-Stimulating Factor." Protein Science. 12: 903-913.

Chi, E.Y., Weickmann, J., Carpenter, J.F., Manning, M.C., Randolph, T.W. (2005). "Heterogeneous Nucleation-Controlled Particulate Formation of Recombinant Human Platelet-Activating Factor Acetylhydrolase in Pharmaceutical Formulation." J Pharma Sci. 94: 256-274.

Cleland, J.L., Powell, M.F., Shire, S.J. (1993). "The Development of Stable Protein Formulations: A Closer Look at Protein Aggregation, Deamidation, and Oxidation." Crit Rev Ther Drug Carrier Syst. 10: 307-377.

Collier, F.C., Dawson, A.D. (1985). "Insulin syringes and Silicone Oil." Lancet. 2: 611.

Dalgleish, D.G., Srinivasan, M., Singh, H. (1995). "Surface Properties of Oil-in-Water Emulsion Droplets Containing Casein and Tween 60." J Agric Food Chem. 43: 2351-2355.

de Jongh H.H.J., Wierenga, P.A. (2006). "Assessing the Extent of Protein Intermolecular Interactions at Air-Water Interfaces Using Spectroscopic Techniques." Biopolymers. 82: 384-389.

de Young, L.R., Fink, A.L., Dill, K.A. (1993). "Aggregation of Globular Proteins." Acc Chem Res. 26: 614-620.

Dickinson, E. (1999). "Adsorbed Protein Layers at Fluid Interfaces: Interactions, Structure, and Surface Rheology." Colloids and Surfaces B: Biointerfaces. 15: 161-176.

Eakins, M.N. (2008). "Offering a New Choice in Glass Pre-fillable Syringes." East Sussex, United Kingdom: ONdrugDelivery. pp 7-10.

Eftink, M.R., Ghiron, C.A. (1977). "Exposure of Tryptophanyl Residues and Protein Dynamics. Biochemistry. 16: 5546-5551.

Eftink, M.R., Ghiron, C.A. (1981). "Fluorescence Quenching Studies with Proteins. Anal Biochem. 114: 199-227.

Faude, A., Zacher, D., Muller, E., Bottinger, H. (2007) "Fast Determination of Conditions for Maximum Dynamic Capacity in Cation-Exchange Chromatography of Human Monoclonal Antibodies. J Chromatogr A. 1161: 29-35.

Fesinmeyer, R.M., Hogan, S., Saluja, A., Brych, S.R., Kras, E., Narhi, L.O., Brems, D.N., Gokarn, Y.R. (2009). "Effect of Ions on Agitation- and Temperature-Induced Aggregation Reactions." Pharmaceutical Research. 26(4): 903-913.

Gabrielson, J. (2006). "Irreversible Association of Monoclonal Antibody with Silicone Oil in Aqueous Formulation Containing Sucrose and Surfactants. In Monoclonal Antibody Aggregation in Therapeutic Formulation: Size and Shape-Distribution Analysis." Ph.D. Thesis: 100-124.

Gajraj, A., Ofoli, R.Y. (2000). "Quantitative Technique for Investigating Macromolecular Adsorption and Interactions at the Liquid-Liquid Interface." Langmuir. 16: 4279-4285.

Givan, A.L. (2002). Flow Cytometry: First Principles. 2nd Edition. Wiley.

Groza, A., A. Surmeian, et al. (2005). "Infrared spectral investigation of organosilicon compounds under corona charge injection in air at atmospheric pressure." Journal of Optoelectronics and Advanced Materials 7(5): 2545-2548.

Halling, P.J. (2009). "Estimation of Flattening Coefficient for Absorption and Circular Dichroism Using Simulation." Anal Biochem. 387(1): 76-81.

Harrison, R.G., Todd, P., Rudge, S.R., Petrides, D.P. (2003). Bioseparations Science and Engineering. New York: Oxford University Press.

Hazra, P., Chakrabarty, D., Chakraborty, A., Sarkar, N. (2004). "Probing Protein-Surfactant Interaction by Steady State and Time-Resolved Fluorescence Spectroscopy." Biochemical and Biophysical Research Communications. 314: 543-549.

Hoehne, M., Samuel, F., Dong, A., Wurth, C., Mahler, H., Carpenter, J.F., Randolph, T.W. (2010). "Adsorption of Monoclonal Antibodies to Glass Microparticles". J Pharm Sci. 1: 1-10.

Hoffman, G. (1977) Isotables, 7th Edition. Lincoln, Neb., ISCO.

Hogg, R., Healy, T.W., Fuerstenau, D.W. (1966). "Mutual Coagulation of Colloidal Dispersions." Trans. Faraday Soc. 62: 1638-1651.

Honciuc, A., Baptiste, D., Campbell, I.P., Schwartz, D.K. (2009). "Solvent Dependence of the Activation Energy of Attachment Determined by Single Molecule Observations of Surfactant Adsorption." Langmuir. 25(13): 7389-7392.

Israelachvili, J.N. (1992). Intermolecular and Surface Forces, 2nd Edition. New York: Academic Press.

Jakupi, P., Halvorsen, Leaist, D.G. (2004). "Thermodynamic Interpretation of the 'Excluded-Volume Effect' in Coupled Diffusion." J Phys Chem B. 108: 7978-7985.

Janeway, C.A., Travers, P.A., Walport, M. (2001). Immunobiology. New York: Garland Publishing.

Jones, L.S., Cipolla D., Liu, J., Shire, S.J., Randolph, T.W. (1999). "Investigation of Protein-Surfactant Interactions by Analytical Ultracentrifugation and Electron Paramagnetic Resonance: The Use of Recombinant Human Tissue Factor as an Example." Pharmaceutical Research. 16: 808-812.

Jones, L.S., Kaufmann, A., Middaugh, C.R. (2005). "Silicone Oil Induced Aggregation of Proteins." J Pharm Sci. 94: 918-927.

Kerwin, B.A. (2008). "Polysorbates 20 and 80 Used in the Formulation of Protein Biotherapeutics: Structure and Degradation Pathways." J Pharma Sci. 97(8): 2924-2935.

Kragel, J., Derkatch, S.R., Miller, R. (2008). "Interfacial Shear Rheology of Protein-Surfactant Layers." Advances in Colloid and Interface Sci. 144: 38-53.

Lubiniecki, A., D. B. Volkin, et al. "Comparability assessments of process and product changes made during development of two different monoclonal antibodies." Biologicals In Press, Corrected Proof.

Ludwig, D.B., Carpenter, J.F., Hamel, J., Randolph, T.W. (2009). "Protein Adsorption and Excipient Effects on Kinetic Stability of Silicone Oil Emulsions." J Pharm Sci. 99: 1721-1733.

Ludwig, D.B., Trotter, J.T., Gabrielson, J.P., Carpenter, J.F., Randolph, T.W. (2010) "Flow Cytometry: A Promising Technique for the Study of Silicone Oil-Induced Particulate Formation in Protein Formulations." J Pharm Sci. 99(4): 1721-1733.

Maas, C., Hermeling, S., Bouma, B., Jiskoot, W., Gebbink, M.F.B.G. (2007). "A Role for Protein Misfolding in Immunogenicity of Biopharmaceuticals." J Biological Chemistry. 282(4): 2229-2236.

Marinova, K. G., R. G. Alargova, Denkov, N.D., Velev, O.D., Petsev, D.N., Ivanov, I.B., Borwankar, R.P. (1996). "Charging of oil-water interfaces due to spontaneous adsorption of hydroxyl ions." Langmuir 12(8): 2045-2051.

Martin, A.H., Meinders, M.B.J., Bos, M.A., Stuart, M.A.C., van Vliet, T. (2003). "Conformational Aspects of Proteins at the Air/Water Interface Studied by Infrared Reflection-Absorption Spectroscopy." Langmuir. 19: 2922-2928.

McLeod, A.G., Walker, I.R., Zheng, S., Hayward, C.P.M. (2000). "Loss of Factor VIII Activity During Storage in PVC Containers due to Adsorption." Haemophilia. 6: 89.

McMillin, C.R., Walton, A.G. (1974). "A Circular Dichroism Technique for the Study of Adsorbed Protein Structure." J Colloid and Interface Sci. 48(2): 345-349.

Moon, Y.U., Curtis, R.A., Anderson, C.O., Blanch, H.W., Prausnitz, J.M. (2000). "Protein-Protein Interactions in Aqueous Ammonium Sulfate Solutions. Lysozyme and Bovine Serum Albumin (BSA)." J Solution Chem. 29(8): 699-717.

Pace, N.C., Trevino, S., Prabhakaran, E., Scholtz, J.M. (2004). "Protein Structure, Stability, and Solubility in Water and Other Solvents." Phil Trans R Soc Lond B. 359: 1225-1235.

Pharmacopedia US. (2006). <788> Particulate Matter in Injections. USF-NF, 24th edition.

Pifferi, G., Restani, P. (2003). "The Safety of Pharmaceutical Excipients." Il Farmaco. 58: 541-550.

Randolph, T.W., Jones, L.S. (2002). "Surfactant-Protein Interactions." Pharm Biotechnology. 13: 159-175.

Rahman, M., Lane, A., Swindell, A., Bartram, S. (2006). "Introduction to Flow Cytometry: Principles, Data Analysis, Protocols, and Troubleshooting." Oxford, United Kingdom, Serotec Incorporated.

Romacker, M., Schoenknecht, T., Forster, R. (2008). "The Rise of Prefilled Syringes from Niche Product to Primary Container of Choice: A Short History. East Sussex, United Kingdom: ONdrugDelivery. pp 4-5.

Rosenberg, A.S. (2006). "Effects of Protein Aggregates: An Immunologic Perspective." The AAPS Journal. 8(3): E501-E507.

Sahin, E., Adeola, A.O., Perkins, M.D., Roberts, C.J. (2010). "Comparative Effects of pH and Ionic Strength on Protein-Protein Interactions, Unfolding, and Aggregation for IgG1 Antibodies." J Pharma Sci. 99(12): 4830-4848.

Sahu, K., Roy, D., Mondal, S.K., Karmakar, R., Bhattacharyya, K. (2005). "Study of Protein-Surfactant Interaction Using Excited State Proton Transfer." Chemical Physics Letters. 404: 341-345.

Salinas, B.A., Sathish, H.A., Bishop, S.M., Harn, N., Carpenter, J.F., Randolph, T.W. (2010). Understanding and Modulating Opalescence and Viscosity in a Monoclonal Antibody Formulation." J Pharma Sci. 99: 82-93.

Schladitz, C., Vieira, E.P., Hermel, H., Mohwald, H. (1999). "Amyloid- $\beta$ -Sheet Formation at the Air-Water Interface." Biophysical Journal. 77: 3305-3310.

Seneviratne, A.K. (2010). "Visible Particles in Protein Therapeutics: Physical Nature, Origin, Detection, and Solutions." 2010 AAPS National Biotechnology Conference, May 16-19, San Francisco.

Sharma, B. (2007). "Immunogenicity of Therapeutic Proteins. Part 2: Impact of Container Closures." Biotechnology Advances. 25: 318-324.

Shugar, D. (1952). "The Measurement of Lysozyme Activity and the Ultraviolet Inactivation of Lysozyme." Biochimica et Biophysica Acta. 8: 302-309.

Sluzky, V., Tamada, J.A., Klibanov, A.M., Langer, R. (1991). "Kinetics of Insulin Aggregation in Aqueous Solutions Upon Agitation in the Presence of Hydrophobic Surfaces." Applied Biological Sciences. 88: 9377-9381.

Smith, J.R., Cicerone, M.T., Meuse, C.W. (2009). "Measuring Hydrogen-Deuterium Exchange in Protein Monolayers." Surf Interface Anal. 41: 878-885.

Strambini, G.B., Gonnelli, M. (2010). "Fluorescence Quenching of Buried Trp Residues by Acrylamide Does Not Require Penetration of the Protein Fold." J Phys Chem B. 114: 1089-1093.

Thirumangalathu, R., Krishnan, S., Speed Ricci, M., Brems, D.N., Randolph, T.W., Carpenter, J.F. (2009). Silicone Oil- and Agitation-Induced Aggregation of a Monoclonal Antibody in Aqueous Solution. J Pharm Sci. 98: 3167-3181.

Tilton, R.D., Gast, A.P., Robertson, C.R. (1990). "Surface Diffusion of Interacting Proteins." Biophysical Society. 58: 1321-1326.

Timasheff, S.N. (1992). "Water as Ligand: Preferential Binding and Exclusion of Denaturants in Protein Unfolding." Biochemistry. 31: 9857-9864.

Turro, N.J., Lei, X.G. (1995). "Spectroscopic Probe Analysis of Protein-Surfactant Interactions: The BSA/SDS System." Langmuir. 11: 2525-2533.

Tyagi, A.K., Randolph, T.W., Dong, A., Maloney, K.M., Hitscherich, C., Carpenter, J.F. (2009). "IgG Particle Formation during Filling Pump Operation: A Case Study of Heterogeneous Nucleation on Stainless Steel Nanoparticles." J Pharm Sci. 98: 94-104.

Tzannis, S.T., Hrushesky, W.J.M., Wood, P.A., Przybycien, T.M. (1997). "Adsorption of a Formulated Protein on a Drug Delivery Device Surface." J Colloid Interface Sci. 189: 216-228.

Walder, R., Schwartz, D.K. (2010). "Single Molecule Observations of Multiple Populations at the Oil-Water Interface." Langmuir. 26(16): 13364-13367.

Walstra, P. (1996). Emulsion Stability. In: Bercher P, editor. Encyclopedia of Emulsion Technology. New York: Marcel Dekker. 4: 1-62.

Wang, W., Nema, S., Teagarden, D. (2010). "Protein Aggregation: Pathways and Influencing Factors." International J Pharmaceutics. 390: 89-99.

Wang, W., Singh, S., Zeng, D.L., King, K., Nema, S. (2007). "Antibody Structure, Instability, and Formulation." J Pharma Sci. 96(1): 1-26.

Wang, W., Wang, Y.J., Wang, D.Q. (2008). "Dual Effects on Tween 80 on Protein Stability." International J Pharmaceutics. 347: 31-38.

Yeung, A., Moran, K., Masliyah, J., Czarnecki, J. (2003). "Shear-Induced Coalescence of Emulsified Oil Drops." J Colloid and Interface Sci. 265: 439-443.

Youan, B.B.C., Hussain, A., Nguyen, N.T. (2003). "Evaluation of Sucrose Esters as Alternative Surfactants in Microencapsulation of Protein by the Solvent Evaporation Method." AAPS PharmSci. 5(2): 1-9.

2005. Mimetibody.com. Online posting. December 15, 2010 <<http://www.mimetibody.com>>.

2010. abcam. Online posting. December 15, 2010 <<http://www.abcam.com/ps/CMS/Images/abstructure.jpg>>.

2010. DOW CORNING 360 Medical Fluid [product information]. Dow Corning Corporation.



2010. “Fluorophores and Their Amine-Reactive Derivatives: Alexa Fluor Dyes Spanning the Visible and Infrared Spectrum.” Molecular Probes: The Handbook. Life Technologies.

2010. “Probes for Lipids and Membranes.” Molecular Probes: The Handbook. Life Technologies.